

**PERFORMANCE OF
ALKALI ACTIVATED SLAG CONCRETE MIXES
INCORPORATING COPPER SLAG
AS FINE AGGREGATE**

Thesis

submitted in partial fulfilment of the requirements for the degree of

DOCTOR OF PHILOSOPHY

by

MITHUN B M

(112021CV11F10)



**DEPARTMENT OF CIVIL ENGINEERING
NATIONAL INSTITUTE OF TECHNOLOGY KARNATAKA
SURTATHKAL, MANGALORE - 575025**

SEPTEMBER, 2017

DECLARATION

by the Ph.D. Research Scholar

I hereby declare that the Research Thesis entitled “**Performance of Alkali Activated Slag Concrete Mixes Incorporating Copper Slag as Fine Aggregate**” Which is being submitted to the **National Institute of Technology Karnataka, Surathkal** in partial fulfilment of the requirements for the award of the Degree of **Doctor of Philosophy in Civil Engineering**, is a bonafide report of the research work carried out by me. The material contained in this Research Thesis has not been submitted to any University or Institution for the award of any degree.

112021CV11F10, MITHUN B M

Department of Civil Engineering

Place: NITK-Surathkal

Date: 14-09-2017

CERTIFICATE

This is to certify that the Research Thesis entitled **Performance of Alkali Activated Slag Concrete Mixes Incorporating Copper Slag as Fine Aggregate** submitted by **Mr. MITHUN B.M**, (Register Number: **112021CV11F10**), as the record of the research work carried out by him, is accepted as the Research Thesis submission in partial fulfilment of the requirements for the award of degree of **Doctor of Philosophy**.

(Dr. Mattur C. Narasimhan)
Professor and Research Guide
Department of Civil Engineering

Chairman - DRPC
Department of Civil Engineering

DEDICATED
TO
MY PARENTS,
FAMILY MEMBERS, TEACHERS
AND
FRIENDS

ACKNOWLEDGEMENT

I would like to express my sincere gratitude to my research supervisor, Dr. Mattur C. Narasimhan, for his Infinite love, care, motivation and invaluable guidance throughout my research work. I am grateful to him for his keen interest in the preparation of this thesis. It has been my pleasure to work with him.

I acknowledge my sincere thanks to Dr. Vasudeva Adhikari, Dept. of Chemistry and Dr. Manu, Dept. of Applied Mechanics and Hydraulics, the members of my Research Progress Assessment Committee, for their valuable suggestions and the encouragement provided at various stages of this work.

I wish to thank Dr. Uma Maheshwar Rao. K, Director of our Institute, Dr. Katta Venkataramana, Prof. D. Venkat Reddy and Dr. A.U. Ravishankar, the former Heads of Civil Engineering Department, Dr. Varghese George, the Head of Civil Engineering Department, and Dr. Babu Narayan, Dr. Sitaram Nayak, Dr. Shrihari, Dr. Subhash C. Yaragal, Dr. Prashanth M.H, Dr. B.B. Das, Dr. Gangadhar Mahesh, Dr. Ramesh. H, Dr. Subrahmanya Kundapura for all their support and encouragement throughout my stay at the NITK campus.

I wish to acknowledge here sincerely the intellectual knowledge, support, and motivation given by the, Dr N.P.Rajmane who can be considered as **Father of Indian Geopolymer Concrete**, which has helped me infinitely throughout.

Special mention is to be made of I appreciate the co-operation and help extended to me by all the members of the technical staff at the laboratories of the Civil Engineering Department. My special thanks to due to Mr. Purushotham, Mr. Ramanath Acharya, Mr. Shashikant, Mr. Vishwanth and Mr. Dheeraj for their kind help in completing my experimental work. I extend my sincere thanks to the members of the office staff, Mrs. Vagdevi, Mrs. Vijay Laxmi and Mr. Monaappa, for their kind supportat various stages of this work

I also like to extend my gratitude to all the members of the teaching faculty and other members of the supporting staff of the Civil Engineering Department, for their encouragement, help and support extended to me during the research work.

I am fortunate to have my friends like, Mr. Sajeev S, Mr. Nitendra Palankar, Mr. Manu D.S, Mrs, Anupama, Mr. Chethan Kumar. B, Mr. Manjunath S P, Mr. Guru Prasad, Mr. Mudaanna, Mr. Gokul Kudva, Mr. Shashi Kumar, Mr. Akshay, Mr. Rohith, Mr. Rajath, Mr. Mohon Kumar, and Mr. Vivek Kumar whose contributions and encouragements have taken me this far. I am very much thankful to all my friends and fellow research scholars of this institute for their continuous encouragement and suggestions during the course of my research work. The informal support and encouragement of my friends has been indispensable.

I am highly indebted to my present place of work, the NMAMIT, Nitte, Karnataka, for providing me to continue my research activities. I am thankful to our beloved Principal Dr Niranjan Chipulankar, Vice-principal, Dr. Mithanthaya, I.R, Dean (R&D) Dr. Sudesh Bekal, Head of Civil Engineering Department Udayakumar G, Former Head of Civil Engineering Department who have supported me and enabled me for successful completion of my research work. My recent colleagues at NMAMIT, Mr. Janakaraj, Mr. Akshay, Mr. Pruthviraj, Mr. Rakshith Shetty, Mr. Pushpa Raj, Mr. Suresh, Mr. Lokesh, Dr. Mahadeve Gowda, Mr. Sundeep Shenoy, Mr. Sriram Marathe, Mr. Shanmuka Shetty, Mr. Anil, Mr. Thusar Shetty, Mr. Pradeep Karanth, Mr. Sabhyath Shetty, Miss. Rajashree, Miss. Swathi Pai, Miss. Shruthi Gatti, Dr. Subramanya Bhatt, also helped me for continuous encouragement and their kind support.

I am especially grateful to my loving parents Sri. Manjunath B V and Smt. Chaya A V, brother Sri. B. M. S Chethan, Sister-in-Law Smt. Meghana, Sister Manasa B. M. C who have provided me the best available education and support and have encouraged in all my endeavors. They have always been a source of inspiration for me.

Finally, I am grateful to everybody who helped and encouraged me during this research work.

NITK, Surathkal

(Mithun B M)

Date: 14-09 -2017

ABSTRACT

The present study attempts a detailed evaluation of the strength and durability performance of Alkali Activated Slag Concrete (AASC) mixes containing Copper Slag (CS) as fine aggregate. Copper slag, a waste product obtained from copper industry, is incorporated in the AASC mixes as a partial/full replacement to river sand. Initially OPC and AASC mixes are designed to obtain M45 grade with river sand as aggregate; subsequently additional AASC mixes obtained with CS as fine aggregate, incorporated as replacement to sand at increasing volumes are also considered. CS replacement at varying levels upto 100% by absolute volume, in increments of 25% of total fine aggregate are attempted. Various strength and durability properties, including under flexural fatigue tests, of these AASC mixes are studied in detail and are compared with those of conventional Ordinary Portland Cement Concrete (OPCC). An attempt is also made to study the flexural performance of experimental reinforced concrete beams prepared using such mixes in terms of their Load-deflection response, first crack loads and ultimate loads, ductility characteristics etc. vis-à-vis OPC-based concrete beams with similar reinforcement. The ecological and economical analysis of all such concrete mixes is also carried out.

The experimental results indicate that the AASC mixes display better mechanical strength as compared to OPCC in normal working environments. While the AASC mixes with CS fine aggregates displayed similar durability performance in an acid rich environment, however, relatively lower performance is exhibited by them in magnesium sulphate solution and elevated temperatures. The fatigue performance of AASC mixes marginally improved with the incorporation of CS. It was also observed that the fatigue data of beams made with different mixes can be satisfactorily modelled using two parameter Weibull-distribution. The reinforced AASC beams with CS as fine aggregate have exhibited acceptable flexural performance, both with respect to flexural strength and deflection, as compared with AASC concrete beams using river sand fine aggregate. The AASC mixes with CS fine aggregates displayed lower energy requirement and lower production cost as compared to OPCC, thus proving them to be eco-friendly. Thus the experimental results have indicated that CS aggregates can be used as alternate fine aggregates in alkali activated concrete mixes for acceptable performance in both structural and pavement quality concrete mixes.

Keywords: Alkali activated slag concrete mixes; Copper slag fine aggregates; Mechanical and durability properties, Fatigue performance, Flexural performance, Waste management.

CONTENTS

No	Title	Page No
	DECLARATION	
	CERTIFICATE	
	ACKNOWLEDGEMENT	
	ABSTRACT	
	CONTENTS	i
	LIST OF FIGURES	v
	LIST OF TABLES	vi
	NOMENCLATURE	vii
1	INTRODUCTION	01
	1.1 GENERAL	01
	1.2 OBJECTIVES OF THE PRESENT RESEARCH	05
	1.3 SCOPE OF WORK	05
	1.4 ORGANIZATION OF THE THESIS	06
2	LITERATURE REVIEW	09
	2.1 GENERAL	09
	2.2 BRIEF HISTORY OF ALKALI ACTIVATED BINDERS	10
	2.3 GROUND GRANULATED BLAST FURNACE SLAG (GGBFS)	11
	2.4 ACTIVATION MECHANISMS OF ALKALI ACTIVATED SLAG	12
	2.5 EFFECT OF TYPE, DOSAGE, AND MODULUS OF ALKALINE ACTIVATORS OF ALKALI ACTIVATED SLAG	14
	2.6 MECHANICAL PROPERTIES OF ALKALI ACTIVATED SLAG CONCRETE MIXES	16
	2.7 EFFECT OF CURING REGIME ON THE MECHANICAL PROPERTIES OF AAS CONCRETE MIXES	18
	2.8 DURABILITY OF ALKALI ACTIVATED SLAG CONCRETE MIXES	18
	2.9 EFFECT OF ELEVATED TEMPERATURE ON THE STRENGTH OF	20

	CONCRETE MIXES	
	2.10 FLEXURAL FATIGUE CHARACTERISTICS OF CONCRETE PAVEMENTS	23
	2.10.1 S-N Curves and Probabilistic Approach	25
	2.11 STRUCTURAL BEHAVIOR OF AASC- BASED REINFORCED CONCRETE BEAMS	27
	2.12 COPPER SLAG	28
	2.12.1 Engineering Properties of Copper Slag Based Concrete Mixes	29
	2.13 SUMMARY	30
3	MATERIALS CHARACTERIZATION AND MIX PROPORTIONS	33
	3.1 INTRODUCTION	33
	3.2 PRELIMINARY INVESTIGATIONS ON CONSTITUENT MATERIALS	33
	3.2.1 Cement	33
	3.2.2 Ground Granulated Blast-Furnace Slag (GGBFS)	33
	3.2.3 Aggregates	33
	3.2.3.1 <i>Copper slag</i>	35
	3.2.4 Water	36
	3.2.5 Super-plasticizer	36
	3.2.6 Alkaline Activators	37
	3.2.7 Reinforcing bars	38
	3.3 EFFECT OF SODIUM OXIDE DOSAGE AND MODULUS ON STRENGTH OF AASCs	39
	3.4 CONCRETE MIX DESIGN	40
	3.5 SPECIMEN DETAILS	41
	3.6 MIXING, PLACING AND COMPACTING CONCRETE MIXES	41
	3.7 CURING OF SPECIMENS	43
	3.8 EXPERIMENTAL PROCEDURES	43
	3.8.1 Workability	43

3.8.2	Mechanical Properties of Concrete Mixes	43
3.8.3	Water Absorption and Total porosity of AASC Mixes	43
3.8.4	Chloride Impermeability Tests	43
3.8.5	Resistance to Sulphate Attack	44
3.8.6	Resistance to Acid Attack	44
3.8.7	Resistance to Elevated-Temperatures	45
3.8.8	Flexural Fatigue Testing Set-up	45
3.8.8.1	<i>Flexural Fatigue Test</i>	45
3.8.8.2	<i>Flexural Fatigue tests of AAS Concrete Beams</i>	46
3.8.9	Flexural tests on AAS concrete beams	47
4	STRENGTH AND DURABILITY OF ALKALI ACTIVATED SLAG CONCRETE MIXES	51
4.1	GENERAL	51
4.2	WORKABILITY	51
4.3	HARDENED PROPERTIES OF CONCRETE MIXES	52
4.3.1	Compressive Strength and Modulus of Elasticity of the Concrete Mixes.	52
4.3.2	Split Tensile and Flexural Strength of AASC Mixes	53
4.4	DURABILITY OF CONCRETE MIXES	55
4.4.1	Water Absorption and Total Porosity of AASC Mixes	55
4.4.2	Chloride Ion Penetration	56
4.4.3	Sulfate Attack Resistance Test	56
4.4.4	Sulphuric Acid Attack	58
4.5	ELEVATED-TEMPERATURE RESISTANCE TEST	61
4.6	SUMMARY	63
5	FLEXURAL FATIGUE PERFORMANCE OF CONCRETE MIXES	65
5.1	GENERAL	65
5.2	S-N CURVE	65
5.3	PROBABILISTIC ANALYSIS OF FATIGUE DATA	66
5.3.1	Graphical Method	67

5.4	STATIC FLEXURAL STRENGTHS OF AASC PRISMS	68
5.5	FLEXURAL FATIGUE BEHAVIOUR OF AASC CONCRETE PRISMS	68
5.6	PROBABILISTIC ANALYSIS OF FATIGUE TEST DATA	71
5.7	GOODNESS-OF-FIT TEST FOR FATIGUE DATA	73
5.8	PREDICTION OF FATIGUE LIFE OF AASC MIXES - APPLICATION OF WEIBULL PARAMETERS	74
6	FLEXURAL BEHAVIOUR OF REINFORCED ALKALI ACTIVATED CONCRETE BEAMS	77
6.1	INTRODUCTION	77
6.2	FLEXURAL BEHAVIOUR OF RCC BEAMS - LOAD CONSIDERATIONS	77
6.2.1	Loads at First Crack	79
6.2.2	Service Load on Beams	79
6.2.3	Ultimate Load on Beams	79
6.3	LOAD DEFLECTION BEHAVIOR - DEFLECTIONS AT MID SPAN	81
6.3.1	Span Deflection Profiles	83
6.4	MOMENT-CURVATURE RELATION FOR AASC BEAMS	84
6.5	CRACK PATTERNS	86
7	ECOLOGICAL ANALYSIS OF CONCRETE MIXES	89
7.1	GENERAL	89
8	CONCLUSIONS	93
	REFERENCES	99
	APPENDIX – I	113
	APPENDIX – II	117
	APPENDIX – III	121
	PUBLICATIONS BASED ON PRESENT RESEARCH	129
	RESUME'	131

LIST OF FIGURES

Figure No	Title	Page No
2.1	Reaction mechanism of alkali activated slag	13
2.2	Modulus of sodium silicate solution Vs 28-day strength for different types of slag	15
2.3	Typical S-N curve	26
3.1	Effect of Ms of alkaline activator on compressive strength	40
3.2	Flexural fatigue testing setup	46
3.3	Typical cross sectional details of reinforced concrete test beams*2L	48
3.4	Formwork for beam specimens	48
3.5	Reinforced concrete beam test setup-schematic	49
4.1	Split tensile strengths of AASC mixes at 28-days	54
4.2	Flexural strengths of AASC mixes	54
4.3	Water absorption of concrete mixes at 28 and 90 days	55
4.4	Total porosity of concrete mixes at 28 and 90 days	55
4.5	Comparison of chloride diffusion coefficient of concrete mixes	56
4.6	Compressive strength of AASC mixes in 10% Na ₂ SO ₄ solution	57
4.7	Compressive strength of AASC mixes in 10% MgSO ₄ solution	58
4.8	Appearance of AASC mixes in pH=1 sulphuric acid solution at 120 days	60
4.9	Weight changes of AASC mixes in H ₂ SO ₄ solution (pH=1)	60
4.10	Loss in compressive strength of AASC mixes in H ₂ SO ₄ solution(pH=1)	61
4.11	Variation in compressive strength ratio of concrete mixes with temperatures	62
4.12	Crack pattern for of concrete mixes at 800 ⁰ C	63
5.1	S-N curves for various concrete mixes	70
5.2	Graphical analysis of fatigue for ACS-100 at stress level of 0.85	72
5.3	Predicted fatigue lives corresponding to different survival probabilities for various concrete mixes	75
6.1	Midpoint deflection curve	81
6.2	Deflection profiles of beams at load at first crack, service and ultimate loads	84
6.3	Moment curvature profiles for test beams	85
6.4	Crack pattern of all test beams	86

LIST OF TABLES

Table No	Title	Page No
2.1	History of Alkali-activated cement systems and alkaline cements	11
2.2	Classification of Alkali activators	14
2.3	Deterioration mechanism of cement paste at different temperatures	22
3.1	Properties of Ordinary Portland cement used	34
3.2	Chemical composition of GGBFS used	34
3.3	Properties of coarse and fine aggregates	35
3.4	Results of sieve analysis - coarse aggregate	36
3.5	Results of sieve analysis- fine aggregates	36
3.6	Chemical composition of copper slag used	37
3.7	Properties of Superplasticizer (Conplast SP 430)	37
3.8	Properties of Liquid Sodium Silicate	38
3.9	Properties of Sodium Hydroxide (97% purity)	38
3.10	Properties of steel reinforcement bars used	38
3.11	Effect of Ms of alkali solution on compressive strength of AASC mixes	39
3.12	Details of mix designations and mix proportions of tested concrete mixes	42
3.13	Details of test specimens used for various tests	42
4.1	Workability, compressive strength and modulus of elasticity of various concrete mixes.	52
5.1	Fatigue test results for OPCC and AASC specimens	69
5.2	Relationship between fatigue cycle (N) and stress level (S)	70
5.3	Values of Weibull parameters for concrete mixes at different stress levels	72
5.4	Kolmogorov–Smirnov test of fatigue life data for ACS-0 at S=0.85	73
6.1	Test details of OPCC and AASC cubes at 28 days	78
6.2	Load at first crack, service and ultimate loads of OPCC and AASC Beams	80
6.3	Mid-span deflections of OPCC and AASC beams at different load levels	82
6.4	Ultimate moments and curvatures for test beams	85
6.5	Test result of crack profiles	87
7.1	Ecological and economic analysis of various concrete mixes	91

NOMENCLATURE

AAB	Alkali Activated Binders
AAFA	Alkali Activated Fly Ash
AAS	Alkali Activated Slag
AASC	Alkali Activated Slag Concrete
AASFC	Alkali Activated Slag-Fly Ash Concrete
A-S-H	Alumino Silicate Hydrate
ASTM	American Society for Testing and Materials
CH	Calcium Hydrate
C-S-H	Calcium Silicate Hydrate
ECO _{2e}	Embodied Carbon Dioxide Emission
EE	Embodied Energy
FA	Fly Ash
FRC	Fiber Reinforced Concrete
GBFS	Granulated Blast-Furnace Slag
GGBFS	Ground Granulated Blast Furnace Slag
HM	Hydration Modulus
HPC	High Performance Concrete
LSS	Liquid Sodium Silicate
Ms	Activator Modulus
M-S-H	Magnesium Silicate Hydrate
N	Fatigue Life
Na ₂ O	Sodium Oxide
NaOH	Sodium Hydroxide
OPC	Ordinary Portland cement
OPCC	Ordinary Portland Cement Concrete
RHA	Rice Husk Ash
R-A-S-H	Alkaline Alumino-Silicate system(R =Na or K)
R-C-A-S-H	Alkaline- Alkaline Earth system
RTPS	Raichur Thermal Power Station
SCRC	Self Compacting Rubberized Concrete
SF	Silica Fume
SFRC	Steel Fibre Reinforced Concrete
SR	Stress Ratio
VPV	Volume of Permeable Voids
w/b	Water to Binder Ratio

CHAPTER 1

INTRODUCTION

1.1 GENERAL

Concrete is one of the most basic and critical component for any type of construction and plays an important role in building the nation's infrastructure. Concrete is a composite material which is composed of coarse and fine aggregates embedded in a matrix and bound together by a binder which fills the space or voids between the aggregates and bonds them together (Mindess et al. 2003). Basically concrete is a mixture of a binder, water, aggregates and additives. The binder generally used for concrete production is Ordinary Portland Cement (OPC), which is mainly responsible for mechanical strength of concrete.

Climate change is one of the most important environmental problems faced by Planet Earth. This is due to the increase of carbon dioxide (CO₂-eq) in the atmosphere for which the built environment is a significant contributor. While in the early eighteenth century, the concentration level of atmospheric CO₂-eq was 280 parts per million (ppm), as at present it is already 450 ppm. Keeping the current level of emissions (which is unlikely to reduce, given the high economic growth of less-developed countries with consequent increases in emission rates) will imply a dramatic increase in CO₂-eq concentration to as much as 731 ppm by the year 2130 leading to a global warming of about 3.7⁰C above pre-industrial temperatures (Han et al. 2015).

The cement industry is responsible for about 7% (and it is rising!) of the world's total CO₂ generation and the production of cement is also a highly energy intensive process (Mehta 2001). It is claimed that the production of one ton of cement leads to a carbon dioxide (CO₂) emission in the range 0.8-1.3 ton along with energy consumption in a higher range 100-150 kWt (Rajamane 2013).

India ranks second in the world amongst the cement and iron producing (and consuming) countries, next only to China. The cement industry of India has a current capacity of 324 Million Tonnes Per Annum (MTPA) and is expected to add

30-40 MTPA of capacity in the next few years. To produce this huge quantity of cement, large quantities of naturally occurring, however non-renewable, materials like limestone, chalk, and clay are to be mined and processed every year. With the dominant use of carbon-intensive fuels like coal in clinker making, the increasing cost of fuels and raw materials in the recent years has been reflected in correspondingly raising cost of cement. Moreover the mining of limestone which is one of the main raw materials for cement production has impact on the land use patterns, hydrology of local water bodies and ambient air quality. Dust emissions from the cement industry also have affected the ambient air quality.

Of course, of late, the cement industry is making sustained efforts to improve and develop better cement production technologies and process efficiency in order to reduce the CO₂ emissions. However, further improvements may be limited as CO₂ generation is inherent and inevitable during the basic process of calcinations of limestone.

A recent forecast estimates that by 2030, urban land cover will increase by 1.2 million km² (equivalent to an area about the size of South Africa). This will be concomitant with an enormous infrastructure boom in road construction, water and sanitation, energy and transport, and buildings (Seto et al. 2012).

Considering the crucial importance of infrastructure development for India and other emerging countries, the demand for cement production has increased rapidly, which have led to increased concerns on the environmental aspects involved in the use and production of concrete. Under these circumstances, an eco-friendly and sustainable development is the need of day which in turn demand developing newer concrete technologies which consume lower natural resources, have lower energy demands and generate less CO₂ without compromising on the strength and durability properties. Eco-friendly technologies and effective management of natural raw materials is necessary to counter the ill-effects occurring from concrete production. It is essential to find methods to make the concrete industry more sustainable by using appropriate replacements for concrete constituents; e.g. Ordinary Portland Cement (OPC) and the

aggregates. It is now believed that, using more durable and less energy-intensive construction materials is inevitable for the construction industry.

In the context of increased awareness to reduce the production of OPC, the concrete research community initially focused, with good success, on the possible use of industrial waste materials such as Fly Ash (FA), Ground Granulated Blast Furnace Slag (GGBFS) etc., as partial replacements to OPC. Subsequently, as of now, newer techniques like Alkali Activated Slag (AAS), Alkali Activated Slag-Fly Ash (AASF), Geo-polymers etc., which involve the complete replacement of OPC based binders are being explored. Alkali activated slag or slag-flyash based binders are being researched as definite alternatives to conventional OPC-based concrete mixes, leading to significant reduction in the use of OPC in the construction industry (Rashad et al. 2012). Along with reduced emission of CO₂ and consumption of energy in their manufacture, the alkali activated binders are also shown to exhibit superior mechanical properties than OPC binders (Morsy et al. 2008). However, technical and economic viabilities of alkali activated slag binder systems is still a topic of recent research endeavors.

Again production of concrete also requires about 60 to 80% of natural aggregate like crushed rock for coarse aggregate; and sand quarried from river beds as fine aggregates. Their increased consumption again stresses the environment (Anurag et al. 2012).

Sand is a very important ingredient for cement mortar and concrete for new constructions and repair works, its prices increasing continuously due to huge demand and such increases in the price leading to more and more sand mining. In nature, the layers of sand have triple roles to play - (i) of supporting the (mangrove) vegetation which protects the riverbeds and hence the length and breadth of river flow (ii) filtering and controlling the water flow rates which in turn provide good environment for aquatic life to grow and flourish, and (iii) re-charging of groundwater as sand particles hold water and also allow lateral and vertical flow of water to neighboring wells. As the demand for sand has increased, mining from the riverbeds has increased, changing their hydrologies - both surface and ground-water flows, and

affecting the aquatic life they are supporting and the yields from the filter point-wells drilled in the river bed, open wells and bore wells constructed along the riparian area.

Thus continued use of river sand as the fine aggregate fraction in concrete-making has started posing serious problems with respect to its availability, cost and environmental impact. This has led to a necessity of looking at substitutes or replacements for river sand for use in concrete industry. Numbers of alternatives are being tried including quarry dust, bottom ash, pelleted fly-ash, coarse blast furnace slags, spent foundry sand and laterite fines etc., Copper Slag (CS) is one such economic alternative being explored for possible use as fine aggregate in concrete mixes. CS is produced during pyro-metallurgical production of copper from copper ores and contains constituents like iron, alumina, calcium oxide and silica etc. For every ton of copper metal produced, about 2.2-3 ton of copper slag is generated. While its addition to fresh concrete would decrease the water demand and consequently the cement content for a given workability and strength requirements, leading to further savings in cost. Obviously the material cost involved in incorporation of the copper slag will vary depending on the source.

While there are previous research studies, though limited, on the effect of addition of copper slag, as fine aggregates, on the properties of conventional concrete mixes, the use of CS as fine aggregate in alkali activated concrete mixes has not been investigated to date. CS incorporated AASC is a new construction material made using two industrial by-products, GGBFS, a byproduct from the iron-making industries as binder and CS a byproduct from copper industry as the fine aggregate. It is a “greener concrete” as it does not use Portland cement clinker; Use of CS in concrete-making decreases the load on the natural sand reserves and its self-curing properties lead to savings in water which is of great advantage especially in regions with severe scarcity of water resources. The present research report documents the results of detailed experimental studies on performance of Alkali Activated Slag Concrete (AASC) mixes made with CS as fine aggregate.

1.2 OBJECTIVES OF THE PRESENT RESEARCH

In the present research work a detailed experimental investigation is aimed to address the performance characteristics of AASC mixes incorporating copper slag as partial/complete replacement to fine aggregate. The main objectives of the present research work are identified as follows:

- Evaluation of strength performance of AASC mixes with copper slag as fine aggregate.
- To study the durability performance of AASC with copper slag as fine aggregate in chloride, sulphate and acid rich environments.
- To investigate the effect of elevated temperatures on strength performance of AASC mixes with copper slag as fine aggregate.
- To study the flexural fatigue performance of AASC mixes incorporating copper slag as fine aggregate.
- Evaluation of the flexural performance of reinforced AASC beams incorporating copper slag as fine aggregate.

Thus, this research focuses on evaluation of the feasibility of utilizing larger amounts of copper slag as fine aggregate in AASC mixtures.

1.3 SCOPE OF WORK

AASC mixes were designed to attain a minimum strength of M45 and compared with a conventional OPC concrete mix of similar grade. AASC mixes were prepared with 100% GGBFS as sole binder. Preliminary tests were carried out to identify the optimal activator modulus and dosage of alkaline activators for each of the AASC mixes. Copper slag as fine aggregates were incorporated in the AASC mixes by replacing the natural fine aggregates by absolute volume replacement method at different levels of replacement, i.e. 0%, 25%, 50%, 75% and 100%. The fresh and hardened properties such as workability, compressive strength, split tensile strength, flexural strength, and modulus of elasticity of different concrete mixes was evaluated as per standard test procedures. The durability of concrete mixes in terms of resistance to sulphuric acid, magnesium sulphate, sodium sulphate, water absorption and volume of permeable voids are investigated. Also the performance of concrete mixes exposed

to elevated temperatures is studied in detail. Flexural fatigue performance of various concrete mixes is determined by carrying out repeated load tests on beam specimens using repeated load testing equipment. The fatigue life data obtained are represented and analyzed using S-N curves to establish fatigue equations. Probabilistic analysis of fatigue data is carried out using two parameter Weibull distribution methods. Further, goodness-of-fit test is done to ascertain the statistical relevance of the fatigue data using Weibull-distribution model. Survival probability analysis to predict the fatigue lives of concrete mixes with a required probability of failure is carried out. The flexural behavior of reinforced AASC beams with copper slag as fine aggregates are evaluated. The ecological and economical benefits of AASC mixes in comparison with conventional OPC concrete are analyzed and discussed.

1.4 ORGANIZATION OF THESIS

This thesis is organized into eight chapters followed by the list of references and Appendixes.

CHAPTER 1

Gives brief note on alkali activated slag and copper slag; need and significance, objectives and scope of the research.

CHAPTER 2

A comprehensive literature review has been carried out to collect adequate information about alkali activated binders, copper slag and other materials. Information gathered about the research works carried out so far on mechanical, durability properties, flexural fatigue and reinforced concrete beams studies of alkali activated slag, copper slag is also presented.

CHAPTER 3

This chapter provides the details of various materials, preliminary investigations, tests carried out, test methodology adopted optimization design parameters of concrete mixes.

CHAPTER 4

This chapter presents the results and discussions on the mechanical properties of concrete mixes, durability tests carried out on AASC mixes with sand/CS in detail,

strength characteristics of AASC mixes with sand/CS on exposure to elevated temperature.

CHAPTER 5

This chapter deals with the detailed discussions of results of fatigue tests conducted on AASC mixes with sand/CS carried out at various stress levels. A probabilistic analysis is carried out on the fatigue data of the concrete mixes.

CHAPTER 6

This chapter presents the results and discussions of flexural performance of reinforced AASC mixes with sand/CS.

CHAPTER 7

The ecological and economical benefits of AASC with sand/CS aggregates are studied and the results are presented in this chapter.

CHAPTER 8

Observations and conclusions drawn based on the investigation; recommendations and scope for the future study are presented in this chapter.

CHAPTER 2

LITERATURE REVIEW

2.1 GENERAL

Alkali Activated Binders (AAB) are the new generation binders which use an alkali rich, clinker-free binder matrix such as Alkali Activated Slag (AAS), Geopolymers, Alkali Activated Slag-Fly ash (AASF) etc., (Puertas 1995). AABs are generally produced by activating the natural minerals or industrial wastes like Ground Granulated Blast Furnace Slag (GGBFS), Fly Ash (FA), Metakaolin (MK), Silica Fume (SF) etc., which are primarily rich in calcium, aluminosilicates and silica, using alkaline solutions (Bernal et al. 2011). The alkali ions are used to release the latent cementitious properties of finely divided inorganic materials (Jiang 1997).

The activation and synthesis of AAS and geo-polymers are quite similar; however they vary widely in their reaction products (Palomo et al. 1999). Amorphous hydrated alkali aluminosilicate is the major reaction product formed in a geopolymer; while Calcium Silicate Hydrate (C-S-H) with low Ca/Si ratio is formed in AAS (Glukhovskiy 1959, Duxson et al. 2007). Studies carried out by researchers like Puertas et al. (2000), claim that the main product formed in AASF to be C-S-H with no existence of Alumino Silicate Hydrate (A-S-H); while others (Chi and Huang 2013) have reported the co-existence of both. Idawati et al. 2013 have found C-A-S-H phase and hybrid C-(N)-A-S-H phases also in smaller quantities.

The raw materials used for the production of AAB's may be classified as pozzolanic or latent hydraulic materials (Caijun and Della 2006). Pozzolans are the materials rich in silica and alumina, possess little or no cementitious properties by themselves, but in finely divided form and in the presence of moisture, undergo chemical reaction with calcium hydroxide at ambient temperatures to form compounds having cementing properties (Malhotra and Mehta 1996). Low calcium (class F) fly ash and silica fume are the most widely used pozzolanic materials. Latent hydraulic materials are finely divided materials similar to pozzolans, which contain sufficient amount of calcium to form compounds with cementitious properties after reacting with water. In general, the latent hydraulic materials cannot undergo direct setting and hardening after

reacting with water in normal conditions. The hardening energy is quiescent and requires an activator such as calcium hydroxide or some other strong alkaline compound to release the cementitious properties. The latent hydraulic materials when blended with Portland cement and water get activated under the influence of calcium hydroxide which is generated during the hydration reaction of cement (Jiang 1997). GGBFS is one of the examples of latent hydraulic materials. Both the pozzolans and latent hydraulic materials may be naturally occurring in nature or may be produced artificially from industrial processes.

2.2 BRIEF HISTORY OF ALKALI ACTIVATED BINDERS

Purdon (1940) carried out extensive laboratory study on clinker-free cements which consisted slag as the binder and caustic alkalis produced by a base and an alkaline salt. Glukhovskiy (1959) discovered a new group of binders which included both of low basic calcium or calcium-free aluminosilicate and alkali metal solutions which were termed “soil cements” and the corresponding concretes termed as “soil silicates”. In 1979, Davidovits developed new group of binders produced by combining sintering products of kaolinite and limestone or dolomite as the aluminosilicate constituents and called those binders as “geopolymers” due to the presence of a polymeric structure. Davidovits (1994) proposed that any source, either from natural geological origin or an industrial by-product material such as fly ash, rice husk ash etc, which are rich in silica and alumina can be activated using highly alkaline liquids solutions. The classification of alkali activated binders based on their chemical composition and characterization of hydration products was done by Krivenko (1994).

The alkaline aluminosilicate systems (R-A-S-H, where R=Na or K) were called “geo-cements”, whose formation process is similar to geological process of natural zeolites and alkaline-alkaline earth systems (R-C-A-S-H) in which the products of hydration included the formation of calcium silicate hydrates i.e. C-S-H with low Ca/Si ratio. Pacheco-Torgal et al. (2008) suggested the use of the term ‘geo-polymer’ in alkali activated cementitious materials only if there is a presence of a zeolite-like phase with amorphous to semi-crystalline characteristics.

The important historic developments of alkali activated binders are summarized by Roy (1999) as shown in Table 2.1.

**Table 2.1 History of Alkali-activated cement systems and alkaline cements
(Roy 1999)**

Author(s)	Year	Significance
Feret	1939	Slags used for cement
Purdon	1940	Alkali-slag combinations
Glukhovskiy	1959	Theoretical basis and development of alkaline cements
Glukhovskiy	1965	First called "alkaline cements" because natural substances used as components
Davidovits	1979	"Geopolymer" term—emphasizes greater polymerization
Malinowski	1979	Ancient aqueducts characterized
Forss	1983	F-cement (slag-alkali-superplasticizer)
Langton and Roy	1984	Ancient building materials characterized (Roman, Greek, Cyprus)
Davidovits and Sawyer	1985	Patent leading to "Pyrament"
Krivenko	1986	D.Sc. Thesis, $R_2O-RO-R_2O_3-SiO_2-H_2O$
Malolepsy and Petri	1986	Activation of synthetic melilite slags
Malek et al.	1986	Slag cement-low level radioactive waste forms
Davidovits	1987	Ancient and modern concretes compared
Deja and Malolepsy	1989	Resistance to chlorides shown
Kaushal et al.	1989	Adiabatic cured nuclear waste forms from alkaline mixtures including zeolite format
Roy and Langton	1989	Ancient concrete analogs
Majumdar et al.	1989	$C_{12}A_7$ - slag activation
Talling and Brandstetr	1989	Alkali-activated slag
Wu et al.	1990	Activation of slag cement
Roy et al.	1991	Rapid setting alkali-activated cements
Roy and Silsbee	1992	Alkali-activated cements: overview
Palomo and Glasser	1992	CBC with metakaolin
Roy and Malek	1993	Slag cement
Glukhovskiy	1994	Ancient, modern and future concretes
Krivenko	1994	Alkaline cements
Wang and Scrivener	1985	Slag and alkali-activated slag microstructure

The field of alkali activated binders has witnessed further contributions from many researchers (Wang et al.1994, Palomo et al.1999, Bakharev et al. 2000, Puertas et al. 2000, Fernández-Jiménez and Puertas 2001, Shi et al. 2006, Pacheco-Torgal et al. 2008, Bernal et al. 2010, Idawati et al. 2013, Rashad 2013a and b).

2.3 GROUND GRANULATED BLAST FURNACE SLAG (GGBFS)

Granulated Blast-Furnace Slag (GBFS), a by-product from iron and steel industry, is a granular material which is produced by quenching the molten blast furnace slag rapidly with water. When this granular GBFS is ground to a fine powder, it is called Ground Granulated Blast-Furnace Slag (GGBFS). It mainly consists of oxides of calcium (CaO), silica (SiO₂), alumina (Al₂O₃)and magnesia (MgO) along with some other minor oxides like SO₃, FeO or Fe₂O₃, TiO₂, K₂O, Na₂O, etc., in small quantities.

GGBFS is probably the most widely investigated, and the most effective supplementary cementitious material used in concrete manufacturing.

The hydraulic activity of GGBFS can be quantified in terms of its basicity coefficient (K_b) which is the ratio between total content of basic constituents to total content of acidic constituents, as given in the equation (2.1) (McGannon 1971).

$$K_b = \frac{CaO + MgO + Fe_2O_3 + K_2O + Na_2O}{SiO_2 + Al_2O_3} \quad (2.1)$$

The equation for calculation of basicity coefficient was further simplified by excluding minor components such as Fe_2O_3 , K_2O , and Na_2O (less than 1%) in the GGBFS (Wang et al. 1994, Bakharev et al. 2000).

$$K_b = \frac{CaO + MgO}{SiO_2 + Al_2O_3} \quad (2.2)$$

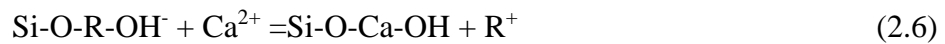
Based on the basicity coefficient (K_b), the GGBFS is classified into three groups as under i.e. Acid ($K_b < 1$), neutral ($K_b = 1$), and basic ($K_b > 1$). Neutral and alkaline slags are preferred as starting materials for activation in AAS binders. Chang (2003) introduced a parameter termed as Hydration Modulus (HM) given in equation 2.3 and suggested that it should be greater than 1.4 in order to ensure good hydration properties.

$$HM = \frac{CaO + MgO + Al_2O_3}{SiO_2} \quad (2.3)$$

2.4 ACTIVATION MECHANISMS OF ALKALI ACTIVATED SLAG

In the activation process of slag (GGBFS), the reaction begins with the attack of alkalis on slag particles thus breaking the outer layer and then continues as poly-condensation of reaction products. The initial reaction products are formed due to the process of dissolution and precipitation. At later stages, however, a solid state mechanism is followed, where the reaction occurs on the surface of formed particles dominated by slow diffusion of the ionic species into the unreacted core

(Wang et al.1994). In the initial stages of hydration, alkali cation (R^+) behaves like a mere catalyst in the cation exchange with the Ca^{2+} ions for the reaction as shown in the following equations (Glukhovsky 1994, Krivenko 1994).



While the alkaline cations act as structure creators, the anions in the solution play a significant role in activation, especially during the early stages, particularly with regard to paste setting (Fernández-Jiménez and Puertas 2001). A descriptive model showing the reaction mechanism is presented in Figure 2.1. The final hydration products in case of activation of slag are similar to the products of OPC hydration i.e. Calcium-Silicate-Hydrate (C-S-H), but with low Ca/Si ratio. However the rate and intensity of activation of slag differ substantially as compared to that hydration of OPC. It is reported that the alkalis are not freely available in the pore solution since they are bound to the reaction products thereby negating the potential for alkali-silica reactivity; however this depends on the concentration of alkali used.

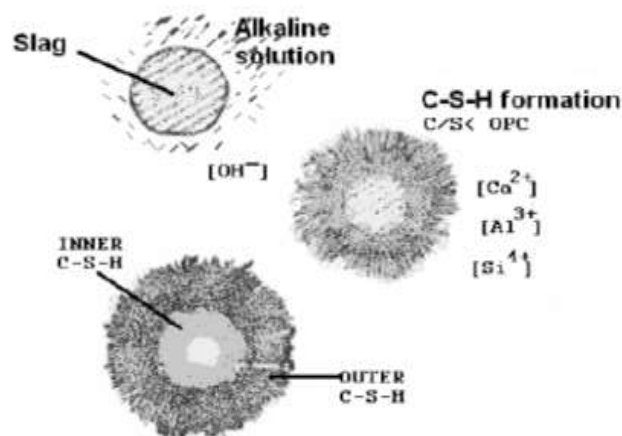


Fig 2.1 Reaction mechanism of alkali activated slag (Fernandez-Jimenez and Puertas 2001).

2.5 EFFECT OF TYPE, DOSAGE, AND MODULUS OF ALKALINE ACTIVATORS ON ALKALI ACTIVATED SLAG

The source materials for alkali activated slag binders need to be activated using strong alkalis in order to form the resulting binding material. Caustic alkalis or alkaline salts are the most widely used alkaline activators. The alkaline activators are classified into six groups based on their chemical compositions and are tabulated in Table 2.2.

Table 2.2 Classification of Alkali activators (Fernandiz-Jimenez et al. 2005)

Type of Alkali Activator	Chemical Formula
Hydroxides	MOH
Non-silicate, Weak acid salts	M ₂ CO ₃ , M ₂ SO ₃ , M ₃ PO ₄ , MF
Silicates	M ₂ O · nSiO ₂
Aluminates	M ₂ O · nAl ₂ O ₃
Alumino-silicates	M ₂ O · Al ₂ O ₃ · (2-6)SiO ₂
Non-silicate, Strong acid salts	M ₂ SO ₄

In the above chemical formulae, M stands for Alkali Metal ion

The alkaline activators generally consist of mixtures of silicates and hydroxides of alkali metals. Sodium silicate (Na₂SiO₃), sodium hydroxide (NaOH), sodium carbonate (Na₂CO₃) or a mixture of sodium or potassium hydroxide (NaOH, KOH) with sodium silicate or potassium silicate respectively or any other combinations are most widely used as alkaline activators. A combination of sodium hydroxide with sodium silicate has been shown to provide the best strength performance for activation of alkali activated binders (Rashad 2013a). The strength of alkali activated slag is governed by the type of alkaline activator, activator modulus and dosage of alkaline activator (Fernandez-Jimenez et al. 1999). The Activator Modulus (Ms) is the ratio of mass ratio of SiO₂ to Na₂O components present in the alkaline activator, while the Dosage (usually referred as %Na₂O) is the total sum of mass of Na₂O present in the alkaline activator (mass of Na₂O present in sodium silicate + mass of Na₂O equivalent in sodium hydroxide, if a combination of sodium silicate and sodium hydroxide is used as the alkaline activator).

Wang et al. (1994) reported that mechanical strength and other properties of AAS mortars are influenced by the nature of the alkaline activators. The dosage and the activator modulus have significant effects in activators containing either sodium silicate or a blend of sodium silicate and sodium hydroxide. They provided a range of activator modulus depending upon the type of GGBFS within which the maximum compressive strength may be obtained.

- a) Acid slag - (M_s - 0.75 to 1.25),
- b) Neutral slag - (M_s - 0.90 to 1.3) and
- c) Basic slag - (M_s - 1.0 to 1.5)

Figure 2.2 presents the variation of 28-day strength with activator modulus for different types of GGBFS. It may be noticed that the strength increases with activator modulus till an optimal activator modulus is reached, however, with further increase in the activator modulus, the strength decreases.

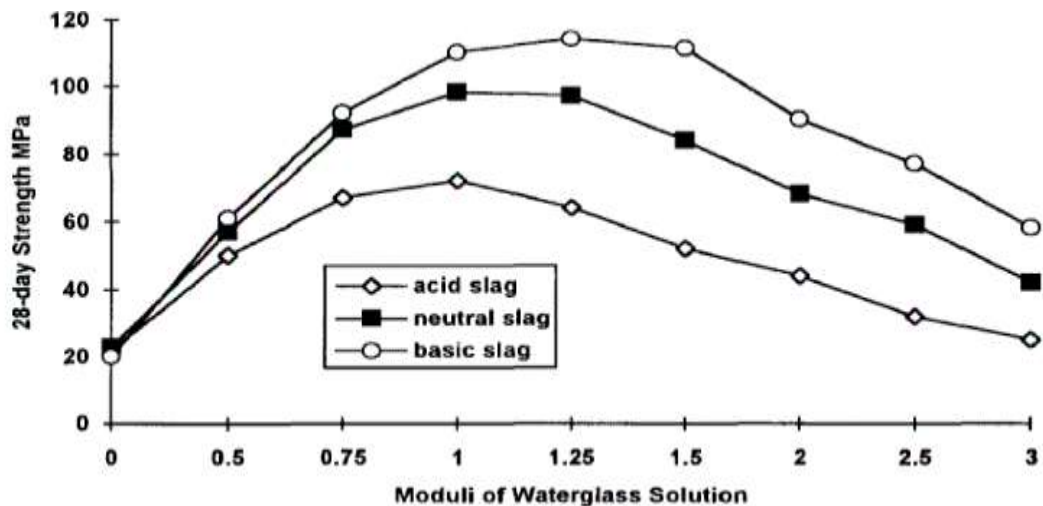


Fig 2.2 Modulus of sodium silicate solution Vs 28-day strength for different types of slag (Wang et al. 1994).

Bakharev et al. (1999) investigated the activation of Australian GGBFS using different activators such as sodium silicate, sodium hydroxide, sodium carbonate, sodium phosphate, and combinations of these activators and recommended sodium silicate solution with 5% Na_2O dosage with 0.75 activator modulus for better results. Fernandez-Jimenez et al. (1999) reported that the mechanical strength of AAS mortars

are mostly influenced by the type and nature of alkaline activator, dosage of alkaline activator and observed that optimum dosage of alkaline activator varies in the range 3% and 5.5 % of Na₂O by mass of GGBFS. Na₂O dosage above this limit may cause efflorescence problems along with inefficient, uneconomical mixtures.

It has been shown that ultimate strength higher than Portland cement can be achieved with GGBFS cements activated using sodium silicate with modulus between 0.6 and 1.5 with appropriate Na₂O dosages (Krizan and Zivanovic 2002). Cengiz et al. (2009) investigated the AAS mortars using different types of activators (sodium hydroxide, sodium carbonate and sodium silicate, with varying activator modulus and with Na₂O dosages in the range 4-8% (mass of GGBFS). They concluded that the compressive and tensile strengths of AAS mortars increased with Na₂O dosage of alkaline activators and also suggested that there exists an optimal alkaline modulus for which the highest compressive and tensile strengths can be obtained. Chi (2012) also has reported that the mechanical and durability properties of AASC mixes were significantly dependent on Na₂O dosage of the alkaline activators. Ravikumar and Neithalath (2013) observed that increasing the modulus of the activator beneficially influences the transport parameters of liquid sodium silicate activated slag concretes.

2.6 MECHANICAL PROPERTIES OF ALKALI ACTIVATED SLAG CONCRETE MIXES

The mechanical properties of AAS concrete mixes are influenced by various parameters such as type and nature of alkaline activators, Na₂O dosage and activator modulus, curing regime, water to binder ratio, chemical admixtures etc., Various studies have reported that the AAS concretes display similar or better mechanical properties as compared to OPC concretes. Collins and Sanjayan (1999) investigated AAS concrete mixes with an emphasis on achieving reasonable workability and equivalent one-day strengths as compared to OPC concrete under normal curing temperatures and concluded that AAS concrete displayed similar one-day strength and superior ultimate strengths as compared to OPC concrete. Sakulich et al. (2009) reported that AAS concretes achieved compressive strengths upto 45MPa and flexural strength upto 4MPa when cured for 28 days under normal room temperatures.

Ravikumar et al. (2010) reported that the activator concentration has a larger influence on the compressive strengths of activated concretes made using fly ash and the activator to binder ratio influences the compressive strengths of activated GGBFS concretes to a greater degree. Bernal et al. (2010) studied the mechanical properties of AAS concrete reinforced with steel fibers at early ages and concluded AAS concrete to be a potential building material with or without steel fibers. Bernal et al. (2011b) also studied the effect of binder content on the strength performance of AAS concretes and reported that regardless of the binder content, AAS concretes developed higher compressive strengths as compared to conventional OPC concrete; however higher binder content led to increase in strength in both AASC and OPCC at 28 days. The use of AAS concrete mixes is, however, associated with certain problems such as high shrinkage and poor workability which impede its large scale practical application (Bakharev et al. 2000).

Investigations on the use of chemical admixtures to overcome such problems related to high shrinkage and poor workability have been carried out by researchers. They have also investigated the effect of use of various chemical admixtures which were used for OPC concrete such as super-plasticizers based on modified naphthalene formaldehyde polymers, air-entraining agents, water-reducing admixtures, shrinkage-reducing admixtures (at dosages of 6±10 ml/kg), and gypsum (6% of slag weight) on AAS mixes. It has been observed that with the use of air-entraining agent, shrinkage-reducing admixtures and gypsum, the shrinkage in AAS concrete mixes got reduced significantly. While the naphthalene based superplasticizer significantly increased the shrinkage and reduced the strength of AAS concrete, use of an air-entraining agent improved the workability without any negative effects on the compressive strength and its use was recommended in AAS concrete. Similar observations were made by several other researchers as well (Douglas and Brandstetr 1990, Wang et al. 1994).

2.7 EFFECT OF CURING REGIME ON THE MECHANICAL PROPERTIES OF AAS CONCRETE MIXES

The properties of AAS mixes are affected considerably with the curing conditions to which they are subjected. Over the years, the properties of AAS mixes have been studied by subjecting the AAS mixes to different curing conditions such as conventional water curing, normal room temperature curing, heat curing and steam curing etc. Altan and Erdogan (2012) studied AAS mortar mixes activated using combination of sodium silicate and sodium hydroxide, at both room temperature and at elevated temperatures. They observed that the heat cured samples gained strength rapidly, however samples cured at room temperature also gained comparable strengths with time. It was also reported that the total heat evolution during hydration of AAS mixes was lesser compared to hydration of OPC mixes and lower water to binder ratio also provides higher strengths at early ages. Aydın and Baradan (2012) reported that high strength mortars with strengths upto 70 MPa can be produced with alkaline activators having alkali content as low as low 2% (by mass of binder) when subjected to autoclave curing. They also observed that AAS mixes provided similar performance as compared to autoclave curing when activated using activator solutions with high activator modulus. Bilim et al. (2015) investigated the AAS mixes with 4 to 6% Na₂O dosages, to study the effect of curing conditions on AAS mixes and reported that curing conditions affected the mechanical behavior of AAS mixes as compared to OPC mixes. The AAS mixes attained higher early strength as compared to OPC mixes when subjected to elevated temperatures.

2.8 DURABILITY OF ALKALI ACTIVATED SLAG CONCRETE MIXES

Concrete is inherently a durable material. Concrete is well known for its strength, ease of production, water tightness and durability properties. However, durability becomes an important issue when concrete is exposed to aggressive environments. Concrete mixes are susceptible to chemical attack in a variety of exposure conditions unless some precautions are taken. The aggressive environments may include natural environments such as in sea waters, acid rains, soils rich in sulphates etc., or man-made such as exposure to chemical effluents from industries, waste waters from

drainage systems etc., which affect the long term performance of concrete elements. Concrete undergoes degradation under the influence of such aggressive environments due to chemical processes involving exchange of ions, thus causing changes in the microstructure of the binding matrix leading to reduction in the mechanical strength.

The cement paste is affected by the presence of acids, sulphates etc., in the surrounding environments. The durability of concrete subjected to chemical attacks such as acids and sulphates are still the aspects of concern. Due to the presence of high calcium compounds in its chemical composition, the resistances of OPC based concrete to acids and sulphates are low. The acids and sulphates usually attack the products of hydration of cement to form products such as gypsum and ettringite along with changes in the C-S-H micro-structure. The formation of these expansive products leads to higher internal stresses which lead to the deterioration of the concrete. Properties of concrete mixes such as water absorption, total porosity and sorptivity are related to the ability of water or fluid to move into mortar and concrete and therefore have significant importance in the durability related properties of concrete structures. Water may enter into the concrete through capillary action of the pore systems. The water so available, in the presence of oxygen, may initiate the corrosion of steel reinforcements in reinforced concrete structures. However, better durability properties of Ordinary Portland Cement Concrete (OPCC) have been reported, with addition of pozzolanic materials such as FA, GGBFS etc. in the binder systems (Gambhir 2004).

Detailed studies on the durability properties of alkali activated binders have been carried out by several researchers (Bakharev 2005, Fernandez-Jimenez et al. 2007, Pacheco-Torgal et al. 2012, Rajamane 2013). The AAS and AASF systems have exhibited better durability properties when exposed to aggressive environments (Duxson et al. 2007). The better durability properties of AAS and AASF based concrete mixes are mainly due to the absence of calcium hydroxide in the reaction products (Bakharev et al. 2002). The durability properties of alkali activated binders are affected by various parameters such as type and concentration of the alkaline activator, activator modulus, binder type, fineness, curing conditions, water/binder ratio, use of admixtures, fibers etc., (Palacios and Puertas 2005, Rodriguez et al. 2008,

Hafa et al. 2011). The mechanisms of sulphate attack on OPC, AAS and AASF systems are expected to be different from one another due to differences in the binder chemistry, reaction products, large differences in the amount and the roles played by calcium ions in these systems (Bakharev et al. 2003). Bakharev et al. (2002) studied in detail the sulphate resistance of AAS systems and reported that AAS samples did not expand, however they showed visible cracks and traces of gypsum. Increase in the strength of AAS and AASF concrete samples have been reported when immersed in sodium sulphate solution due to the ongoing binder formation reactions; however strength decreased when immersed in magnesium sulphate solution (Bakharev et al. 2002). Varaprasad (2006) reported that ambient-cured alkali activated binder mixes containing both fly ash and GGBFS, blended in proper proportions, as source materials can attain excellent durability properties. Rajamane et al. (2013) investigated resistance of AAS and AASF mixes in sulphuric acid. They reported that both AAS and AASF concretes, when immersed in 2% and 10% sulphuric acids, displayed reduced losses in weight, thickness and strength as compared to Portland pozzolana cement concrete. Chi (2012) investigated the effect of Na₂O dosage and curing conditions on the sulphate attack resistance of AAS concrete and concluded that durability in terms of resistance to sulphate attack improved with increase in dosage of Na₂O and also stated that AAS concrete cured at 60⁰C displayed the best durability performance followed by air curing and limewater curing. Chi and Huang (2013) have reported reduction in the water absorption with increasing GGBFS and decreasing FA content in AAS/AASF concrete mixes.

2.9 EFFECT OF ELEVATED TEMPERATURE ON THE STRENGTH OF AAS CONCRETE MIXES

The human life and assets are enormously affected by uncontrolled fire incidents especially with fire incidents occurring in underground constructions which result in severe damage putting several lives at risk. (Sakkas et al. 2013). Besides this, uncontrolled fire accidents lead to considerable damage to physical structures (Khoury 1992, Phan 2008, Sakkas et al. 2013). Every civil engineering structure generally consists of two important components i.e. concrete and steel. Although, concrete is incombustible, it undergoes severe damages in the form of spalling,

degradation of mechanical strength etc., during fire accidents. Such damages are mainly due to impulsive release of huge amounts of heat and aggressive fire gases. The phenomenon of concrete spalling and reduction of concrete strengths generally occur after being exposed to temperatures beyond 300⁰C (Sakkas et al. 2013).

The resistance to degradation of OPC concrete when exposed to elevated temperatures are dependent on the type of constituent material. Hardened cement paste is the least stable constituent in concrete when exposed to elevated temperatures. At elevated temperatures, beyond 400⁰C or so, both chemical and physical properties display deteriorations which are due to loss of interlayer and chemically bound water occurring during the decomposition of Calcium Hydroxide (CH) and Calcium Silicate Hydrate (C-S-H) (Seleem and Rashaad 2011). Such decompositions are associated with consequent increase in volume that occurs during cooling, due to rehydration of calcium oxide accounting to a volume increase by about 44%, and thus leading to severe cracking (Bazant and Kalpan 1996, Handoo et al. 2002). The severity of deterioration is dictated by the mineralogy and porosity of aggregates used (Hosny and Abu 1994). It is further suggested that strength degradation, the cracking and softening phenomena in concrete surface, when exposed to fire, is due to the expansion which is followed by shrinkage of OPC paste on account of conversion of calcium hydroxide to calcium oxide in the temperature range of 450⁰C- 500⁰C, the degradation of calcium oxide being an expansion reaction. (Petzold and Röhrs 1970, Georgali and Tsakiridis 2005). In addition to all these, there is reduction in the load carrying capacity of concrete structures due to explosive spalling which occurs at temperatures between 480⁰C and 510⁰C (Chan et al. 1999). The following effects, as detailed in Table 2.3 occur, in that order, when cement paste is exposed to elevated temperatures (Özge et al. 2008).

Studies carried out by researchers have reported improved mechanical properties of concrete exposed to elevated temperatures with partial replacement of OPC with GGBFS (Sullivan and Sharshar 1992, Poon et al. 2001, Xiao et al. 2006). In a study carried by Wang (2008) by replacing 80% OPC with GGBFS with a low water/binder ratio of 0.23, it was observed that the compressive strength improved along with reduction in the cracking at elevated temperatures.

Table 2.3 Deterioration mechanism of cement paste at different temperatures (Özge et al. 2008).

Capillary and gel water evaporate	100-150 ⁰ C
Shrinkage and cracking accompanied by a tensile strength reduction	150-250 ⁰ C
Evaporation of chemically bound water from aluminous and ferrous constituents with the beginning of compressive strength reduction	250-300 ⁰ C
CH dehydrates to calcium oxide with an accompanying 44% volume reduction along with strength reduction	400 ⁰ C
Decomposition of C-S-H with significant strength reduction	600 ⁰ C

There is limited literature available on the study of effect of elevated temperatures on the behavior of AAS concrete mixes. AAS concrete mixes activated using sodium hydroxide are reported to have retained upto 25% of their original strength after exposure to 800⁰C as in the case of OPC concrete (Jumppanen et al. 1986). Mejía de Gutierrez et al. (2004) concluded that residual strength characteristics of AAS exposed up to 1000⁰C were similar to OPC regardless of the activator type used and suggested that decalcification of C-S-H led to strength decrease as in OPC-based concrete. AAS mortars activated by sodium silicate were tested for thermal properties by Zuda et al. (2007) by exposing specimens to elevated temperatures up to 1200⁰C and it was concluded that AAS mortars have a great potential for use in high temperature applications. Guerrieri et al. 2009 reported that the residual compressive strengths of slag concrete activated by sodium silicate powder and hydrated lime were approximately 76, 73, 46 and 10% of their original compressive strength when exposed to 200, 400, 600 and 800⁰C respectively.

Studies carried out by various researchers (Cheng and Chui 2003, Guerrieri et al. 2010) have reported better stability of AAS concrete as compared to OPCC when exposed to elevated temperatures which may be due to the presence of a highly

condensed binder gel, the low content of chemically bonded water in the alkali-activated gel products and the absence of CH as a reaction product in AAS systems. Although, there have been studies conducted on the performance of AAS mixes in comparison with OPC, there has not been any study regarding the behavior of AASC mixes with copper slag as fine aggregate, exposed to elevated temperatures up to date.

2.10 FLEXURAL FATIGUE CHARACTERISTICS OF CONCRETE PAVEMENTS

Fatigue failure is one of the major modes of failure in various structures and so also in concrete pavements which are subjected to repeated application of loads. The fatigue failure in concrete pavements can occur even under the influence of repetitive or cyclic loads, whose peak values are considerably lower than the safe loads estimated through static tests. In fatigue failure, the material fails by repeated application of load which is not large enough to cause failure due to single application. Fatigue failure causes progressive, localized and permanent damage in concrete structures due to dynamic, moving or cyclic loads. In concrete pavements, the failure due to fatigue occurs as a result of development of internal cracks and progressive growth of such cracks under the action of cyclic loadings, at stresses much smaller than the modulus of rupture of the concrete (Hui et al. 2006, Lee and Barr 2004). Although studies on fatigue failure began over many decades, there is still lack of understanding regarding the nature of fracture mechanisms in cementitious composite materials due to fatigue. This is due to complex nature of cementitious composite materials and their properties which are influenced by a large number of parameters. The fatigue failure in plain concrete is influenced by parameters such as composition and quality of the concrete, age of the concrete, moisture conditions, load frequency, minimum stress used in load cycle, stress levels, rest period, waveform of cyclic load etc. (Naik et al.1993).

Fatigue loading can be classified as low-cycle and high-cycle loading. Low cycle loading is the one which involves application of a few load-cycles at higher stress levels; while high cycle loading involves application of large number of load cycles at lower stress levels. Generally, concrete pavements in highways and airport pavements are evaluated under as high cycle loading (Hsu 1981). Fatigue strength is one of the

important parameters to be considered while designing concrete pavements for highways and airfields.

Generally, resistance of plain concrete mixes to fatigue is considered.

- Fatigue resistance in compression
- Fatigue resistance in tension
- Fatigue resistance in flexure

The development of reliable flexural fatigue life prediction model is one of the toughest challenges in concrete research (Phull and Rao 2007).

Over the years, various studies on fatigue behavior of plain OPC concrete mixes, OPC concrete containing mineral admixtures, fiber reinforced concrete mixes, high performance concrete mixes etc. have been carried out by researchers. However, there are very meager number of research studies available on the fatigue performance of alkali activated binder based concrete mixes. The performance of alkali activated GGBFS-Fly ash concrete mixes incorporating steel fibers under fatigue was investigated by Kumar (2011). The addition of steel fibers improved the fatigue life of GGBFS-Fly ash concrete mixes. It was concluded that GGBFS-Fly ash concrete mixes with 1% steel fibers displayed better strength as compared to the one with 0.5% steel fibers. Silva et al. (2004) studied in detail and reported that the AAS concrete mixes performed better than OPC-based concrete under fatigue which may be mainly due to the strong matrix/aggregate bonding in AAS concrete.

The fatigue behaviour of concrete made with two different types of lightweight aggregate, at stress levels in the range of 40-80 % of the ultimate static compressive strength was studied by Gary et al. (1961) and it was reported that the fatigue behavior of light weight concrete was almost similar to that of normal concretes. Klaiber et al. (1979) investigated the effect of aggregate types (gravel and crushed limestone) on the fatigue behavior of plain concrete in flexure and it was observed that the concrete made with gravel aggregates displayed better fatigue performance as compared to limestone aggregates. Hui et al. (2006) investigated the flexural fatigue performance of plain concretes containing nano-particles of TiO_2 and SiO_2 and reported improved fatigue life and sensitivity to change in stress. Heeralal et al.

(2009) investigated fatigue behavior of steel fiber reinforced concrete with different proportions of recycled aggregate under both static, and fatigue loading at different stress levels. The results of the study suggested that the inclusion of steel fibers improves the fatigue performance of recycled aggregate concrete. Guo et al. (2010) reported that the addition of FA and GGBFS to concrete will have considerable impact on the fatigue crack propagation and damage accumulation under high/low stress levels and concluded that mixes with such mineral admixtures display improved fatigue resistance.

2.10.1 S-N Curves and Probabilistic Approach

The flexural fatigue behavior of concrete mixes are most commonly characterized with two important parameters; first, the Stress Ratio (SR) which is ratio of stress applied to the modulus of rupture of concrete and the second, the Fatigue Life (N) which is the number of cycles to failure. In studies on the fatigue behavior of concrete mixes, it is generally intended to arrive at a relationship between the stress ratio and fatigue life, in the form of a S-N curve (often referred to as Wohler curve). The S-N curve is a plot between with stress level S verses log N where N denotes the fatigue life. The employment of S-N curves for the representation of fatigue data gives a clear idea on the distribution of fatigue lives under different stress ratios. It is also generally accepted that non-dimensionalized S-N curve is independent of the test parameters like shape of the specimen; strength of concrete, curing condition, age, moisture condition at loading etc. Typical S-N curves for a plain concrete mix and a set of FRC mixes are presented in Figure 2.3 (Naik et al.1993).

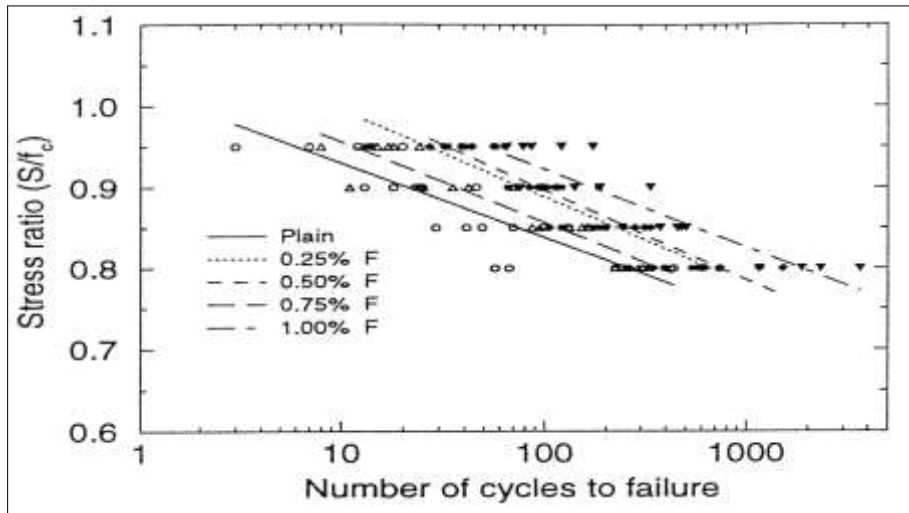


Fig 2.3 Typical S-N curve

(Source: <http://www.columbia.edu/cu/civileng/meyer/research/fati1.html>)

In order to obtain statistically reliable information of the fatigue behavior of concrete mixes, it is necessary to test several specimens at every stress level. This is due to the fact that the results of fatigue tests generally display a large scatter and variability in the number of cycles to failure. This scatter and variability in fatigue data of concrete is mainly due to influence of several parameters like variability in material strength, applied loads, testing conditions etc. Therefore, the fatigue design process is associated with lot of uncertainties from the numerous assumptions made in the analysis and material variability. Hence probabilistic concepts are implemented to model the fatigue data in order to evaluate fatigue resistance of concrete structures (Naik et al. 1993). The probabilistic procedures can be used to obtain the number of cycles to failure at any required probability of failure. A probabilistic approach to determine the fatigue reliability of concrete was first introduced by Oh (1986) and the results of his study reported that Weibull distribution provided a better representation of the experimental data than the log normal distribution and suggested that it can be used to describe the fatigue behavior of concrete mixes. Oh (1991) investigated the distributions of fatigue life of OPC based concrete at different stress ratios i.e. 0.85, 0.75 and 0.65 using specimens of size (100mm x 100mm x 500mm) loaded using the third-point loading system at a frequency of 250 cycles/min. The results indicated that the probabilistic distributions of fatigue life of concrete depended upon stress ratios

and thus shapes of Weibull distribution to describe fatigue life of concrete depended upon levels of applied stress. Singh and Kaushik (2001) carried out a detailed study on the fatigue strength of Steel Fiber Reinforced Concrete (SFRC) on specimens of size (100mm x 100mm x 500mm) under four-point flexural fatigue loading. The results indicated that the statistical distribution of fatigue-life of SFRC was in agreement with the two-parameter Weibull distribution. Chandrashekar et al. (2013) carried out investigations on the fly ash based SFRC using two different types of fibers and reported that the use of steel fibers improved the fatigue performance of fly ash based SFRC as compared with conventional OPCC. Ganesan et al. (2013) have investigated the flexural fatigue behaviour of Self-Compacting Rubberized Concrete (SCRC), with and without steel fibers, and concluded that the probabilistic distribution of fatigue life of SCRC mixes at a given stress-level also can be appropriately modelled using a two-parameter Weibull-distribution.

2.11 STRUCTURAL BEHAVIOR OF AASC-BASED REINFORCED CONCRETE BEAMS

Over the years, relatively limited studies have been carried out on the flexural characteristics of structural beams, with steel rebar reinforcement, made up of alkali activated concrete mixes. Kathirvel and Kaliyaperumal, (2016) studied the influence of varying proportions of recycled coarse aggregates on the flexural properties of reinforced AAS concrete beams and reported that the incorporation of recycled aggregate improved the strength and flexural characteristics of AAS concrete. Extensive studies on reinforced beams and columns prepared using FA-based geopolymer concrete were carried out by Sumajouw and Rangan (2006). The study reported that the failure modes and behavior of FA-based geopolymer concrete based columns and beams were similar to those observed in conventional reinforced OPCC columns and beams.

Dattatreya et al. (2011) studied the flexural characteristics of ambient cured reinforced geopolymer flexural members with binder containing different proportions FA and GGBFS ratios, whose compressive strength varied in the range of 17 to 63 MPa. The study reported that the load carrying capacities of geo-polymer beams were

marginally higher than conventional OPCC beams. However, for geo-polymer beams higher deflections were observed at different stages including service and peak load stages. The study concluded the conventional RC beam theory could be used for computation of flexural capacity, deflection, and crack-width of AAS beams with reasonable accuracy. Studies carried out by Narasimhan et al. (2011) also reported similar load-deflection curves of reinforced fly ash and GGBS based geopolymer beams to those of conventional RC beams. The study recorded appreciable first crack load and ultimate load with the ratio of ultimate load to first crack load in the same range between 1.7-2.7. Pradeep et al. (2012) have studied flexural behavior of heat cured fly ash and GGBS based geopolymer concrete and observed that with increase in tensile reinforcement, first crack load and stiffness of the beam also increased. They observed that at service load deflections were well within limits as per IS 456-2000, which again predicts the ultimate moment capacity of the beams very well. Sarker (2015) Concluded that the current provisions for OPC concrete can be conservatively used for design of reinforced geopolymer concrete members.

2.12 COPPER SLAG

Copper Slag (CS), a by-product obtained from the manufacture and decontamination of copper, can be identified as a potential replacement for sand (Al-Jabri et al. 2009a) The production of one ton of copper produces about 2 to 2.3 tons of CS as a by-product. About 2.5 million tons of CS is generated annually in India, which is to be disposed-off as an industrial waste. According to Lye et al. (2015), annual production of CS globally is around 35 million tonnes, which is sufficient for producing about 100 million cubic metres of concrete, even if 50% of natural sand is replaced with CS. CS is a granular material which can be made to match the size fractions and standards of natural sand used for concrete production. The chemical compositions of CS vary slightly from source to source based on the composition of copper ore, type of furnace and metallurgical treatment techniques employed in the processing.

2.12.1 Engineering Properties of Copper Slag Based Concrete Mixes

Several studies have been carried out on the use of CS as fine aggregate in conventional OPC-based concrete mixes. The workability of concrete mixes was found to increase significantly with the incorporation of CS (Al-Jabri 2011). The high density and glassy surface texture of CS may often lead to undesirable effects in concrete mixes such as excessive bleeding, leading to weaker top surface layers and the formation of water pockets below bigger particles of coarse aggregate. Such adverse effects are known to increase with higher contents of CS in the concrete mixes. However, it has been shown that, by limiting the CS content up to 40% or by adding fines in the concrete, the extent of bleeding can be controlled (Shi et al. 2008).

Studies carried out by different researchers have reported that the concrete and mortar attain sufficient strength with CS as component of concrete, if the concrete mixes are properly designed. Studies conducted on High Performance Concrete (HPC) mixes using CS as fine aggregates have recorded better workability and 28-day strength increments with mixes containing upto 50% CS as fine aggregates. However, replacement of sand with CS beyond 50% (by weight) has resulted in the decline in the strength properties (Al-Jabri et al. 2009a). However, concrete mixes produced even with 100% of sand replaced by CS (by weight) have recorded better compressive strength when constant workability was maintained (Al-Jabri et al. 2009b). According to Lye et al. (2015), if CS is used properly in compliance with specifications for sand for making concrete (particularly in terms of its particle size and grading), it will be possible to replace sand with CS at any replacement level, even up to 100%. Studies carried out by Ghosh (2007) and Dhir (2009) have suggested that the use of CS improves the modulus of elasticity of concrete. Studies carried out by researchers on effect of CS on the permeation properties such as water absorption, permeability (Al-Jabri et al. 2009a, Dhir 2009, Brindha et al. 2010) suggest that natural sand replaced with CS upto about 40% can improve the permeation properties, however, higher replacement beyond 40%, may degrade them. The CS-admixed concretes display slightly lower acid corrosion, although, CS is a very sound and hard material with lower porosity as compared to natural sand.

Brindha and Nagan (2011) conducted tests on the acid corrosion resistance of concrete mixes with CS and reported lower performance of concrete made with CS as compared to natural sand. Various studies have been carried out to determine the resistance of concrete mixes made with different CS content from (0 to 100%) to sodium sulfate (Na_2SO_4) (Ayano et al. 2000, Brindha et al. 2010), using different w/c ratios from 0.45 to 0.62 and with / without wetting and drying cycles. The studies have reported that the sulfate attack resistance of concrete mixes made with CS is similar to that of concrete mixes made with natural sand.

2.13 SUMMARY

From the detailed literature review, it is observed that the strength and durability of alkali activated slag mixes are significantly affected by many factors such as type of binder, chemical composition of the binder, water-to-binder ratio, type of alkali activator, modulus of alkaline activator, Sodium oxide dosage (Na_2O), water content, type of curing, etc. The AAS mixes if designed properly, may obtain higher strength and better durability as compared to conventional OPCC. AASC mixes can attain sufficient strength even at ambient room temperatures, when subjected to air curing, i.e., without any need for heat curing or other methods. The combination of sodium hydroxide and liquid sodium silicate used as alkaline activator provides the best activation for alkali activated slag-based binders. There exist an optimal combination of activator modulus (M_s) and sodium oxide dosage (Na_2O) at which the maximum strength of alkali activated slag-based binders can be attained. The optimal sodium oxide dosage varies between 3% and 5.5% (Na_2O , by weight of binder) for AAS mixes, whereas higher dosages may lead to uneconomical mixtures and efflorescence problems. The optimal activator modulus (M_s) is found to vary between 0.75 and 1.5 for AAS mixes. Thus all the design parameters like the water to binder ratio, sodium oxide dosage (Na_2O), activator modulus (M_s) etc., need to be well controlled in order to obtain mixes of the required strength and workability. Copper slag, an industrial by-product can be looked upon as a potential replacement for sand as fine aggregate in concrete. Improved or satisfactory performance of copper slag aggregates have been reported by various researchers when used in conventional OPC concrete mixes. However, there is limited research available on strength, durability and fatigue

performance of alkali activated slag-based concrete mixes incorporating copper slag as fine aggregate. The present research is hence focussed on a detailed study of the properties of air-cured AASC mixes with copper slag as fine aggregate which in turn facilitates conservation of natural raw materials leading to a sustainable concrete technology.

CHAPTER 3

MATERIALS CHARACTERIZATION AND MIX PROPORTIONS

3.1 INTRODUCTION

This chapter describes the details of all the experimental work conducted in the present investigation. Preliminary test results on constituent materials, design of AAS concrete mixes, methodology adopted, preparation of test specimens and results of preliminary investigations, methods of tests conducted on AASC mixes, both in fresh and hardened states, are discussed.

3.2 PRELIMINARY INVESTIGATIONS ON CONSTITUENT MATERIALS

3.2.1 Cement

Cement is the most important constituent of a concrete mix. In the present study, Ordinary Portland Cement of 43 grade, conforming to IS 8112-2013 was used in the preparation of test specimens of a reference concrete mix used for comparison purposes. The properties of the cement used are given in Table 3.1.

3.2.2 Ground Granulated Blast-Furnace Slag (GGBFS)

For the various tests conducted in the present investigation, GGBFS conforming to IS 12089-1987 was procured from M/s JSW Iron and Steel Plant, Bellary, India. The properties of the GGBFS used are given in Table 3.2.

3.2.3 Aggregates

All the aggregates used herein were tested as per relevant Indian standard codes. Crushed granite chips of maximum nominal size of 20 mm were used as coarse aggregate. The specific gravity and water absorption of the coarse aggregate were 2.69 and 0.5%, respectively. The specific gravity, water absorption and Fineness Modulus (FM) of river sand used were 2.64, 1.50% and 2.58, respectively. The results of various tests conducted on different aggregates are presented in Tables 3.3 to 3.5. All aggregates were used in saturated surface dry condition.

Table 3.1 Properties of Ordinary Portland cement used

SL. No	Test	Results	Limits as per IS 8112-2013
1	Specific gravity	3.13	-
2	Standard consistency, %	30	-
3	Fineness of cement (m ² /kg) (Blaine's air permeability)	330	≥225
4	Setting time - Initial (minutes)	65	≥30
	- Final (minutes)	375	≤600
5	Compressive strength (MPa) 3-Days	27	≥23
	7-Days	41	≥33
	28-Days	54	43-58

Table 3.2 Oxide composition and properties of GGBFS used

Constituent	Oxide Content (% by weight)
CaO	33.77
Al ₂ O ₃	16.70
Fe ₂ O ₃	1.20
SiO ₂	32.43
MgO	9.65
Na ₂ O	0.16
K ₂ O	0.07
SO ₃	0.88
Insoluble Residue	4.03
Loss of Ignition	0.4
Glass Content	92%
Blaine fineness	370 m ² /kg
Specific gravity	2.9
Basicity (k _b)	0.88 (Acidic Slag)
Hydration Modulus (HM)	1.85 (>1.4)

3.2.3.1 Copper Slag

The chemical composition of CS used in this study is shown in Table 3.6. It is observed that the CS, as-received from the industry, consists of 3.3% of friable particles when tested as per ASTM C-142-10. It is expected that better bonding between the cement paste and CS particles can be realized by excluding such weaker particles. Therefore, 20 kg of CS per batch was ground in Los Angeles abrasion testing machine for 30 minutes, with 10 standard steel balls each weighing 390 to 445 gms, as the charge, along with 100 g of water to eliminate dust while removing copper slag from the machine. The specific gravity, water absorption and fineness modulus (FM) of resulting CS were 3.6, 0.50% and 2.61, respectively and such processed CS is used in the present investigation. A comparison of sieve-analysis of sand and CS processed as above, both used as fine aggregates here in this study, are shown in Table 3.5. The results show that both sand and CS are acceptable for concrete-making and conform to Zone II, as per IS 383-1970 specifications.

Table 3.3 Properties of coarse and fine aggregates used

SL. No	Test	Coarse Aggregate	Fine Aggregates	
			Sand	Copper Slag
1	Specific gravity	2.69	2.64	3.60
2	Dry bulk density			
	a) Loose	1493 kg/m ³	1443 kg/m ³	2045 kg/m ³
	b) Compacted	1717 kg/m ³	1634 kg/m ³	2383 kg/m ³
3	Aggregate crushing value	26%	-	-
4	Los angeles abrasion value	28%	-	-
5	Aggregate impact value	17%	-	-
6	Flakiness index	13%	-	-
7	Elongation index	25%	-	-
8	Remarks: All the aggregates were found to be acceptable for use in concrete			

Table 3.4 Results of sieve analysis - coarse aggregates

IS Sieve Designation (mm)	Percentage Passing	Remarks
25	100	Coarse aggregate used satisfies requirements of aggregates as IS 383-1970.
20	99	
10	45	
4.75	2	

Table 3.5 Results of sieve analysis - fine aggregates

Sieve Size	Percentage Passing	
	Sand	Copper Slag
10mm	100	100
4.75mm	99.0	100
2.36mm	96.4	99.6
1.18mm	75.7	76.8
600 μ	53.5	48.8
300 μ	14.3	11.9
150 μ	2.8	1.5
Grading (as per IS 383-1970)	Zone II	Zone II

3.2.4 Water

Tap water available in the institute laboratory was used for preparation of alkaline activator solution, for mixing of the AAS concrete mixes and for mixing and curing of OPC- based concrete specimens in the present investigation.

3.2.5 Super-plasticizer

A commercially available, Sulfonated Naphthalene Formaldehyde (SNF)-polymer based high-range water-reducing admixture was used as a superplasticizer in the present investigation. Properties of the super-plasticizer used are given in Table 3.7.

Table 3.6 Oxide composition and properties of copper slag used

Chemical Constituents	Weight (%)
CaO	0.84
Al ₂ O ₃	16.06
Fe ₂ O ₃	49.30
SiO ₂	32.74
MgO	0.20
Na ₂ O	0.14
K ₂ O	0.03
SO ₃	0.13
Insoluble residue	17.97
Loss of ignition	0.25

Table 3.7 Properties of super-plasticizer used (Conplast SP 430)

Specific gravity	1.20
Chloride content	Nil
Solid content	40%
Recommended dosage	5ml to 20ml/kg of binder
Operating temperature	10 to 40 ⁰ C
Color	Dark brown liquid

3.2.6 Alkaline Activator

The alkaline activator used in this study was a mixture of sodium silicate solution and sodium hydroxide flakes of 97% purity. Both the liquid sodium silicate and sodium hydroxide flakes were procured from a local supplier. Properties of sodium silicate are determined as per IS 14212-1995 and properties of both the ingredients are shown in Tables 3.8 and 3.9 respectively. The alkaline solution was prepared by dissolving sodium hydroxide flakes in sodium silicate solution to obtain a desired modulus (Ms) and water was then added to bring the total water/binder ratio of alkali solution to 0.2.

The solution was stirred well, immediately transferred to an air tight container and was left at least for one day. To this solution, extra water was added to bring the total w/b ratio of 0.4, just before mixing of various AASC mixes Details are given in **Appendix- II**.

Table 3.8 Properties of liquid sodium silicate

Constituent	% by weight
Na ₂ O	14.7
SiO ₂	32.8
Solids	47.5
Water content	52.5
Ms (SiO ₂ /Na ₂ O)	2.23
Specific gravity	1.57

Table 3.9 Properties of sodium hydroxide flakes (97% purity)

Molecular formula	NaOH
Molar mass	39.9971 g/mol
Appearance	White solid
Specific gravity	2.1
Solubility in water	114 g/100 ml (25 ⁰ C)

3.2.7 Reinforcing bars

Two different sizes of deformed steel bars were used as the longitudinal and shear reinforcement while casting reinforced concrete beam specimens. Samples of steel bars were tested in the laboratory. The results of the tests conducted are in Table.3.10.

Table 3.10 Properties of steel reinforcement bars used

Diameter (mm)	Nominal Area (mm ²)	Yield Strength (MPa)	Ultimate Strength (MPa)
8	50.26	470	580
12	113.1	460	575

3.3 EFFECT OF SODIUM OXIDE DOSAGE AND MODULUS ON STRENGTH OF AASC MIXES

Alkali solution was prepared as a mixture of sodium silicate and sodium hydroxide, with different Na₂O dosages (3% and 4%) and Ms (0.5-1.5), with constant GGBS content of 440 kg and w/b of 0.4. Volume changes due to change in specific gravities of various Na₂O dosage has been adjusted by varying total aggregate content. There was considerable effect on the strength of AASC mixes (Table 3.11). In solutions with dosages of Na₂O at both 3% and 4%, highest 28-day compressive strengths was achieved with a modulus of alkali solution Ms of 1.25 (Figure 3.1). Thus, it is observed that the Ms of sodium silicate solution is critical in determining the strength level of AASCs.

Table 3.11 Effect of Ms of alkali solution on compressive strength of AASC mixes (w/b ratio = 0.4)

Na ₂ O Dosage (% by weight of binder)	Modulus Ms (SiO ₂ /Na ₂ O)	Compressive Strength 28-days (MPa)
3	0.5	28.8
	0.75	31.4
	1	34.9
	1.25	39.4
	1.5	35.1
4	0.5	44.7
	0.75	49.6
	1	57.1
	1.25	62.9
	1.5	58.3

In view of above, in the present study, alkaline activator solution with a constant modulus Ms of 1.25 and with a constant Na₂O dosage of 4% was adopted for preparing all candidate AASC mixes, which were further investigated in detail for their strength and durability characteristics.

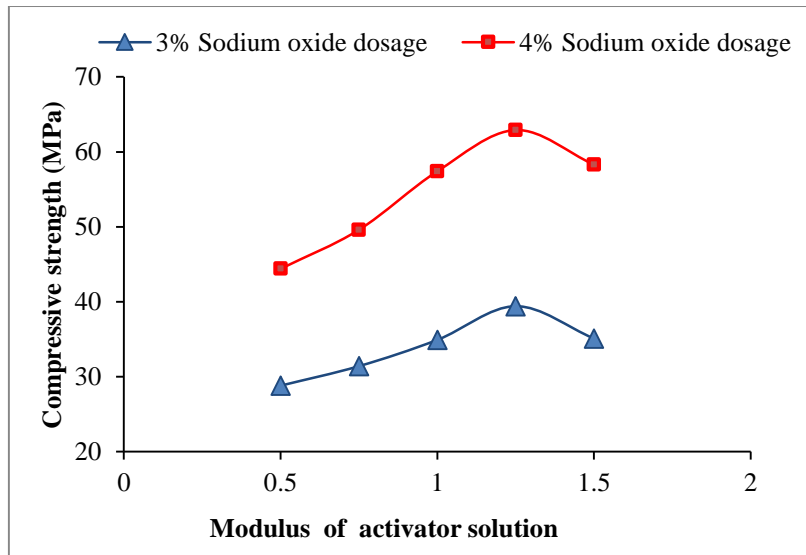


Fig 3.1 Effect of Ms of alkaline activator on compressive strength (w/b = 0.4)

3.4 CONCRETE MIX DESIGN

For the purpose of the durability studies, the selection of the candidate AASC mixes to be used was made based on assumption of severe conditions of exposure. Hence a moderately higher reference compressive strength, corresponding to a mix-grade of M45 was chosen for design of the mixes. This grade was chosen to replicate a standard strength for site-mixed concrete and to investigate whether AASC mixes with CS would perform satisfactorily in durability tests.

The mix-proportions of OPC-based reference concrete mix were calculated following the general guidelines specified in IS 10262-2009. The mix was proportioned to achieve an initial slump of 50-75 mm, with 440 kg/m³ of OPC and an effective water/cement ratio of 0.4. The volumes of fines (only river sand) and coarse aggregate were respectively chosen as 36% and 64% of the total aggregates respectively. The calculations of the proportion of ingredients for OPC-based reference concrete mix are given in **Appendix- I**.

Systematic modifications, with the design parameters of the OPC-based control mix as a basis, were now made to develop the mix-proportions of a new class of AASC mixes. The amount of binder (at 440 kg of GGBFS alone) and the total water/binder ratio of 0.4 were maintained in all the AASC mixes too, as in the reference OPC-

based mix. The total volumes of aggregates were appropriately varied in these mixes. The alkaline activator solution was incorporated in the mixes with a constant dosage of 4% Na₂O, and with a constant modulus $M_s = 1.25$ maintained in it.

With the known properties of all ingredients, AASC mixtures containing 25%, 50%, 75% and 100% of CS, as replacement for river sand fine aggregate (by volume), were prepared. The total volume of fine aggregate comprising of sand and CS was kept constant in all the AASC mixtures. The mass fraction of CS used were more than that of sand of equal volume at each replacement level due to much higher density of the CS. Sample mix design calculations for an AASC mix are given in **Appendix II**. Details of mix quantities of ingredients in all the trial mixes tested herein are presented in Table 3.12. AASC mixes prepared with sand/CS showed no indications of segregation or bleeding.

3.5 MIXING, PLACING AND COMPACTING THE CONCRETE MIXES

Mixing of concrete ingredients was carried out using a ribbon mixer of 125 kg as follows:

- a) Dry mixing of the material introduced to the mixer, in the order - coarse aggregate, sand, OPC or GGBFS, for about thirty seconds.
- b) Water premixed with super-plasticizer in case of OPCC or, alkaline solution in case of AASC, was added during the next 30 seconds and the mixing was continued for further two minutes.
- c) The mixer was stopped, mix was discharged, and its slump was measured.
- d) The total mixing time was about three minutes.
- e) The mix was then placed in moulds kept ready with their inner surfaces well oiled and are compacted on a table vibrator.

3.6 SPECIMEN DETAILS

In order to evaluate the strength and durability characteristics of various mixes, specimens were tested at different ages viz. 3, 7, 28, 56 and 90 days. The details of the specimens used for various tests are given in Table 3.13.

Table 3.12 Details of mix designations and mix proportions of concrete mixes**(All ingredient contents are in kg/m³)**

Mix ID	OPC	GGBFS	Fine Aggregates		Coarse Aggregate	LSS	NaOH	Added water	Total water	SP	Total quantity
			Sand	CS							
OPCC	440	-	650	-	1178	-	-	174.4	176	2.64	2445
ACS-0	-	440	630	-	1141	67.1	10	140.8	176	-	2429
ACS-25	-	440	473	216	1141	67.1	10	140.8	176	-	2488
ACS-50	-	440	315	432	1141	67.1	10	140.8	176	-	2547
ACS-75	-	440	156	648	1141	67.1	10	140.8	176	-	2606
ACS-100	-	440	-	864	1141	67.1	10	140.8	176	-	2665

Note: OPCC-Portland Cement Based Control Mix; LSS - Liquid Sodium Silicate. ACS-X- represents AASC mixes with X (% by volume) of sand replaced with copper slag.

Table 3.13 Details of test specimens used for various tests

SL No.	Types of Test	Specimen Geometry	Specimen Dimensions (mm)	Relevant Standards
1	Cube compression	Cubes	100x100x100	IS 516-1959
2	Split tensile strength	Cylinders	100(dia)x200(height)	IS 5816-1999
3	Modulus of rupture	Beams	100x100x500	IS 516-1959
4	Modulus of elasticity	Cylinders	150(dia)x300(height)	IS 516-1959
5	Water absorption and total porosity	Cubes	100x100x100	ASTM C642-06
6	Chloride impermeability	Cylinders	100(dia)x200(height)	NT BUILD 443
7	Sulphate and acid attack	Cubes	100x100x100	-
8	Elevated temperatures	Cubes	100x100x100	-
9	Flexural behavior of reinforced alkali-activated slag concrete beams	RCC Beams	150x250x2550	-
10	Flexural fatigue characteristics	Beams	100x100x500	-

3.7 CURING OF SPECIMENS

The test specimens of AASC mixes were cured in ambient air laboratory conditions, having temperature $27\pm 3^{\circ}\text{C}$, with relative humidity $85\pm 10\%$. Test specimens of OPCC-mix concrete were cured in a curing water tank for specified number of days (3, 7, 28, 56 and 90 days) until they were tested.

3.8 EXPERIMENTAL PROCEDURES

3.8.1 Workability

In the present investigation the levels of workability of the mixes were measured using the standard Abraham's slump cone. Tests were conducted as per IS 1199-1959.

3.8.2 Mechanical Properties of Concrete Mixes

For each mix, specimens were tested in triplicates using calibrated testing machines. Cube compression tests, flexural strength (on prisms) and modulus of elasticity tests on concrete cylinders of all the mixes were conducted as per the guidelines in IS 516-1959, while split-tensile strength tests on cylindrical specimens were performed as per provisions of IS 5816-1999. Tests were conducted at specified ages.

3.8.3 Water Absorption and Total porosity of AASC Mixes

Total porosity and water absorption were calculated based on the results of tests conducted conforming to the standard procedure in ASTM C642-06.

3.8.4 Chloride Impermeability Test

Concrete specimens for chloride permeability test were prepared according to the specifications in NT Build 443. Penetration of chloride ions was assessed with colorimetric analysis, using 0.1M AgNO_3 solution, applied after 90 days of immersion in 5% NaCl solution and the depth of chloride ion penetration was measured from the colour change along the thickness of the specimen at six positions on each split piece and their average was taken to calculate the diffusion coefficient (Basheer 2001).

3.8.5 Resistance to Sulphate Attack

The strength of the concrete gets degraded, as a result of chemical reactions occurring when concrete is exposed continuously to a sulphate solution of adequately high concentration. Such deterioration of concrete under sulfate attack is widespread in arid provinces where sulfate minerals are present in the soil and groundwater. Weakening of concrete due to sulfate attack is normally attributed to hydration products of Portland cement reacting with sulfates to form expansive reaction products like ettringite and gypsum leading to high internal stresses and succeeding in disruption of the concrete (Shi et al. 2006). Sulfate resistance tests were carried out on 100 mm cubes of various concrete mixes. Concrete specimens after 28-days of curing, were immersed in two solutions, containing 10% Na₂SO₄ and 10% MgSO₄, separately. The solutions in containers were replaced every 2 weeks for the first 2 months, and then replaced every month upto 12 months. The compressive strength of test specimens were measured from time to time upto 12 months.

3.8.6 Resistance to Acid Attack

Sulphuric acid resistance tests were conducted on 100 mm-sized concrete cube specimens immersed in containers filled with 1% sulfuric acid solution (pH=1). This concentration of sulfuric acid is representative of that found in sewers that are in a state of deterioration (Meyer and Ledbetter 1970, Sand and Bock 1984). The containers were interconnected by 2.5 cm diameter plastic pipes. The sulphuric acid solution was kept agitated and circulated through the acid containers by means of a multi-speed electrical pump with a flow rate of 0.5 liters/min, to inhibit any stagnation effect. The pH levels of the sulphuric acid solutions were examined daily by means of a portable digital pH-meter (standard error ± 0.05). Concentrated sulphuric acid was added to the solutions at regular intervals to maintain the pH level. Acid solution was replaced with fresh solution for every 15 days. The compressive strengths and mass changes were measured at regular intervals upto 4 months.

3.8.7 Resistance to Elevated Temperatures

The elevated-temperature resistance tests were done on 100 mm cubes; concrete specimens from each mix were placed in a temperature controlled furnace and heated from room temperature (30⁰C) to elevated temperatures on the range 200-800⁰C at a rate of 6⁰C/min. The specimens were held, soaked at the particular high temperature for four hours and then immediately removed from furnace. They were allowed to cool in air gradually to room temperature. The concrete specimens were then tested for their residual compressive strengths.

3.8.8 Flexural Fatigue Test

The flexural fatigue tests on OPCC and alkali activated concrete beam samples were carried out on beam specimens of dimensions (100mm x 100mm x 500mm) on a 5-tonne capacity MTS servo-controlled, hydraulic, repeated load testing machine.

3.8.8.1 Flexural Fatigue Testing Set-up

Accelerated fatigue testing equipment (Make:- M/s Spranktronics, Bangalore) was used in this study (Figure 3.2).

The following are the main components of this sophisticated equipment.

1. Loading frame and loading system
2. Load sensing devices
3. Deflection recording system (LVDTs)
4. Servo amplifier system
5. Control unit to monitor load and repetitions
6. Computer system

The loading system consisted of a double acting hydraulic cylinder with suitable mounting flanges. It is associated with a power pack unit consisting of pump coupled with motor (1 HP, 3-phase, 1440 rpm), valves and filters, heat exchanger (cooling system), servo-valve, pressure gauge etc. Load cells (Transducers) are used to sense the applied load to the specimen during testing. The load cell used for testing is of capacity 50 kN (5000 kg).



Fig 3.2 Flexural fatigue testing setup

Deflection Recording: LVDTs were used to sense the deflections with the help of suitable signal conditioners and display panels.

Frequency and Waveform of Loading: The loading is generally with half sinusoidal waveform (zero - maximum load - zero). The application frequency can be between 1-5 Hz with or without rest period.

Servo Amplifier System: It is used to link the function generator and the servo-valve. Control Unit is used to monitor the load and the repetitions. It is connected to the PC with an 'ADD ON' data acquisition card to acquire and store the experimental data.

3.8.8.2 Flexural Fatigue tests of AAS Concrete Beams

The fatigue tests were conducted on OPCC and AASC samples with 0%, 50% and 100% with CS aggregates. Five specimens were tested for each mix at each stress level. The static flexural strength of the mixes was recorded at 90 days before the fatigue test was conducted. The beam specimens were tested at the 1/3rd point loading on a total span of 400 mm. The test specimens were subjected to loading using

constant amplitude half sinusoidal wave form at a frequency of 4 Hz without any rest period. The test setup was calibrated applying initial loading and the frequency of loading was maintained constant throughout the test for all specimens. The minimum load is maintained as zero while the maximum load was adjusted based on the required stress ratio (ratio of applied stress to the modulus of rupture of concrete). The fatigue tests were conducted at different stress ratios i.e. 0.85, 0.80, 0.75 and 0.70 to obtain a relationship between different stress ratios (S) and the number of cycles to failure (N). The Fatigue life (N) i.e. the number of cycles up to failure of the sample were recorded. The test was conducted at the end of 90 days of curing of concrete specimen in order to eliminate the errors occurring due to any strength development of the concrete mixes after 28-days of curing.

3.8.9 Flexural Tests on AAS Concrete Beams

The following parameters were considered in the present experimental investigations for evaluating the performance of reinforced concrete beams made using different AAS concrete mixes. Only ACS-0, ACS-50 and ACS-100 mixes, with 0%, 50% and 100% of sand (by volume) replaced with copper slag respectively, were considered for this study.

a. Constant parameters:

- i) Grade of concrete: M45
- ii) Target slump: 50 to 75 mm
- iii) Curing period (ages): 28 days
- iv) Reinforcement: The reinforcement provided for all beams were the same. Three number of grade 415, 12mm diameter bars were provided as tension reinforcement. Higher area of shear reinforcement provided than that required by the shear design, so that shear failure is totally prevented. 2-legged stirrups of diameter 8mm (grade 415 steel), spaced at a uniform spacing of 125mm c/c were provided throughout the span in all the RC beam specimens (Figure 3.3).

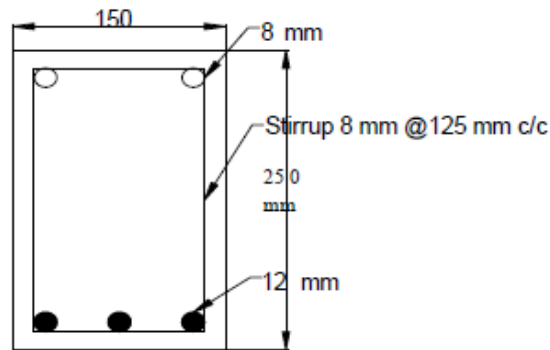


Fig 3.3 Typical cross sectional details of reinforced concrete test beams*2L

Companion cube specimens (150 mm-size) were also simultaneously cast, with the beams, with both Alkali Activated Slag Concrete (AASC) and Ordinary Portland Cement Concrete (OPCC) mixes and were cured for 28-days, for ascertaining the cube compressive strengths of the respective mixes used in the reinforced beams. These cubes were also tested in a Compression Testing Machine (CTM) as per IS 516-1999.

b. Casting of the beam Specimens

To facilitate easy de-moulding, wooden beam forms of size 150mm x 250mm x 2550 mm were fabricated for casting the reinforced AAS/OPC concrete beams. They were coated with oil on their inner surfaces. A constant cover of 25 mm was maintained to the individual reinforcement bars using cover blocks (mortar) at regular intervals. On these cover blocks, the reinforcement cage was placed (Figure 3.4). Each beam was provided with two hooks at equal distance from the ends to facilitate in easy lifting and transportation.



Fig 3.4 Formwork for beam specimens

c. Setup for testing the reinforced AAS beams

The surfaces of the beams were cleaned and white washed with a thin coat to facilitate easy detection of cracks and the propagation of cracks. The beam was placed in the loading frame, with roller supports at both the ends. The positions at which the two-point loads are to be applied in a 4-Point loading scheme and the center of the beam were marked. A schematic diagram of test setup is shown in the Figure 3.5. Deflection dial gauges are placed at both the loading points and also at the mid-span of the beam.

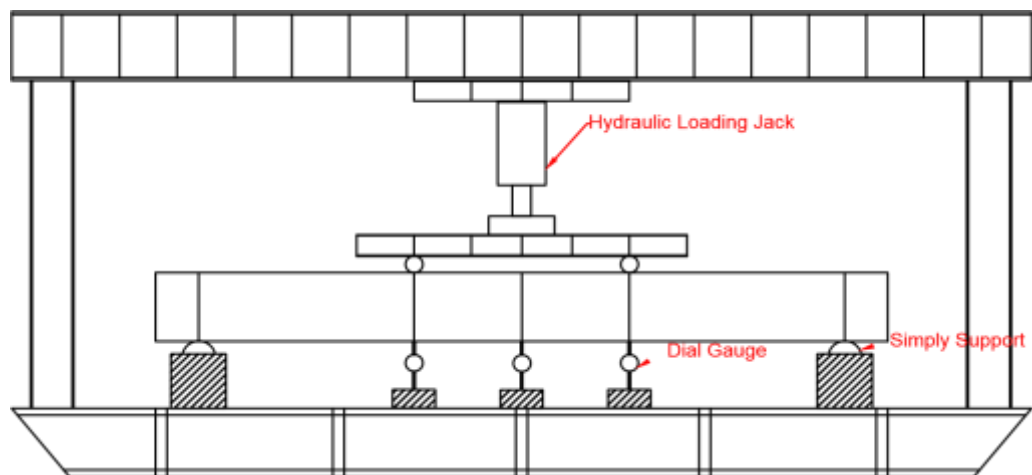


Fig 3.5 Reinforced concrete beam test setup-schematic

(d) Instrumentation and measurements

- Loading jack: A hand operated pneumatic jack was used for the purpose of loading.
- Dial gauges: The deflections were measured using 'dial gauges (least count = 0.01mm) having a magnetic base.

(e) Method of testing the beams

All beams were tested with two point loads applied symmetrically at one-third span points, so as to have a pure bending zone in the middle of the beam. The load was distributed to the two points by means of rigid spreader beam and rollers. The pressure jack was placed over the center of distributing beam such that there was no

eccentricity of the load. Load was indicated by pressure gauge provided in the loading jack. After arranging the loading system, dial gauges were placed just below the load points and at the center span of the beam. Before application of loading, that is at zero loads, initial readings of all the dial gauges were noted. Using a hand operated pneumatic jack, the load was gradually applied on the beam in increments. Dial gauge measurements were recorded at regular load intervals. The load corresponding to the first crack was noted. At each load increment, the appearance of any fresh crack and the propagation of old cracks were closely monitored and clearly marked. The crack widths were also measured using a crack measuring microscope (Elcometer). The respective load levels were also marked. After failure, the crack patterns were sketched using a marker pen and the photograph of each of the beam was taken.

CHAPTER 4

STRENGTH AND DURABILITY OF ALKALI ACTIVATED SLAG CONCRETE MIXES

4.1 GENERAL

The present chapter discusses the mechanical and durability performance of the AASC mixes in comparison with OPCC. Results of workability, strength and different durability tests conducted on various trial Alkali-Activated Slag Concrete (AASC) mixes, with copper slag used a partial/total replacement to river sand as fine aggregate, are analyzed and discussed in the present chapter. Various durability properties such as water absorption, total porosity, acid resistance, sulphate resistance and chloride ion penetration are discussed here. The behavior of AASC mixes, incorporated with different percentage of copper slag as fine aggregates, after exposure to elevated temperatures is also discussed here and is compared with the behaviour of a conventional OPC-based concrete mix. The concrete mixes are exposed to elevated temperatures of 200⁰C, 400⁰C, 600⁰C and 800⁰C and the residual compressive strengths are evaluated.

4.2 WORKABILITY

A slump in the range 50-75 mm had been aimed at, for the various concrete mixes, during the mix design stage. At a moderately lower w/c ratio of 0.40, this was achieved with a small dosage (0.6 % by weight of cement) of a super-plasticizer for the OPC-based concrete mix. However desired level of workability was achieved in the various AASC mixes with no requirement of a super-plasticizer (Table 4.1). No significant changes were observed herein, in the workability of AASC mixes, in contrast to the observations of the earlier researchers, who have, in general reported an increase in workability of the mixes with increasing replacement of sand with CS (Al Jabri et al. 2009a, Al-Jabri et al. 2009b, Wei et al. 2010). This may be possibly due to similar grain-size distribution (and hence the fineness modulus) of both the river sand and CS used herein, and also the differences in the mix proportions.

4.3 HARDENED PROPERTIES OF CONCRETE MIXES

4.3.1 Compressive Strength and Modulus of Elasticity of the Concrete Mixes.

The compressive strength at various specified ages and modulus of elasticity at a reference 28-days age, of the reference OPC-based mix and all the AASC mixes, are also presented in Table 4.1. The split tensile strength at different ages with respect to the 28-day strength for mixes are depicted in Figure 4.1. It is observed that the compressive strength of the OPCC mix gradually increased as curing period progressed up to 90-days. All the mixes attained at 28-days, strengths in the range 60 ± 5 MPa. Increasing replacement of sand with CS did not have any significant effect on the compressive strength of the concrete mixes at a given age. The AASC mixes with sand/CS, however, showed development of higher early-strengths as compared to the control OPCC mix; such initial strength development can prove very advantageous in the construction industry, from the view-point of cost-effectiveness in terms of early formwork removal and faster advancement of work. While the OPCC mix achieved around 70% of the 28-days strength at 7-days of curing, all the AASC mixes with sand/CS attained an average of about 84% of the 28-days strength at 7-days of curing. However, by 90-days of curing, both the OPCC and AASC mixes displayed similar strengths.

Table 4.1 Workability, compressive strength, and modulus of elasticity of various concrete mixes.

Mix Designation	Mean Slump (mm)	Compressive Strength (f_{ck}) (MPa)					Modulus of Elasticity (GPa)
		3-day	7-day	28-day	56-day	90-day	28-day
OPCC	75	24.1	41.5	59.2	65.5	69.4	33.1
ACS-0	65	41.6	54.2	62.1	66.7	71.6	30.3
ACS-25	70	38.7	52.3	60.8	68.2	73.0	30.8
ACS-50	65	42.2	51.0	61.7	65.1	72.2	31.5
ACS-75	75	40.9	53.6	64.4	64.9	74.1	32.0
ACS-100	80	42.4	50.7	63.0	69.3	73.8	32.7

The modulus of elasticity of the reference OPCC mix is marginally higher than that of any of the AASC mixes. It can also be observed that moduli of elasticity of all the AASC mixes, with the varied percentages of CS, are almost comparable.

Early strengths of AASC mixes with sand/CS are 1.6 to 1.72 times that of OPCC due to the physical and structural characteristics of the binders formed in these mixes. The hydration reactions of alkali activated slag are controlled by dissolution and precipitation, whose kinetics in the highly alkaline environment as available, are much faster than the diffusion-controlled reaction processes which take place during the hydration of OPC (Roy and Silsbee 1992, Wang and Scrivener 1995). The use of sodium silicate based-activators leads to the advance of binders whose structure is mainly a Calcium Silicate Hydrate (C-S-H) (Richardson et al. 1994, Wang and Scrivener 1995, Fernández-Jiménez and Puertas 2001) which is primarily responsible for strength development. The interfacial transition zones in AASCs have been reported to be highly dense and uniform, with very minimal differences in these regions (Wang and Scrivener 1995). During the alkali-activation reactions, the silicate ions, both supplied by the activator and obtained from the dissolution of the slag, deliver to the system the species essential to endorse the reactions with the calcium released from the slag. As the reactions advance further, the silicate ions supplied by the alkali-activator get exhausted but dissolution of slag continues. Condensation and cross-linking of these species leads to gelation, resulting in a C-S-H type product with a low to moderate Ca/Si ratio (Wang and Scrivener 1995, Fernández-Jiménez and Puertas 2001, Wang and Scrivener 1995).

4.3.2 Split Tensile and Flexural Strength of AASC Mixes

Figure 4.1 depicts the results for 28-day split tensile strengths of different AASC mixes with sand/CS. All AASC mixes have gained higher split tensile strengths in the range of 9-10% than that of the control OPC. Tensile strengths of AASCs, however, do not seem to be very sensitive to the level of replacement of sand with CS.

The flexural strengths of AAS concrete mixes at different ages (7, 28 and 90 days) are depicted in Figure 4.2. It can be observed that flexural strength of river sand-based AASC mix is higher than that of the control OPCC mix. At 28 days, it was observed

that the AASC mixes gained higher strength in the range of 4-5% as compared to control OPC mixes, Again replacing increased percentages of sand by CS in AASC has not led to any appreciable changes in their flexural strengths.

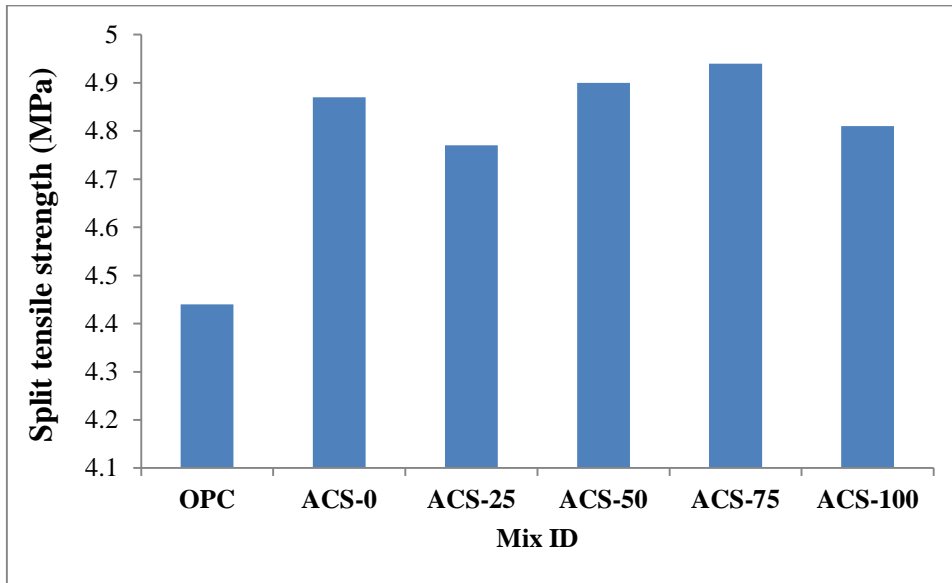


Fig 4.1 Split tensile strengths of AASC mixes at 28-days

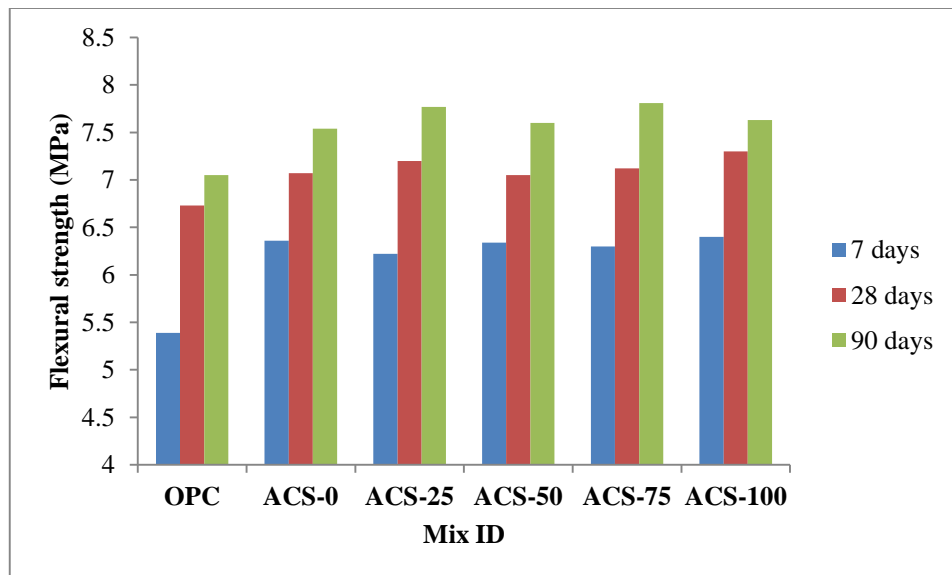


Fig 4.2 Flexural strengths of AASC mixes

4.4 DURABILITY OF CONCRETE MIXES

4.4.1 Water Absorption and Total Porosity of AASC Mixes

Figures 4.3 and 4.4 depict the results of water absorption and total porosity test on the mixes tested herein respectively. AASCs, having same binder content and water-binder ratio, show sufficiently reduced water absorption values at all levels of replacement of sand by CS, at both 28 days and 90 days as compared to the control OPC mix. This may be due to a result of the presence of a refined, tortuous and closed porosity in the AASC samples (Collins and Sanjayan 2000), through which water does not readily penetrate, and also the continuing hydration reactions even at advanced ages of curing (Bernal et al. 2011).

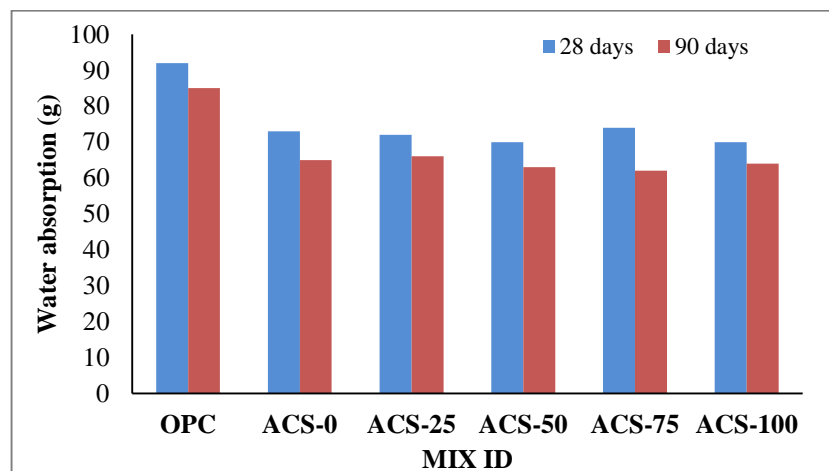


Fig 4.3 Water absorption of concrete mixes at 28 and 90 days

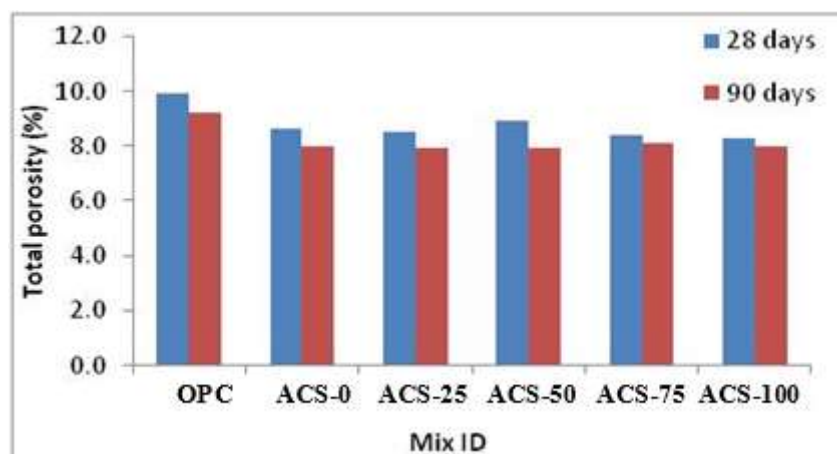


Fig 4.4 Total porosity of concrete mixes at 28 and 90 days

4.4.2 Chloride Ion Penetration

The chloride ion diffusion coefficients as measured for different concrete mixes are plotted and are shown in Figure 4.5. Even though, both AASC with sand/CS and OPC mixes can be classified as low permeable concrete as diffusion coefficient results are very much less than $1 \times 10^{-12} \text{ m}^2/\text{s}$, as per the recommendations of the Concrete Society (Basheer, 2001), AASC mixes with sand/CS further lower than OPC based control concrete, which is explained by the increased tortuosity, lower total porosity and lower water -absorption properties of AASC mixes than OPCC. Such lower chloride diffusion coefficients also suggest better corrosion protection to rebars embedded in structural concrete made of AASC mixes.

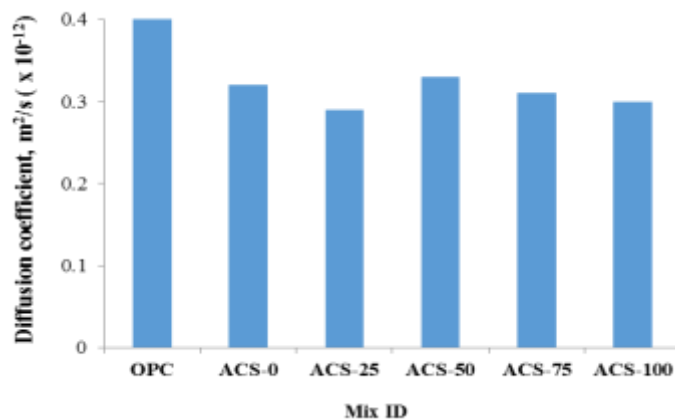


Fig 4.5 Comparison of chloride diffusion coefficient of concrete mixes

4.4.3 Sulfate Attack Resistance Test

The test results of sulfate attack on the compressive strength of various concrete mixes, subjected to 10% sodium sulfate and 10% magnesium sulfate solutions up to an extended duration of one year are presented in Figures 4.6 and 4.7, respectively. While no strength degradations were observed for any of the mixes over this long period, from the results (Figure 4.6), it may be observed that the AASC mixes with sand/CS display marginally better performance as compared to OPCC considering the strength variation when immersed in sodium sulphate solution. However, a continued reduction in compressive strength of test specimens of all concrete mixes was observed on exposure to 10% magnesium sulphate solution. The AASCs with sand/CS displayed higher strength-loss in the range of 23-26% as compared to 15%

strength loss in case of OPCC when subjected to magnesium sulphate environment at the end of 12 months. The lower performance of AASCs with sand/CS in magnesium sulphate environment may be due to the absence of calcium hydroxide $[Ca(OH_2)]$ (Bakharev et al. 2002) which restricts the formation of protective brucite layer (as formed in OPCC), thus leading to the direct attack of magnesium ions on the C-S-H structure resulting in the formation of M-S-H and gypsum. Both M-S-H and gypsum are expansive in nature and their volumes cannot get accommodated in the limited pore spaces in AASC mixes thus leading to cracking of concrete specimens. Some earlier studies (Hughes 1985, Mangat and El-Khatib 1992, Al-Amoudi et al. 1995) also have reported similar poor performance of dense hydrated cements in magnesium sulphate environments.

The results obtained indicate that the rate and effects of deterioration in sulphate environment are mainly governed by the cations which accompany the sulphate anions. The exposure of concrete mixes to magnesium sulphate can have deleterious effects on the strength of concrete mixes; however the effect of sodium sulphate of similar concentration may have little or no effect on the strength of the AASC mixes.

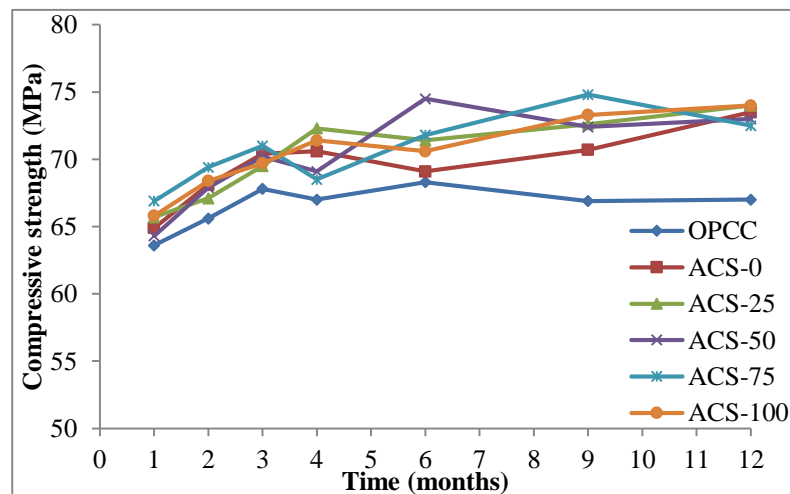


Fig 4.6 Compressive strength of AASC mixes in 10% Na_2SO_4 solution

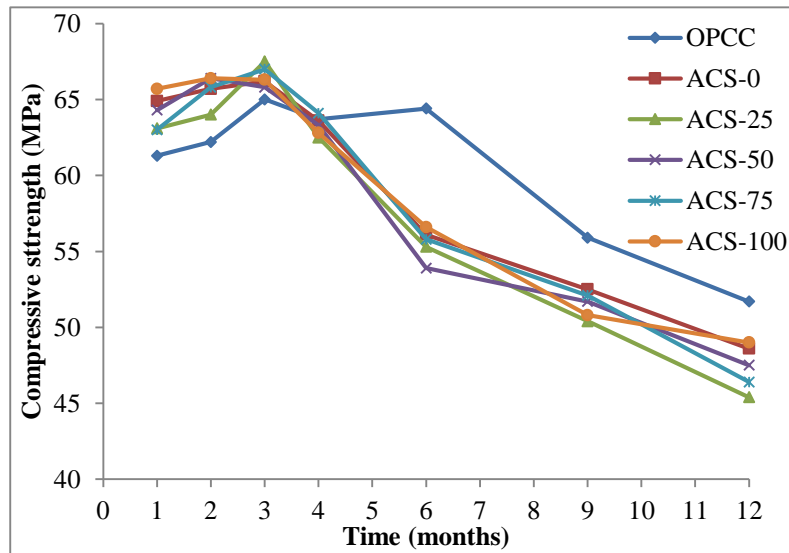


Fig 4.7 Compressive strength of AASC mixes in 10% MgSO₄ solution

4.4.4 Sulphuric acid attack

The photographs of the cube specimens of both OPCC and AASCs (with sand and/or CS) exposed to Sulphuric acid solution (pH=1) for 4 months are presented in Figure 4.8 (a-f). The OPCC specimens (Figure 4.8 a) have got the coarse aggregate completely exposed while, the AASC specimens (with sand and/or CS fine aggregates) show expansion cracks due to extensive formation of gypsum in the regions close to the surfaces (Allahverdi and Frantisek 2000) which in-turn is reflected in an increase in the mass of all AASC specimens as depicted in Figure 4.9. The AASC with CS fine aggregates displayed reduced mass-gains as compared to AASC specimens with sand. However, with time it was observed the mixes displayed mass losses. AASC mixes with CS recorded greater mass-losses as compared to AASC specimens with sand. The mix ACS-100 displayed mass-loss at 45 days while for ACS-0 mix mass-loss took place at 120 days, which may be attributed to solubility of CS fine aggregates in acid medium (Robin and Horst 2005).

The compressive strength development during the experiments for the different mixes are shown in Figure 4.10. Compared to specimens tested at 28-days of curing, OPCC samples had about 50% loss at 60-days and 71% at 120-days. Corresponding losses in strength at 120 days for ACS-0, ACS-25, ACS-50, ACS-75 and ACS-100, are much lower at about 21%, 28%, 34%, 40% and 45% respectively. Thus, ACS-0

mix performed better than OPCC when exposed to the sulphuric acid solution and with increased replacement of CS to river sand in AASC mixes, the loss in compressive strengths is much faster. This may be attributed to CS aggregates which are dissolved earlier in acid solution and the space left is substituted by acid filled



(a) OPCC



(b) ACS-0



(c) ACS-25



(d) ACS-50



(e) ACS-75

(f) ACS-100

Fig 4.8 (a-f) Appearance of AASC cubes exposed to sulphuric acid (pH=1) at 120 days

pores. Further increased dissolution of CS increases the acid filled pores and hence the diffusion of acid through these pores accelerates the transportation of acid to greater depths, leading to higher acid corrosion (Robin and Horst, 2005).

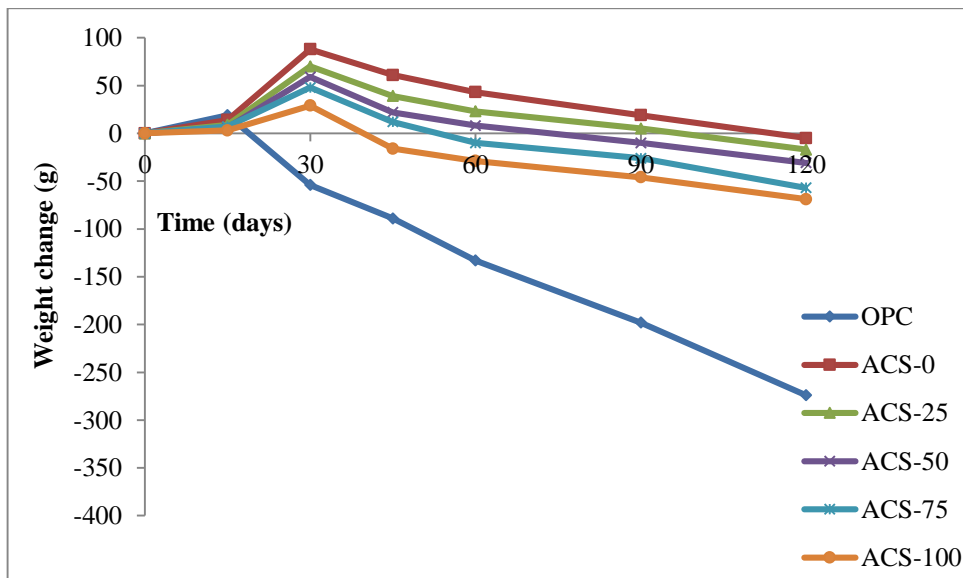


Fig 4.9 Weight changes of AASC mixes in H₂SO₄ solution (pH=1)

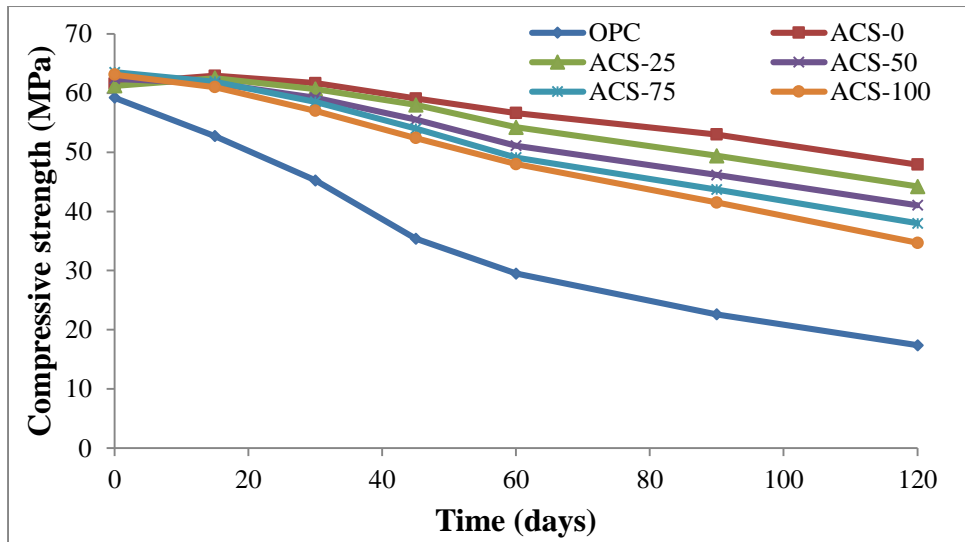


Fig 4.10 Loss in compressive strength of AASC mixes in H₂SO₄ solution (pH=1)

4.5 ELEVATED-TEMPERATURE PERFORMANCE OF AASC MIXES

The loss of structural integrity of RC structures on exposure to elevated temperatures is a major concern in many situations. Deterioration of the strength characteristics of OPCC and AASC mixes with various levels of CS replacements, on exposure to elevated temperatures in the range of 200⁰-800⁰C are shown in terms of the residual compressive strengths of cube specimens (Figure 4.11).

Compressive strength of concrete has a significant influence on the performance of concrete members when exposed to elevated temperature. It is found that for exposure temperature upto 200⁰C, OPCC mix shows a marginal 2% increase in its compressive strength, whereas AASC mixes with sand/CS shown increase of 10-7%, possibly owing to the increase in ‘Vander Waals’ forces due to the removal of moisture content (Khoury 1992). At 400⁰C, OPCC recorded a 10% reduction in compressive strength while in AASC only 1% decrease is observed. However as the CS replacement level increased, strength reduction reached a value of about 9% for ACS-100. A sharp reduction in the strength however occurred beyond 600⁰C, due to the loss of crystal water and cracks occurred on the surface of concrete possibly as a result of differences in the rates of thermal expansion of aggregates and cement paste (Poon et al. 2001, Xu et al. 2001, Li et al. 2004). Once again at 800⁰C, as the replacement of CS increased, strength reduction is also increased, loss in strength for ACS-0 is as

high as 86% and for ACS-100 it is a higher 92%. However OPC based concrete retained up to 37% of its strength. Figure 4.12 (a-f) shows the crack pattern observed at 800°C for different mixes. It can be observed that OPC based concrete mix shows less crack-density over ACS-0 mix and the crack density increased with increased replacement of CS.

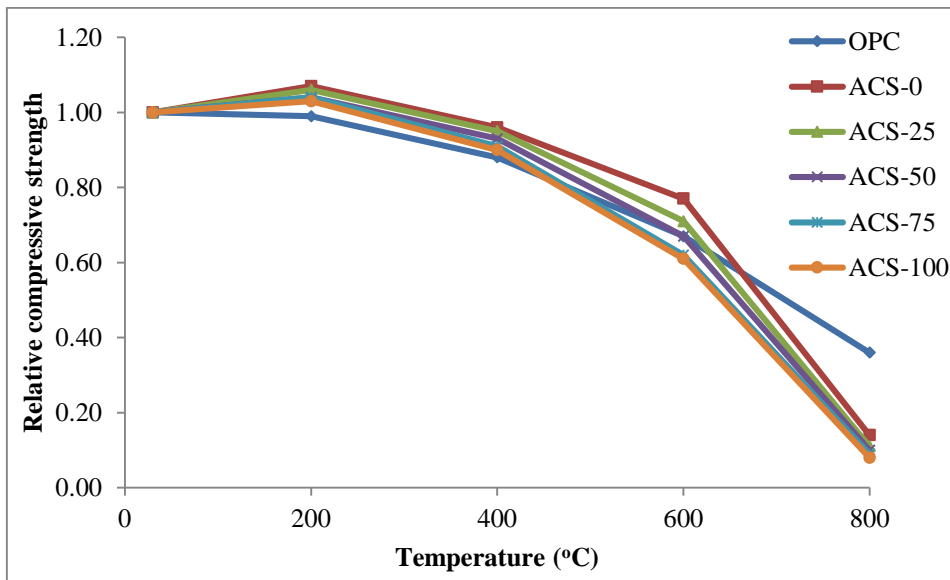


Fig 4.11 Variation in compressive strength ratio of concrete mixes under elevated temperatures



(a) OPC

(b) ACS-0

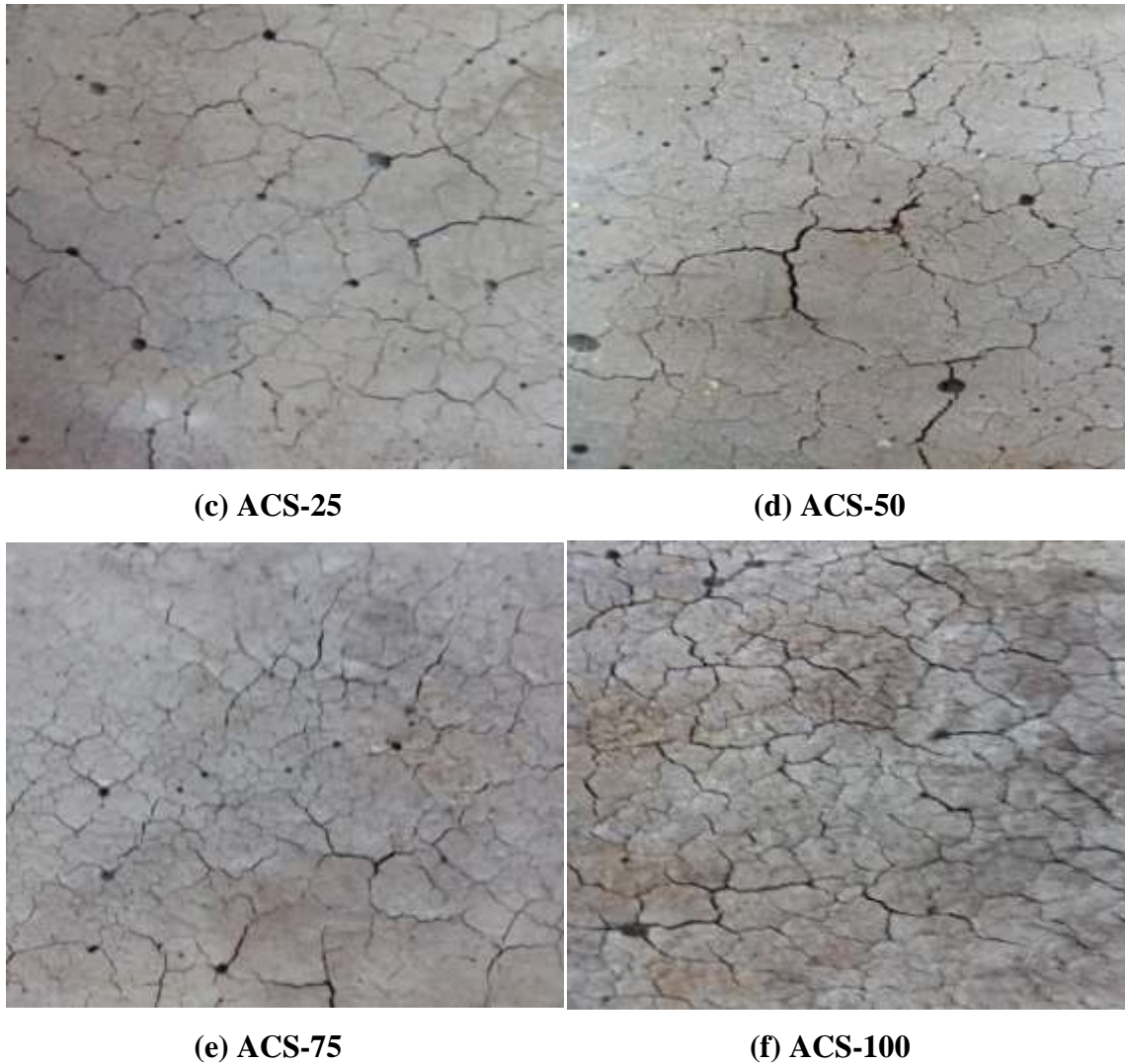


Fig 4.12 (a-f) Crack pattern for of concrete mixes at 800°C

4.6 SUMMARY

In the present chapter, the relative performance of alkali activated slag concrete mixes with CS as fine aggregate, is compared to conventional ordinary Portland cement concrete (OPCC) mix in terms of their workability, strength and durability parameters and performance on exposure to elevated temperatures. The results indicate that, AASC mixes with CS, as a replacement to sand upto 100% (by volume), show no marked losses in their strength-characteristics. AASC mixes with either sand or CS possess similar modulus of elasticity, lower total porosity, lesser water absorption and reduced chloride ion penetrations as compared to those of control OPCC mix. Strength-retention characteristics of AASC mixes with sand/CS on exposure to

magnesium sulfate showed higher rate of strength deterioration than OPCC, as measured at the end of one year. The deterioration rate of OPCC samples subjected to sulfuric acid attack was much higher than that of ACS-0. While, increased replacement of copper slag increased the rate of deterioration of compressive strength, due to solubility of copper slag in the acid medium, but still such deterioration is much less compared to that of conventional OPCC. AASC specimens with/without CS are prepared and exposed to elevated temperatures in the range of 200-800⁰C in an electric furnace, residual compressive strength results indicated that relative compressive strengths of AASCs with sand/CS were higher than that of OPC-based control concrete upto 600⁰C. The strength loss at 800⁰C for AASCs with/without CS was found to be severe. It may be concluded that the AASC mixes with sand/CS significantly promotes the residual mechanical strength properties upto a temperature of 600⁰C. However, after 600⁰C, the replacement of sand with CS reduces the resistance of AASC mixes to elevated temperatures.

CHAPTER 5

FLEXURAL FATIGUE PERFORMANCE OF CONCRETE MIXES

5.1 GENERAL

Concrete pavements may undergo failure in different types under the action of vehicular loads during their service life; one such type of failure may be due to fatigue. The fatigue strength of concrete structures such as pavements, bridges etc., subjected to repetitive loads, is one important parameter to be considered in the design of such structures. Fatigue is often described by a parameter “Fatigue life” which essentially represents the number of cycles the material can withstand under a given pattern of repetitive loading, before failure. The failure due to fatigue occurs as a result of development of internal cracks and progressive growth of cracks under the action of cyclic loadings, that leads to failure of the pavements at loads smaller than the modulus of rupture of the concrete (Li and Liu 2007, Lee and Barr 2004). In general, fatigue testing is a very time-consuming and expensive process and a large number of samples have to be tested at varied stress-levels. Again the uncertainties involved in such tests are also high. The cyclic stress levels applied on the specimens are generally described as a percentage of the static flexural strength. In this study, the performance of the different AASC mixes under cyclic stresses at levels conforming to 70% to 85% of their respective static flexural strengths is considered, at which the number of cycles to failure are determined in the tests. The tests were terminated when the failure of the specimen occurred or an upper limit of number of cyclic applications was reached, whichever was earlier. An upper limit of 1,00,000 cycles was considered in the tests conducted during the present investigation. A probabilistic analysis of fatigue test data was carried out to ascertain the fatigue life of the material.

5.2 S-N CURVE

Most of the researchers adopted the relationship between stress level (ratio of maximum applied stress to the modulus of rupture) and the number of repetitions ‘N’ causing failure, to predict the fatigue behaviour of the material. The relationship established is known as Wohler equation and is shown by S-N Curve or Wohler curve

(Oh, 1986). The use of S-N curve or Wohler curve is the most basic method of representing the fatigue behaviour of concrete specimen. The S-N curve is an important parameter in the analysis of fatigue data, where ‘S’ denotes the stress amplitude and ‘N’ denotes the number of cycles to complete failure. This S-N curve enables one to predict the mean fatigue life of concrete under given stress level or amplitude of cyclic stress (Roylance 2001).

5.3 PROBABILISTIC ANALYSIS OF FATIGUE DATA

As the fatigue test data of concrete shows a considerable scatter and is random in nature, a probabilistic approach can be introduced for analyzing the fatigue data and evaluating the probability of unfavorable performance (Oh 1986). The ASTM guidelines for fatigue testing and the statistical analysis of fatigue data (ASTM STP 91-1963) suggest that the fatigue life may be assumed to be normally distributed and thus a lognormal distribution is extensively used (Mohammadi and Kaushik 2005). Later experimental studies on the basis of physical valid assumptions have shown that the distribution of fatigue life of concrete under given stress level follows the Weibull-distribution and is most commonly employed in assessing reliability of composite structures (Sakin and Ay 2008). A Weibull-distribution is characterized by three parameters:

- 1) Shape parameter (α) which describes the shape of the distribution;
- 2) Characteristic life or scale parameter (μ); and
- 3) Location parameter (n_0).

The hazard function (Mohammadi and Kaushik 2005) can be obtained from

$$h_N(n) = \alpha \left(\frac{n-n_0}{\mu-n_0} \right)^{\alpha-1}; n \geq n_0 \quad (5.1)$$

The hazard function or failure rate function of Weibull-distribution increases with time or with an increase in the number of cycles for $\alpha \geq 1$ only, which is compatible with the expected fatigue behaviour of engineering material (Singh and Kaushik 2001). When the location parameter is set to zero ($n_0=0$), it is reduced to two parameter Weibull-distribution.

There are several methods of estimating external parameters namely: 1) Graphical method 2) Method of maximum likelihood and 3) Method of moments, etc.

5.3.1 Graphical Method

The survival function of Weibull distribution can be expressed as follows:

$$L_N(n) = \exp \left[- \left(\frac{n}{\mu} \right)^\alpha \right] \quad (5.2)$$

'n' represents specific value of random variable, ' α ' represents shape parameter or Weibull slope at stress level 'S' and μ characteristic life at stress level 'S'.

Taking twice the logarithm of both sides of Eq. 5.2.

$$\left[\ln \left[\ln \left(\frac{1}{L_N(n)} \right) \right] \right] = \alpha \ln(n) - \alpha \ln(\mu) \quad (5.3)$$

Eq. 5.3 may be written in the following form:

$$Y = \alpha X - B \quad (5.4)$$

$$\text{Where; } Y = \left[\ln \left[\ln \left(\frac{1}{L_N(n)} \right) \right] \right],$$

$$X = \ln(n)$$

$$\text{and } B = \alpha \ln(\mu).$$

The distribution parameters ' α ' and ' μ ' can be obtained from the straight line, if fatigue life data follow Weibull-distribution, which is possible if the relationship between X and Y in Eq.5.4 is linear. Hence, linear regression analysis for fatigue life data needs to be performed to get the relation for each stress level 'S' as in Eq.5.4.

In order to obtain a graphic form of Eq.5.4, the fatigue life data at a given stress level are arranged in ascending order of cycles to failure. The empirical survivorship function $L_N(n)$ for each fatigue life data ranked in the order of number of cycles to failure at a given stress level is calculated using mean rank.

The empirical survivorship function $L_N(n)$ for each fatigue life data at a given stress level is calculated using the following Eq.6.5 (Mohammadi and Kaushik 2005).

$$L_N(n) = 1 - \frac{i}{k+1} \quad (5.5)$$

Where 'i' represent failure order number and 'k' represents sample size under consideration at a particular stress level.

By plotting a graph between $[\ln[\ln(\frac{1}{L_N(n)})]]$ and $\ln(n)$, the parameters ' α ' and ' μ ' of Weibull distribution can be directly obtained; where the slope of the line provides shape factor ' α ', while the characteristic life ' μ ' can be calculated from the equation, $B = \alpha \ln(\mu)$. The graph between $[\ln[\ln(\frac{1}{L_N(n)})]]$ and $\ln(n)$ is plotted for all the stress levels and for all concrete mixes and the Weibull distribution parameters are calculated.

5.4 STATIC FLEXURAL STRENGTHS OF AASC PRISMS

The average 90-days static flexural strengths of OPCC and AASC mixes as discussed in section 4.3.2 are considered to study the fatigue performance. The Stress Ratio (S) (ratio of applied stress to static flexural strength) are fixed to 0.70, 0.75, 0.80 and 0.85, taking into consideration, the 90-days static flexural strengths obtained in Table 4.2 of section 4.3.2.

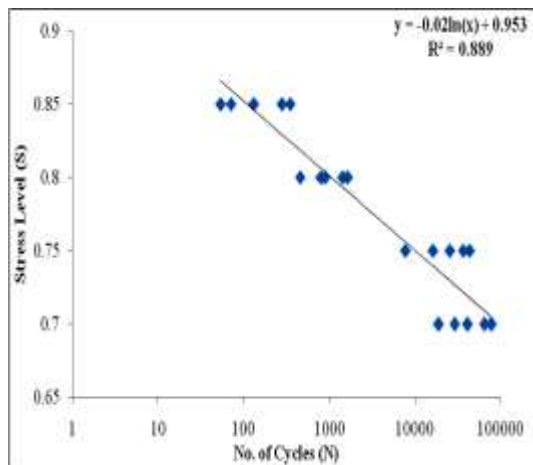
5.5 FLEXURAL FATIGUE BEHAVIOUR OF AAS CONCRETE PRISMS

The fatigue lives of concrete were obtained as per procedure mentioned in section 3.3.8. Table 5.1 presents the results of fatigue tests conducted herein on the standard prism specimens cast with OPCC and the AASC mixes, with decreasing amplitude of the repeated load.

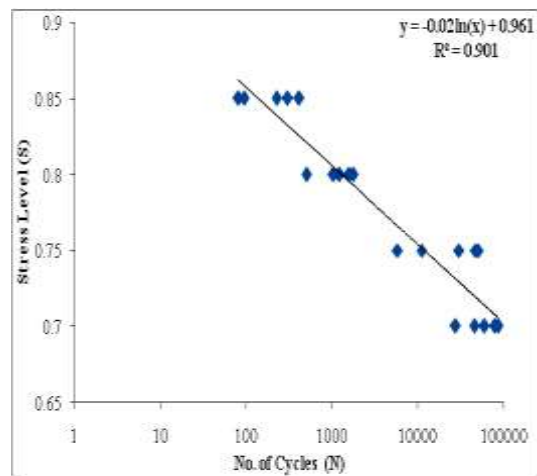
**Table 5.1 Fatigue test results for OPCC and AASC specimens
- Number of cycles N to Failure for individual test sample**

Number of Cycles to Failure (N)				
Stress Ratio (S)	OPCC	ACS-0	ACS-50	ACS-100
0.85	54	81	70	88
	71	94	110	121
	132	225	125	177
	282	302	299	312
	350	410	459	481
0.80	455	501	369	542
	794	1036	832	987
	893	1212	902	1365
	1433	1577	1345	1874
	1634	1748	1887	1991
0.75	7766	5786	10475	9698
	16347	11024	14586	18142
	25756	29786	30789	34859
	36447	46975	39486	42578
	43684	49876	56789	51476
0.70	18978	27232	15763	22786
	28967	45141	40327	32499
	41367	59201	52166	63897
	64333	78209	66896	80278
	78956	85476	88789	96178

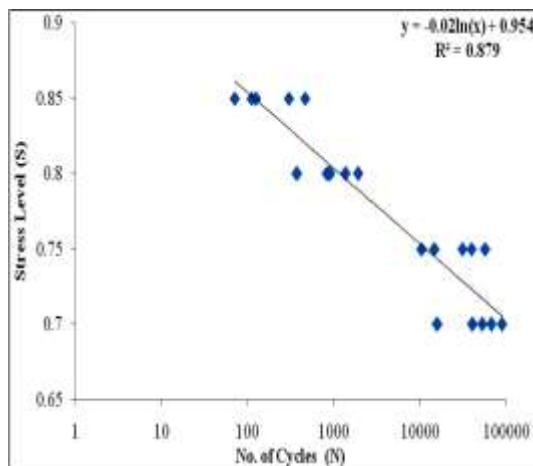
The load applied on the test specimens is represented in terms of the stress ratio. Only 50% and 100% replacement of river sand with copper slag fine aggregates used in these fatigue tests. Five test specimens are tested for each of the mixes and in Table 5.1, the number of cycles N to failure for each of the individual specimen is listed. The results of the fatigue tests are graphically represented in the form of S-N curves (Figure 5.1). The best-fit straight-line relations between Stress Ratio (S) and number of fatigue cycles (N), obtained from the experimental results for each of the concrete mixes are then obtained as listed in Table 5.2.



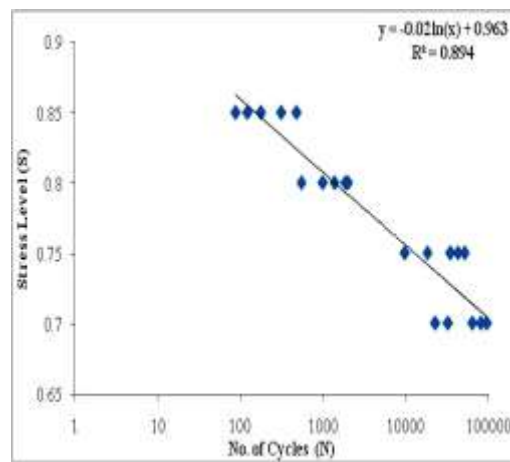
(a) OPCC



(b) ACS-0



(c) ACS-50



(d) ACS-100

Fig 5.1 S-N curves for various concrete mixes

Table 5.2 Relationship between fatigue cycle (N) and stress level (S)

Mix ID	Equations	R ²
OPCC	$\ln(N)=(0.953-S)/0.02$	0.889
ACS-0	$\ln(N)=(0.961-S)/0.02$	0.901
ACS-50	$\ln(N)=(0.954-S)/0.02$	0.879
ACS-100	$\ln(N)=(0.963-S)/0.02$	0.894

From Table 5.1, it can be seen that AASC mixes display a comparable or marginally higher fatigue performance as compared to that of an OPCC mix, which can be

attributed to the possible presence of denser interfacial zone between the aggregate and paste (Jin-Keun and Yun Yong 1996) resulting in delayed formation and slower propagation of cracks under the action of repeated loads. The ACS-100 displays better fatigue life than OPCC, ACS-0 and ACS-50 at all stress levels. A stronger bond between the copper slag and the binder paste and better packing would prove effective in transmitting higher stresses through the composite resulting in an improved fatigue resistance as compared to OPCC and AASC mixes with sand (Erdem and Blankson, 2014). While the fatigue life of any of the concrete mix is found to decrease drastically at higher stress levels (stress ratio=0.85) i.e. lower number of cycles to failure; at lower stress levels (say stress ratio=0.70), however, the number of cycles exponentially increase. From Figure 5.1, it can be observed that the fatigue data of all concrete mixes, both OPCC and AASC mixes, show a similar trend with increasing stress levels. It can also be noticed that all the mixes generally display a higher degree of scatter in their S-N Curves. However, quite satisfactory correlation coefficients (R^2) in the range of 0.88-0.90 have been recorded for the best-fit lines plotted in Figure 5.1.

5.6 PROBABILISTIC ANALYSIS OF FATIGUE TEST DATA

The Weibull distribution parameters for various concrete mixes are obtained by plotting graphs between $[\ln[\ln(\frac{1}{L_N(n)})]]$ and $\ln(n)$. A sample plot for ACS-100 at stress level of 0.85 is depicted in Figure 5.2. The Weibull distribution parameters, α and μ , for all of OPCC, ACS-0, ACS-50 and ACS-100 mixes, at different stress levels are presented in Table 5.3. It can be noticed from the Table 5.3, that the statistical coefficients of correlation range from 0.91 to 0.99 at different stress levels, for all the mixes which signify that the Weibull distribution describe the distribution of fatigue data of OPCC and AASC mixes sand/CS, fairly well.

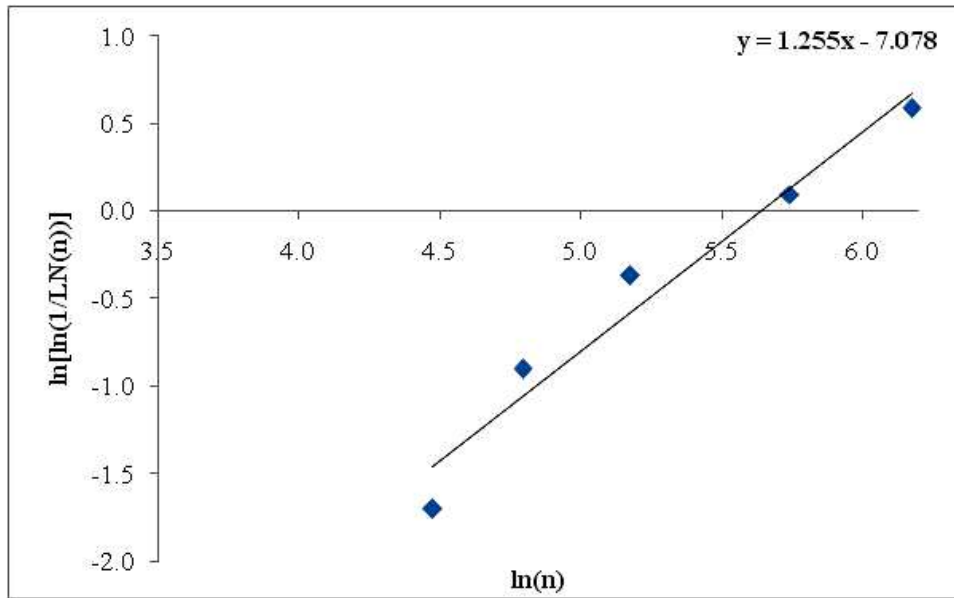


Fig 5.2 Graphical analysis of fatigue for ACS-100 at stress level of 0.85

Table 5.3 Values of Weibull parameters for concrete mixes at different stress levels

Mix ID	OPCC			ACS-0		
	α	μ	R^2	α	μ	R^2
0.85	1.044	215	0.938	1.191	271	0.927
0.80	1.711	1234	0.97	1.739	1451	0.938
0.75	1.266	31677	0.971	0.909	35388	0.945
0.70	1.518	55396	0.987	1.893	69676	0.977
Mix ID	ACS-50			ACS-100		
Stress Level	α	μ	R^2	α	μ	R^2
0.85	1.100	255	0.916	1.255	281	0.955
0.80	1.420	1289	0.965	1.685	1551	0.913
0.75	1.241	36890	0.967	1.265	38305	0.965
0.70	1.308	65226	0.955	1.412	71877	0.959

5.7 GOODNESS-OF-FIT TEST FOR FATIGUE DATA

It has been established that the fatigue life data of an OPCC mix and AASC mixes with or without copper slag, can be modeled using Weibull-distribution at various stress levels. However, it would be far more convincing to perform a goodness-of-fit

test; the results of such goodness-of-fit tests would then indicate whether Weibull-distribution is a valid distribution model for statistical description of fatigue life of OPCC and AASC mixes or not. (Mohammadi and Kaushik 2005). The Kolmogorov-Smirnov test is adopted in the present investigation for this purpose. The pertinent calculations for the said test are indicated for a typical mix ACS-0 at stress ratio of 0.85 in Table 5.4

Table 5.4 Kolmogorov–Smirnov test of fatigue life data for ACS-0 at S=0.85

Stress Ratio (S)	<i>I</i>	<i>X_i</i>	$F^+(X_i) = i/k$	$F(X_i)$	$F^+(X_i) - F(X_i)$
0.85	1	81	0.2	0.2113	0.0113
	2	94	0.4	0.2467	0.1533
	3	225	0.6	0.5512	0.0488
	4	302	0.8	0.6794	0.1206
	5	410	1	0.8055	0.1945

From the Table 5.4, it can be noted that the maximum difference D_t is 0.1945 (for $i=5$) for ACS-0 at stress ratio of 0.85. From Kolmogorov-Smirnov Table (Kennedy and Neville 1986), the critical value D_c for $n=5$ and at 5% significance level, is found to be 0.563. Since $D_t < D_c$ ($0.1945 < 0.563$), the present two-parameter Weibull-distribution model for fatigue life at stress ratio $S=0.85$ is assumed to be acceptable at the 5% significance level. Such goodness-of-fit tests are performed for the fatigue life data for the OPCC and all the three AASC mixes, at the different three stress ratios and the models were found to be acceptable at 5% level of significance, in each of the case.

5.8 PREDICTION OF FATIGUE LIFE OF AASC MIXES – APPLICATION OF WEIBULL PARAMETERS

The analysis carried out in the preceding sections has shown that the fatigue data of AASC mixes can be well described using the two-parameter Weibull distribution. Now that the Weibull parameters α and μ are known, for any of the mixes, at corresponding stress ratios, they can be used to calculate the fatigue lives of flexural beams under cyclic loading. The fatigue life at different probabilities of failure (P_f) can be expressed as follows:

$$n = \exp \left[\frac{\ln \left\{ \ln \left(\frac{1}{1-P_f} \right) \right\} + \alpha \ln(\mu)}{\alpha} \right] \quad (5.6)$$

The values of α and μ attained from Weibull distribution analysis are substituted in the Eq.5.6 to predict fatigue lives of concrete beam samples at different probabilities of failure (P_f). As an illustration, the expected fatigue lives at different survival probabilities i.e. (0.05, 0.5 and 0.95) are calculated for OPCC, AASC mixes with sand/CS fine aggregates and the results are depicted in Figure 5.3. From the different graphs in Figure 5.3, it is apparent that at a specific stress ratio, with decrease in probability of failure, the number of cycles for failure increases exponentially. The expected number of cycles is greater at lower probabilities of failure. Figure 5.3 can be used to forecast the probable fatigue life of OPCC, AASC mixes with sand/CS fine aggregate, at any specified stress ratio at a specific probability of failure.

5.9 SUMMARY

The present chapter summarizes the results of the fatigue experiments carried out on concrete mixes. The flexural fatigue performance of AASC mixes incorporating 0%, 50% and 100% (by volume) CS fine aggregate have been investigated. The specimens were subjected to different stress ratios (0.70, 0.75, 0.80 and 0.85) and the number of cycles for failure of the specimen was determined. The fatigue data were represented using S-N curves. A probabilistic analysis of the obtained fatigue test data was carried

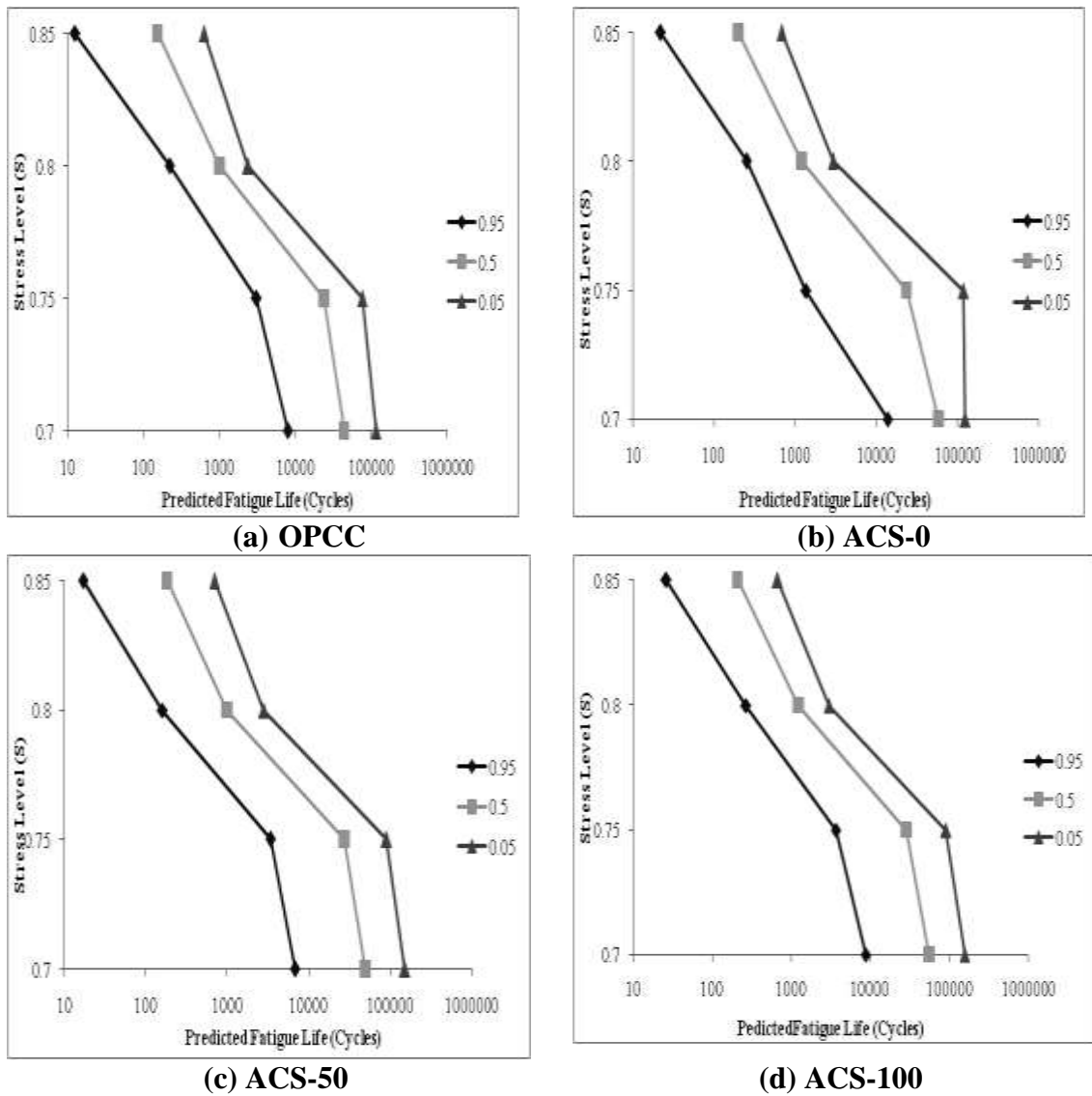


Fig 5.3 Predicted fatigue lives corresponding to different survival probabilities for various concrete mixes

out to ascertain the fatigue life of the material using two parameter Weibull distributions. Graphical method was adopted to determine the Weibull parameters. The tests for goodness-of-fit are carried out to verify the statistical significance of the obtained data. The outcomes of the Weibull distribution are analyzed to predict the fatigue life of concrete mixes with the desired probability of failure. The flexural strength of AASC mixes with sand/CS is also higher compared OPCC of similar compressive strength. The AASC mixes with sand/CS shows better fatigue life as compared to that of OPCC due to dense and uniform interfacial transition zone. All

the concrete specimens were found to fail in the flexure zone. The two parameter Weibull-distribution has been utilized for the statistical analysis and it can be used for approximate modeling of fatigue data of OPCC and AASC mixes with sand/CS statistical correlation higher than 0.87. The parameters obtained from Weibull distribution may be utilized for carrying out prediction modeling with survival probability for OPCC and AASC with sand/CS mixes. The goodness-of-fit test is performed for the fatigue life data for OPCC, ACS-0, ACS-50 and ACS-100 at different stress levels and the model was found to be acceptable at 5% level of significance. The expected fatigue lives at different survival probabilities i.e. (0.05, 0.5 and 0.95) are determined for OPCC, AASC mixes with sand/CS and it was found that at a specific stress level; the number of cycles for failure increases with decrease in probability of failure.

CHAPTER 6

FLEXURAL BEHAVIOUR OF REINFORCED, ALKALI ACTIVATED CONCRETE BEAMS

6.1 INTRODUCTION

All Portland cement-based matrices are quite weak in tension (as compared to compression), and hence in all structural components, appropriately designed steel reinforcement is required to be provided to resist the tensile stresses. Thus, providing steel reinforcement is essential in structures. The efficiency of any structural component then depends on the realization of a perfect bond between the concrete and the steel rebars. Increased application of AASC in structures would then require the demonstration of such bond between steel rebars and concrete matrix and hence good structural performances of beams and columns made of AASC mixes. Such an evaluation of the flexural behaviour of reinforced AASC beams incorporating sand/CS as fine aggregate in comparison to that of a conventional reinforced OPC-based concrete beam is hence necessary and the same is attempted as detailed in this chapter.

The details of geometry and reinforcement provided in the test beams have been discussed in section 3.10. The simply supported beams have been designed as under-reinforced beams, provided with adequate shear reinforcement so as to prevent failure in shear. The beams are tested under conventional third point loading test. The flexural behaviour of OPCC and AASC beams under monotonically increasing load is evaluated in terms of parameters like load at first crack, service load, ultimate load, and the corresponding deflections. Moment-Curvature relations are also derived for the beams and development of cracks in such beams under higher loads are also studied.

6.2 FLEXURAL BEHAVIOUR OF RCC BEAMS- LOAD CONSIDERATIONS

Tests were conducted on a total of twelve beams of rectangular cross-section. Each beam had a width of 150mm, overall depth of 250mm and a total length of

2550mm. Three beams were tested for each of the four representative mixes. The grade of concrete considered was M45. Tensile reinforcement at approx. 1.032% provided in the form of three, 12mm dia bars, corresponding to an under reinforced section, was used in each of the beams tested. In all the beams, shear stirrups were of 2L, 8mm size and spaced at 125mm c/c throughout the span. Two 8 mm diameter hanger bars were provided on the compression side to support the stirrups. All the beams were tested at 28-days of curing, under three-point loading (Figure 3.4). Details of 28-day compressive strength of concrete mixes used in OPCC beams and AASC beams are tabulated in Table 8.1. All the pertinent theoretical calculations with respect to computation of load at first-crack, service load, ultimate load and deflections etc., as per provisions of IS 456-2000, are illustrated with respect to OPCC beam in **Appendix III**.

A comparison of flexural performance of AASC beams of sand/CS as fine aggregate with OPCC beams is presented in the following order:

- Load at First-Crack, Service and Ultimate Loads
- Load-Deflection Behavior of Beams
- Moment-Curvature Relations of the Beams
- Cracking Pattern

Table 6.1 Test details of OPCC and AASC cubes at 28 days

SL. No	Beam Designation	Reinforcement (%)	28-day Compressive Strength (MPa)
1	OPCC	1.032%	53.0
2	ACS-0		55.2
3	ACS-50		54.5
4	ACS-100		53.8

6.2.1 Loads at First-Crack

Table 6.2 compares the first-crack loads experimentally determined with their theoretical values (determined as per IS 456-2000) of all the beams tested. It can be seen that the experimental values of the first-crack loads in OPCC beams are found to be very much comparable in magnitude to AASC beams with sand/CS fine aggregate

From Table 6.2, the first-crack load for OPCC beam is 18.2 kN. The experimental values of first-crack load for different beams are found to be almost 8-15% lower than their respective theoretical values, for both OPCC and AASC beams with sand/CS fine aggregate.

6.2.2 Service Loads on Beams

From Table 6.2, it is observed that the service load, for the OPCC beam (54.0kN) is very much comparable to the service loads for the three AASC beams with sand/CS fine aggregate. (54.6-56.1kN). It is also seen that experimental values of service loads are 12-17% greater than their theoretical values for OPCC and AASC beams.

6.2.3 Ultimate Loads on Beams

The experimental and theoretical ultimate loads of the beams tested are also tabulated in Table 6.2. Again it is to be noted that the experimental ultimate loads of all the AASC mixes with sand/CS beams are similar in magnitude to that of the OPCC beam. Increase in percentage of CS replacement in AASC mixes has shown no significant changes in the ultimate load carrying capacity of reinforced AASC beams.

From Table 6.2, For OPCC and all AASC beams, the first crack load is 0.22-0.23 times that of ultimate load. It is seen that experimental ultimate load values are higher than the theoretical values. The ratio of experimental ultimate loads to their theoretical values ($P_{u(\text{exp})} / P_{u(\text{theo})}$) (in the range of 1.12-1.17) are more than one for OPCC and AASC beams with sand/CS which indicates that the theoretical values are conservative.

Table 6.2 Load at first crack, service and ultimate loads of OPCC and AASC Beams

SL. No	Beam Designation	Flexural strength values of AASC beams (kN)									Ratios		
		First-Crack load (P_{cr})			Service Load (P_s)			Ultimate load (P_u)					
		Exp. P_{cr} (Exp)	Avg. P_{cr} (Exp)	Theo. P_{cr} (Theo)	Exp. P_s (Exp)	Avg. P_s (Exp)	Theo. P_s (Theo)	Exp. P_u (Exp)	Avg. P_u (Exp)	Theo. P_u (Theo)	$\frac{P_{cr} (Exp)}{P_{cr} (Theo)}$	$\frac{P_s (Exp)}{P_s (Theo)}$	$\frac{P_{cr} (Exp)}{P_u (Exp)}$
1	OPCC	17.9	18.2	19.7	53.8	54.0	48.0	80.7	81.0	72.1	0.92	1.12	0.22
		18.6			55.2			82.8					
		18.1			53.0			79.5					
2	AASC-0	18.8	19.1	22.6	55.7	54.6	48.2	83.5	81.9	72.3	0.85	1.13	0.23
		19.6			54.0			81.0					
		19.0			54.2			81.4					
3	AASC-50	18.4	19.2	22.1	55.9	55.7	48.2	81.5	82.8	72.3	0.87	1.15	0.23
		19.3			54.6			81.9					
		19.8			56.6			84.9					
4	AASC-100	19.2	19.6	22.9	56.1	56.1	48.1	84.1	84.3	72.2	0.86	1.17	0.23
		20.0			57.1			85.7					
		19.5			55.3			83.0					

6.3 LOAD DEFLECTION BEHAVIOR - DEFLECTIONS AT MID SPAN

Comparison of structural response of AASC beams (with sand/CS fine aggregate) with that of an OPCC beam is carried out with respect to their load deflection behavior under flexure. Deflections are measured at mid span and at load points at all increments of the load. The measured mid span deflections, with increasing load are plotted for one candidate beam specimen for each of the OPCC and AASC mixes (with sand/CS fine aggregates), in Figure 6.1.

To discuss the load deflection behavior, deflections at three load levels namely, deflections at first crack-load (Δ_{cr}), at service load (Δ_s) and at ultimate load (Δ_u) are considered. Experimental and theoretical mid-span deflections of OPCC and AASC beams tested are presented in Table 6.3.

Typical results are also graphically presented in Figure 6.2. 15% higher are the experimental deflection values at service loads vis-à-vis the theoretical deflection values for OPCC, while the experimental values are up at 39-51% more than theoretical values for the AASC beams.

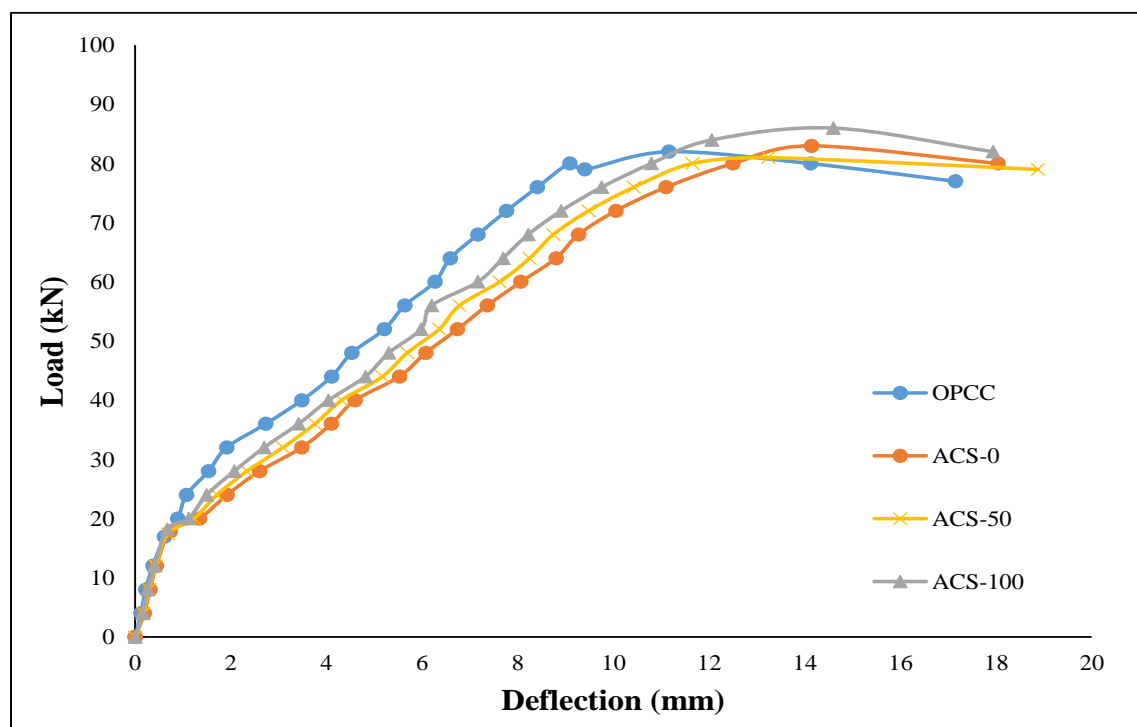


Fig 6.1 Deflections at Mid-span for reinforced OPCC and AASC beams

Table 6.3 Mid-span deflections of OPCC and AASC beams at different load levels

Designation	Mid –Span Deflections									
	Experimental Values						Theoretical Values		Ratios	
	Δ_{cr} (mm)	Avg. Δ_{cr} (mm)	Δ_s (mm)	Avg. Δ_s (mm)	Δ_u (mm)	Avg Δ_u (mm)	Δ_{cr} (mm)	Δ_s (mm)	$\frac{(\Delta_{cr})_{Exp}}{(\Delta_{cr})_{Theo}}$	$\frac{(\Delta_s)_{Exp}}{(\Delta_s)_{Theo}}$
OPCC	0.61	0.61	5.34	5.38	11.33	11.10	0.67	4.67	0.91	1.15
	0.60		5.48		11.04					
	0.61		5.32		10.92					
ACS-0	0.68	0.68	7.26	7.34	14.12	14.23	0.82	4.86	0.83	1.51
	0.67		7.36		14.06					
	0.68		7.42		14.52					
ACS-50	0.66	0.66	6.55	6.52	13.24	13.55	0.78	4.78	0.85	1.36
	0.67		6.44		13.76					
	0.66		6.56		13.60					
ACS-100	0.64	0.65	6.38	6.39	13.68	13.29	0.78	4.71	0.83	1.35
	0.65		6.35		13.04					
	0.65		6.44		13.24					

6.3.1 Span Deflection Profiles

Deflection profiles along the span are plotted in Figure 6.2, for the OPCC beam and the AASC beams, at the same three load levels indicated earlier i.e., load at first-crack, service load and ultimate load. These profiles clearly indicate that the deflection experienced by the OPCC beam is much smaller in comparison to those in the AASC beams. Again, as the replacement of CS increases, deflections are seen to decrease due to increased modulus of elasticity of CS-admixed concrete mixes.

At the first-crack load levels, the magnitude of measured deflections of ACS-0, ACS-50 and ACS-100 beams are respectively 1.11, 1.08 and 1.07 times the deflections of the OPCC beam, while at the service load level, the magnitude of these deflections are respectively 1.36, 1.21 and 1.19 times the deflection of the OPCC beam (Table 6.3). At ultimate loads, the magnitude of measured deflections of ACS-0, ACS-50 and ACS-100 beams are comparatively higher at 1.28, 1.22 and 1.20 times the deflection of the OPCC beam respectively.

It is also observed from results in Table 6.3 that the experimental values of deflection are lesser than theoretical deflections at first crack load while they are higher at the service load, for both OPCC and AASC beams with sand/CS fine aggregates. The experimental mid-span deflection value at first crack load is 0.91 times the theoretical deflection in OPCC beam, while in AASC beams, experimental mid-span deflections at first crack load are again comparable 0.83, 0.85 and 0.83 times the theoretical values for ACS-0, ACS-50 and ACS-100 beams respectively. Similarly at their respective service loads such experimental mid-span deflections are on an average 1.15, 1.51, 1.36 and 1.35 times their theoretical values in the OPCC beam and the AASC beams ACS-0, ACS-50 and ACS-100 respectively.

Again the experimental deflections at mid-span of all the OPCC and AASC (with sand/CS aggregates) beams are well within the limit of the maximum allowable deflection at service loads, as specified in IS: 456-2000 i.e. $\text{Span}/250$.

It is observed that all AASC beams are relatively more ductile than OPCC beams; but as the CS replacement increases in the AASC mixes, the ductility of AASC beams

appear to decrease; however the ductility in them is marginally greater than in the OPCC beam.

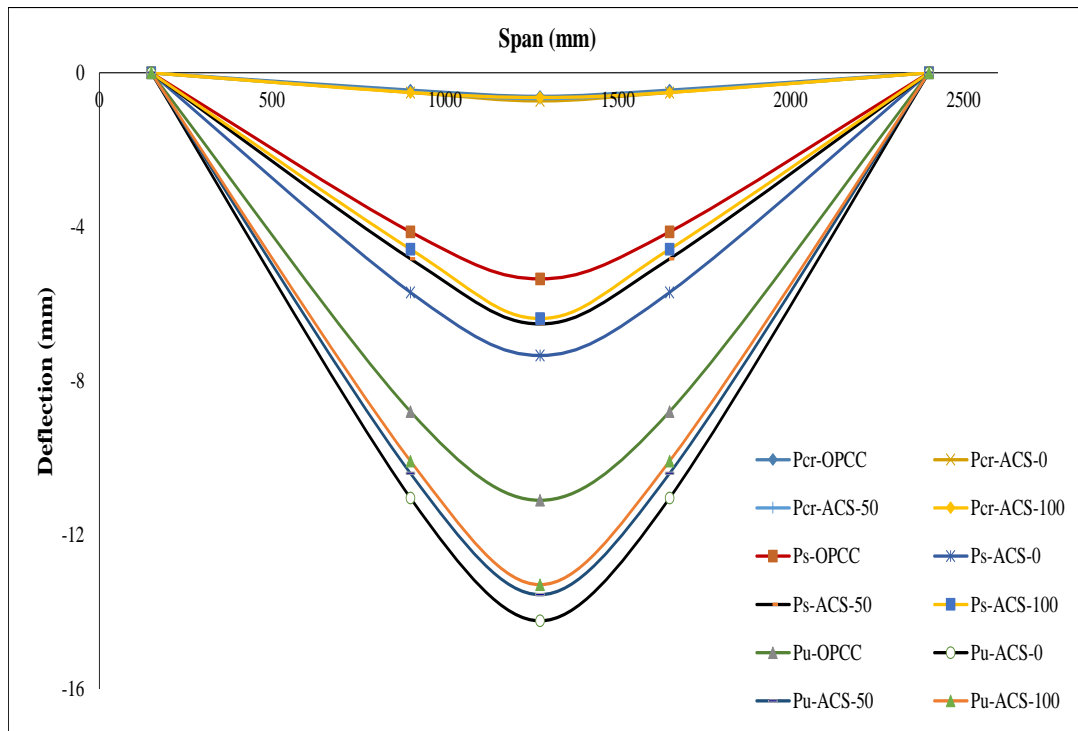


Fig 6.2 Deflection profiles of beams at load at first crack, service and ultimate loads

6.4 MOMENT-CURVATURE RELATION FOR AASC BEAMS

A study of moment-curvature relations of RCC beams assists in evaluating the rotation capacities of the beam and helps in assessing the capacity of the structure to redistribute the moment after yielding. The ultimate moments and corresponding curvatures of all the OPCC beam and AASC beams with sand/CS fine aggregates are computed based on the test results and are tabulated in Table 6.4.

Variation of curvatures with increasing magnitude of the bending moments, in the central sections of the test beams, are depicted in Figure 6.3. It can be observed from the test results plotted herein that there is no considerable difference in ultimate moment carrying capacities between OPCC and AASC beams with sand/CS fine aggregate. From Table 6.4, it is clear that ultimate moment carrying capacity of OPCC beams is approximately same as the ultimate moments of AASC beams, which

again are not varying much with increasing percentage of CS used as fine aggregate. The ultimate curvature of AASC beam with 100% sand is found to be higher than that of the OPCC beam and with increasing replacement of sand by CS, the ultimate curvatures are found to decrease very marginally.

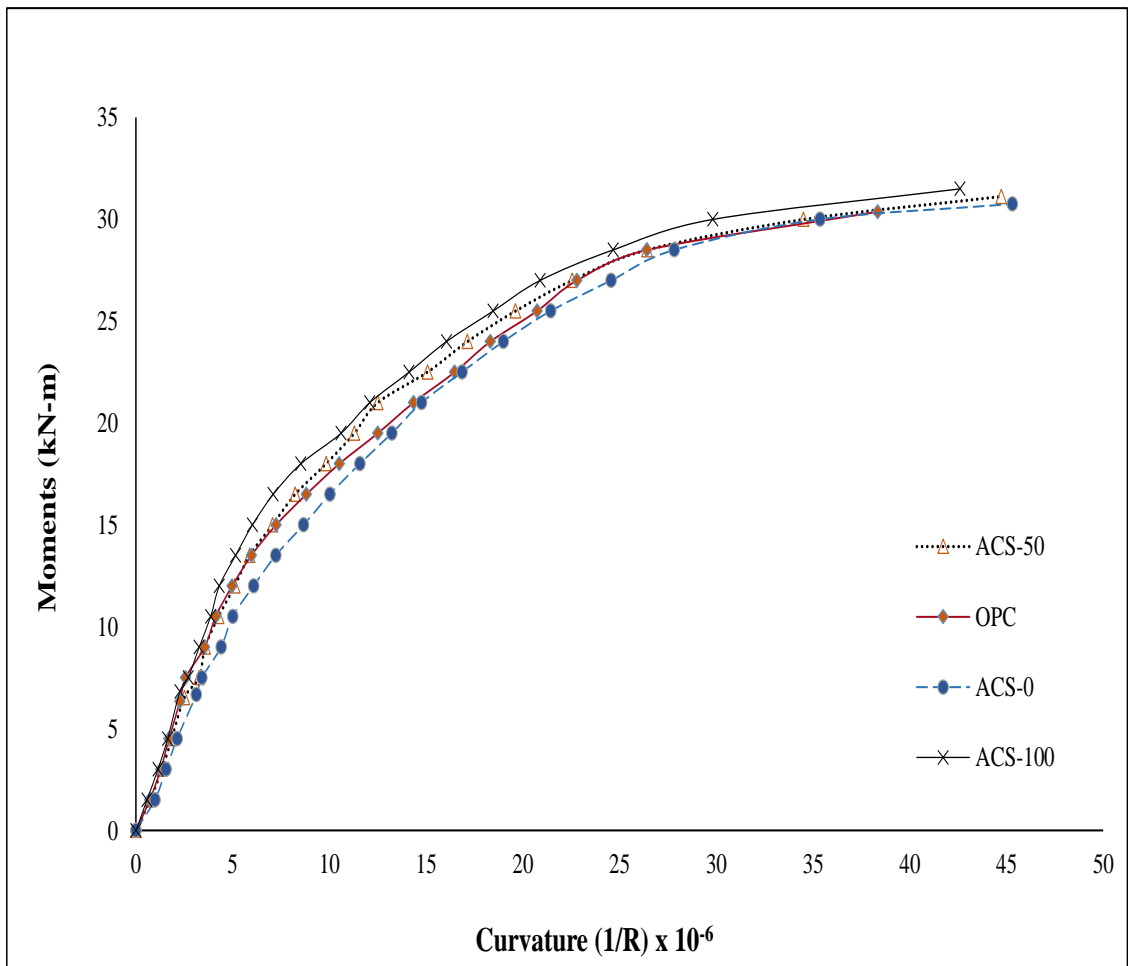


Fig 6.3 Moment curvature profiles for test beams

Table 6.4 Ultimate moments and curvatures for test beams

SL. No.	Beam Designation	Ultimate Moment (kN-m)	Ultimate Curvature (Radians/mm 10^{-6})
1	OPCC	30.4	38.3
2	ACS-0	30.8	45.3
3	ACS-50	31.1	44.7
4	ACS-100	31.5	42.6

6.5 CRACK PATTERNS

As expected, flexural cracks got initiated in the pure bending zone. As the load is increased, existing cracks propagated and new cracks developed along the span. Flexural cracks in the shear span turned into inclined cracks due to the effect of shear force. The width of cracks varied along the span. The cracks at the mid-span opened widely near failure. Near failure load, the beams deflected significantly, thus indicating that the tensile steel to have yielded, at failure. At the ultimate load of the beams, the concrete in the compression zone started getting crushed. The failure mode was, by design, typical of that of an under-reinforced concrete beam.

The crack patterns of test beams are shown in Figure 6.4. Number of cracks in flexural zone and shear zones, total number of cracks and maximum crack widths at both of the service load and at ultimate load are tabulated in Table 6.5, for the representative test beams for comparison purposes.

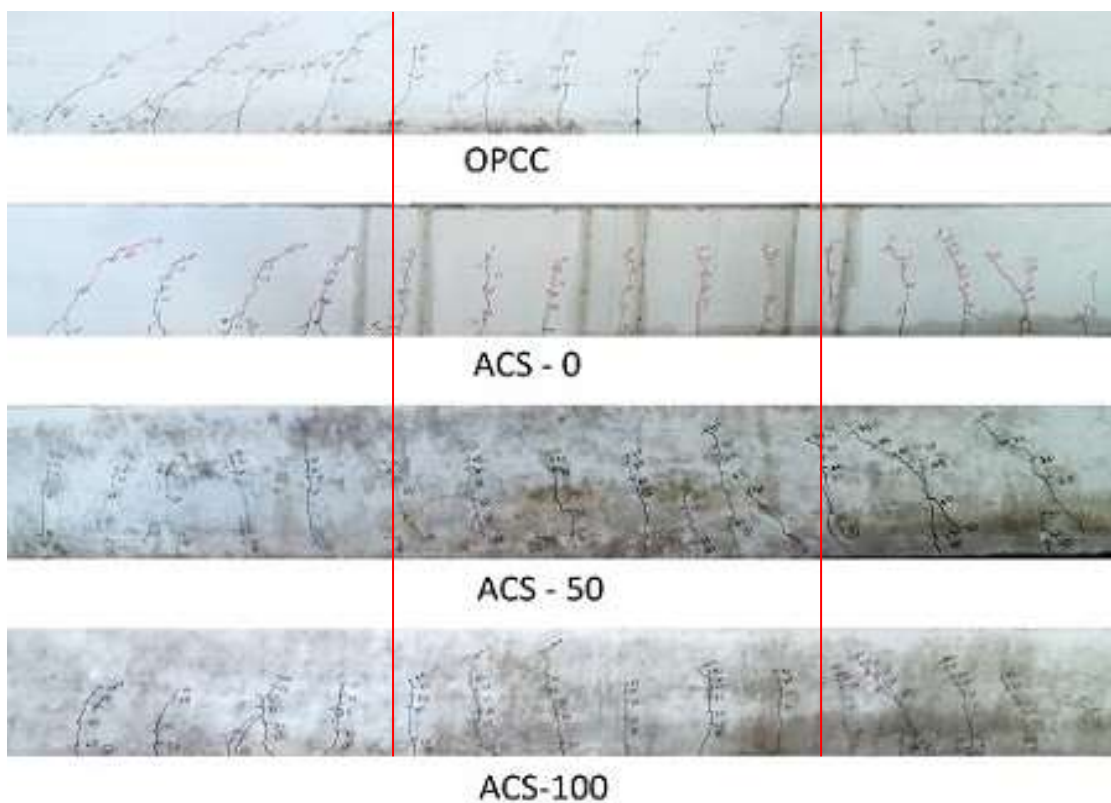


Fig 6.4 Crack pattern of all test beams

Table 6.5 Test result of crack profiles

SL. No.	Beam Designation	Total No of Cracks at Ultimate load	No of Cracks in Flexural Zone	No of Cracks in Shear Zone	Width of First Crack at Service Load (mm)	Width of First Crack at Ultimate Load (mm)
1	OPCC	14	6	8	0.25	0.33
2	ACS-0	15	6	9	0.29	0.37
3	ACS-50	15	7	8	0.27	0.35
4	ACS-100	15	6	8	0.27	0.34

Between OPCC and AASC beams with sand/CS, not much difference between numbers of cracks at failure was observed. Final Crack-widths were just marginally more in case of AASC beams than OPCC beams and they decreased, though very marginally, with increasing CS replacement.

In all, failure behavior and the final crack patterns observed for reinforced AASC beams with sand/CS were very much similar to those in a reinforced OPCC beam.

6.6 SUMMARY

Summing up, it can be said that it is possible to obtain quite a comparable flexural response in reinforced AASC beams, with either sand or CS (upto 100% replacement level) fine aggregates as obtained in a control OPC based concrete beam, with respect to each of load or moment carrying capacity, stiffness (deflection or curvature) and cracking behavior.

CHAPTER 7

ECOLOGICAL ANALYSIS OF CONCRETE MIXES

7.1 GENERAL

Cement is manufactured from a combination of naturally occurring minerals - calcium (60% by weight) mainly from limestone (CaCO_3), silicon (20%), aluminum (10%), iron (10%) and small amounts of other ingredients and heated in a kiln to about 1500°C to get the clinker. The main sources of emission of CO_2 herein is in the use of fossil fuels in the burning process and the calcination process where CaCO_3 is broken down to calcium oxide, other sources being processes such as operation of mining equipment to extract the raw materials and transportation of the raw materials to the cement plant (NRMCA, 2008). Global CO_2 emissions from cement production (377 million metric tons of carbon in 2007) represent 4.5% of global CO_2 releases from fossil-fuel burning and cement production (Marland et al. 2007). Concrete uses about 7% to 15% cement by weight, average being around 250 kg/m^3 of concrete; with concrete density of 2400 kg/m^3 , about 100 to 300 kg of CO_2 is embodied in concrete which amounts to 5% to 13% of the weight of concrete (Marceau, 2007). It is also estimated that 33% to 57% of the CO_2 emitted from calcination will be reabsorbed through carbonation of concrete surfaces over a 100-year life cycle (Pade et al. 2007). It is reported that building industry contributes 22% of CO_2 emissions in the world (Reddy 2010).

Now that there are continuous demands on lowering the energy requirements in an otherwise continuously developing world of concrete infrastructure, an attempt has been made here in to compute the Embodied Energy (EE) and embodied carbon dioxide emission (ECO_2e) of the alternate concrete mixes to examine their ecological effects. The EE is the energy consumed and ECO_2e is the total CO_2 released during the entire duration of the product life (starting raw material extraction, transportation, manufacture, assembly, installation, disassembly and deconstruction for the concrete system tested herein). The data-base for computation of EE and ECO_2e for the

ingredients and the concretes are taken from the literature (Rajamane 2013). The details of the calculations are indicated in Table 7.1.

The EEs of OPCC, ACS-0 and ACS-100 have been computed at 3701, 2142 and 2091 MJ/m³ (Table 7.1) respectively and thus ACS-100 was found to be 43.5% lower in energy requirement as compared to OPCC. Similarly the ECO_{2e} of OPCC, ACS-0 and ACS-100 mixes have been calculated at 433, 221 and 218 kg CO_{2e}/m³ respectively with 50.3% lower values in CO₂ emission for ACS-100 mix as compared to OPCC. These results are found to be in agreement with those of Yang et al. (2013).

Therefore in the light of above calculations, the AASC mixes with CS fine aggregate prove to be more eco-friendly. Cost calculations also suggest that, because of high cost of OPCC, the cost of ACS-100 works out to be about 24% cheaper. Higher early strengths, even at 3-days, offer many construction advantages, which are not accounted here in costing, lead to further cost-reductions. Thus, it may be concluded that the AASC mixes with sand/CS prove advantageous ecologically and economically as compared to conventional OPCC based concrete mix. Ecological and economic analysis of concrete mixes presented here can be taken as only indicative in nature; and detailed computations need to consider many more parameters such as transportation costs etc.

Table 7.1: Ecological and economic analysis of various concrete mixes

Ingredients		Data for each material (per kg)			EE (MJ/m ³)			ECO _{2e} (kgCO _{2e} /m ³)			Cost (INR/m ³)		
		EE (MJ)	ECO _{2e} (kgCO _{2e})	Cost (Rs)	OPCC	ACS- 0	ACS- 100	OPCC	ACS- 0	ACS- 100	OPCC	ACS-0	ACS- 100
Binder	GGBFS	1.60	0.083	4.00	-	704	704	-	36.52	36.52	-	1760	1760
	OPC	4.80	0.93	8.00	2111.1	-	-	409.2	-	-	3520	-	-
Activator Solution	NaOH	20.5	3.20	22.00	-	205	205	-	32	32	-	220.0	220.0
	LSS	10.2	2.00	14.00	-	684.4	684.4	-	134.2	134.2	-	939.4	939.4
	Water	0.20	0.0008	0.01	34.88	28.16	28.16	0.14	0.11	0.11	1.74	1.40	1.40
Admixture	Super plasticizer	11.5	0.60	75.0	30.28	-	-	1.58	-	-	198.0	-	-
Aggregates	Sand	0.08	0.0051	1.00	52.65	51.03	-	3.31	3.213	-	650.0	630.0	-
	Copper slag	-	-	0.05	-	-	-	-	-	-	-	-	43.20
	Coarse Aggregate	0.083	0.0048	1.00	97.83	94.76	94.76	5.71	5.53	5.53	1178.	1141.0	1141.0
	Curing water*	0.20	0.0008	0.05	1000	-	-	4.0	-	-	250.0	-	-
Processing		0.15	0.0038	1250	375	375	375	9.5	9.5	9.5	1250.	1250.0	1250.0
Total					3702	2142	2091	433	221	217	7048.	5943.0	5355.0

Note: EE = Embodied energy, ECO_{2e} = Embodied CO₂ emitted,

** curing water = cost inclusive of labour, considering typical residential building roof slab 10 m x 10 m, depth of ponding 0.05m*

CHAPTER 8

CONCLUSIONS

8.1 GENERAL

The development and understanding of AASC mixes with industrial waste materials as aggregates are of significant interest because these new materials can be made cost-competitive to Ordinary Portland Cement (OPC) based concrete mixes, while exhibiting superior chemical, mechanical and durability properties, with lower carbon footprint. The present thesis presents details of detailed investigations carried out on the suitability of Ground Granulated Blast Furnace Slag (GGBFS) (as binder) and Copper Slag (CS) (as fine aggregate) to produce such concrete mixes. Results of the investigations have confirmed that the AASC mixes can be designed so as to develop required strength and durability characteristics for their possible application in both non-structural and structural concrete elements.

The following conclusions are drawn based on the results of experiments during the present investigation on the engineering and durability properties of a class of AASC mixes with copper slag (CS) as fine aggregate.

A. Strength and Durability of AASC Mixes

1. Strengths of AASC mixes depend on the modulus of the alkaline solution and concentration of alkalis. GGBFS exhibits selectivity towards the modulus (M_s) of sodium silicate solution based activator. For a given sodium oxide dosage (3%, 4%), use of sodium silicate solution with $M_s = 1.25$ resulted in the highest 28-day compressive strengths exceeding those of the other AASC mixes with same binder content and w/b ratio.
2. Increase in replacement of sand by CS in AASC mixes show no significant changes in the workability of the mixes.
3. AASCs show marginally higher tensile strength properties than those of control OPCC mix of similar compressive strengths but reduced modulus of elasticity. Replacing CS even up to 100% showed no marked loss in

strength parameters and increase in the CS replacement (for sand), increased the modulus of elasticity of AASC mixes.

4. AASC mixes with sand/CS exhibited lesser total porosity, lower water absorption and reduced chloride permeability than the conventional OPCC mix.
5. The compressive strength measurements showed that the strength of OPCC and AASC mixes with sand/CS showed no strength deterioration up to 12 months in 10% Na₂SO₄ solutions, with AASC mixes showing slightly higher strength increments than OPCCs. In 10% MgSO₄ solution, however, AASC mixes with sand/CS showed higher rate of strength deterioration in the range of 23-26% as compared to 15% strength loss in case of OPCC, as measured at the end of one year.
6. The deterioration rate of OPCC samples subjected to sulfuric acid attack had about 50% loss at 60-days and 71% at 120-days. Corresponding losses in strength at 120 days for ACS-0, ACS-25, ACS-50, ACS-75 and ACS-100, are much lower at about 21%, 28%, 34%, 40% and 45% respectively. While, increased replacement of CS increased the rate of deterioration of compressive strength, due to solubility of CS in the acid medium, but still such deterioration is much less compared to that of conventional OPCC.
7. ACS-0 performed better at elevated temperature up to 600⁰C by retaining higher levels of strengths, when compared to OPCC. At 800⁰C, as the replacement of CS increased, strength reduction is also increased; loss in strength for ACS-0 is as high as 86% and for ACS-100 it is a higher 92%, while OPC based concrete retained up to 37% of its strength. Increased replacement of sand with CS in AASCs, surges the strength reduction with amplified crack intensity compared to ACS-0.

B. Flexural Fatigue Performance of Concrete Mixes

8. The AASC mixes with sand/CS shows better fatigue life as compared to that of OPCC.
9. The two-parameter Weibull distribution has been utilized for the statistical analysis and it has been shown that it can be used for a satisfactory modeling of fatigue data of OPCC and AASC mixes with sand/CS statistical correlation coefficient of atleast 0.87 having been achieved.
10. The parameters obtained from Weibull distribution may be utilized for predicting the fatigue life for a given survival probability, for both OPCC and AASC with sand/CS mixes.
11. The goodness-of-fit test is performed for the fatigue life data for OPCC, ACS-0, ACS-50 and ACS-100 at different stress levels and the Weibull 2-parameter model was found to be acceptable at 5% level of significance.
12. The expected fatigue lives at different survival probabilities i.e. (0.05, 0.5 and 0.95) are determined for OPCC, AASC mixes with sand/CS and it was found that at a specific stress level; the number of cycles to failure decreases with increase in probability of failure.

C. Flexural Behavior of Reinforced AASC Beams

13. Reinforced beams of different AASC mixes with sand/CS exhibited marginally higher first crack load (19.1-19.6 kN), due to their higher flexural strengths than that of OPCC mix (18.2 kN).
14. The load deflection characteristics of reinforced AASC beams with sand/CS are almost similar to those of the reference OPCC-based RCC beam. Again the deflections of RC beams of AASC mixes with sand/CS are marginally higher than beams of OPCC mixes.
15. The ultimate loads taken by reinforced AASC beams with sand/CS fine aggregate (81.9-84.3 kN) are comparable to reinforced OPCC beams (81.0 kN). Experimental ultimate loads for all beams were also found to be more than theoretical ultimate loads (72.1-72.3 kN, based on IS: 456-2000

recommendations) showing that theoretical calculations are conservative.

16. The crack patterns observed for different reinforced AASC beams tested were similar to those observed in conventional OPCC beams. Beyond the ultimate load, the number of flexural cracks stabilized and the cracks at the mid span opened widely. There were not much differences between numbers of cracks at ultimate load observed in both OPCC and AASC beams with sand/CS. Crack-widths were generally larger for ACS-0 than OPC-based concrete mixes and they decreased with increased CS replacement.
17. Moment carrying capacity of reinforced OPCC (30.4 kN-m) beam was approximately same as the moment carrying capacities of AASC beams with sand/CS (30.8-31.5 kN-m). The moment carrying capacities of different reinforced AASC beams, with increasing percentage CS, do not differ significantly. The maximum curvature of ACS-0 beam ($45.3 \text{ Radians/mm } 10^{-6}$) is found to be higher than OPCC ($38.3 \text{ Radians/mm } 10^{-6}$) and higher replacement of sand by CS decreases the curvature ($42.6 \text{ Radians/mm } 10^{-6}$).

The results of large number of tests conducted on various strength and durability considerations have revealed that, the performance of CS-based AASC concrete mixes, have been generally at par or marginally better than the conventional OPC-based concrete mixes with sand as fine aggregates. It has also been brought out that, except for acid exposure, 100% replacement of sand with CS is possible in concrete mixes without compromising on the functional requirements of the concrete material/structural elements.

It can be also said that, use of AASC mixes with CS as fine aggregates can have eight- fold advantages over OPCC namely

- Uses industrial wastes (CS, GGBFS)
- Reduces consumption of sand which in-turn reduces environmental and ecological problems associated with sand mining

- Reduction in CS stock piles, which or else would create environmental problems
- Saving in water due to air-curing
- High early-strength development can be effectively used for early strip-off of formwork and removal of scaffolding helping faster construction, with added economical benefits associated with it
- Consumes lesser energy
- Produces less CO₂
- Economical
- Consumes industrial by product (GGBFS) which in turn saves non-renewable resources like limestone, iron ore, coal etc., which are necessary basic materials for the production of cement.

All the AASC mixes with CS tested herein have shown satisfactory results for their use in structural and highway applications. Use of AASC mixes will result in consequent reduction of use of OPC in construction industry and in turn can contribute to lowering of CO₂ emissions: Utilization of CS in AASC mixes not only creates opportunities for the conservation of natural aggregates but also helps in solving its disposal problem smelting industry.

Hence efforts should be made, with government patronage, to popularize use of these types of alternate binder systems (where copper industries /copper slag are available) in concrete infrastructure projects in developing countries.

8.2 SCOPE FOR FUTURE STUDY

The present investigation can be extended to:

- Extensive study of the development of micro-structures with age and their effect on macro-structural behaviour of alkali activated slag concrete mixes with CS as fine aggregates can be carried out.
- Comparative study of AASC with CS subjected to different types of curing processes such as heat curing, steam curing etc., can be studied.

REFERENCES

- Al-Amoudi, O. S. B., Maslehuddin, M., and Saadi, M. M. (1995). "Effect of magnesium sulfate and sodium sulfate on the durability performance of plain and blended cements". *ACI Materials Journal*, 92(1), 15-24.
- Al-Jabri, K. S., Al-Saidy, A. H., and Taha, R. (2011). "Effect of copper slag as a fine aggregate on the properties of cement mortars and concrete". *Construction and Building Materials*, 25(2), 933-938.
- Al-Jabri, K. S., Hisada, M., Al-Saidy, A. H., and Al-Oraimi, S. K. (2009a). "Performance of high strength concrete made with copper slag as a fine aggregate". *Construction and Building Materials*, 23(6), 2132-2140.
- Al-Jabri, S.K., Makoto, H, Al-Oraimi, K. S., Al-Saidy, H. S. (2009b). "Copper slag as sand replacement for high performance concrete". *Cement and Concrete Composites*, 31(7), 483-488.
- Allahverdi, A., and Škvára, F. (2000). "Acidic corrosion of hydrated cement based materials". *Ceramics– Silikáty*, 44(4), 152-160.
- Altan, E., and Erdoğan, S. T. (2012). "Alkali activation of a slag at ambient and elevated temperatures". *Cement and Concrete Composites*, 34(2), 131-139.
- Anurag, M., Arora, A. N., Pawan, K., Himanshu, G., and Vimal, G. (2012). "Strength, permeability and carbonation studies on wollastonite, fly ash and silica fume added concrete". *ICI Journal*, 13(3), 15-20.
- Ayano, T., Kuramoto, O., and Sakata, K. (2000). "Concrete with copper slag fine aggregate". *Journal of Society of Materials Science Japan*, 49, 1097-1102.
- Aydın, S., and Baradan, B. (2012). "Mechanical and microstructural properties of heat cured alkali-activated slag mortars". *Materials and Design*, 35, 374-383.
- Bakharev, T. (2005). "Durability of geo-polymer materials in sodium and magnesium sulfate solutions". *Cement and Concrete Research*, 35(6), 1233-1246.
- Bakharev, T., Sanjayan, J. G., and Cheng, Y. B. (1999). "Alkali activation of Australian slag cements". *Cement and Concrete Research*, 29(1), 113-120.
- Bakharev, T., Sanjayan, J. G., and Cheng, Y. B. (2000). "Effect of admixtures on properties of alkali-activated slag concrete". *Cement and Concrete Research*, 30(9), 1367-1374.

- Bakharev, T., Sanjayan, J. G., and Cheng, Y. B. (2002). "Sulfate attack on alkali-activated slag concrete". *Cement and Concrete Research*, 32(2), 211-216.
- Bakharev, T., Sanjayan, J. G., and Cheng, Y. B. (2003). "Resistance of alkali-activated slag concrete to acid attack". *Cement and Concrete Research*, 33(10), 1607-1611.
- Basheer, P. A. M. (2001). "Permeation analysis". in Handbook of Analytical techniques in concrete science and technology - principles, techniques and applications", *J. J. Noyes*, USA, 658-737.
- Bazant, Z. P., and Kaplan, M. F. (1996). "Concrete at high temperatures: material properties and mathematical models". *Harlow Longman*.
- Beddoe, R. E., and Dorner, H. W. (2005). "Modelling acid attack on concrete: Part I. The essential mechanisms". *Cement and Concrete Research*, 35(12), 2333-2339.
- Bernal, S. A., De Gutiérrez, R. M., Pedraza, A. L., Provis J. L., Rodriguez, E. D. and Delvasto, S (2011). "Effect of binder content on the performance of alkali-activated slag concretes". *Cement and Concrete Research*, 41(1), 1-8.
- Bernal, S. A., De Gutierrez, R., Delvasto, S., and Rodriguez, E. (2010). "Performance of an alkali-activated slag concrete reinforced with steel fibers". *Construction and Building Materials*, 24(2), 208-214.
- Bernal, S. A., Provis, J. L., Rose, V., and De Gutierrez, R. M. (2011). "Evolution of binder structure in sodium silicate-activated slag-metakaolin blends". *Cement and Concrete Composites*, 33(1), 46-54.
- Bilim, C., Karahan, O., Atiş, C. D., and İlkentapar, S. (2015). "Effects of chemical admixtures and curing conditions on some properties of alkali-activated cementless slag mixtures". *KSCE Journal of Civil Engineering*, 19(3), 733-741.
- Brindha, D., and Nagan, S. (2011). "Durability studies on copper slag admixed concrete". *Asian Journal of Civil Engineering (Building and Housing)*, 12(5), 563-578.
- Brindha, D., Baskaran, T., and Nagan, S. (2010). "Assessment of corrosion and durability characteristics of copper slag admixed concrete". *International Journal of Civil and Structural Engineering*, 1(2), 192-210.
- Caijun, S., and Della, R. (2006). "Alkali-activated cements and concretes". *Taylor and Francis. London and New York*.

- Cengiz, D., Atis, C. B., Zlem, O., Elik, C., and Okan, K. (2009). "Influence of activator on the strength and drying shrinkage of alkali-activated slag mortar". *Construction and Building Materials*, 23(1), 548-555.
- Chan, S. Y. N., Peng, G. F., and Anson, M. (1999). "Fire behavior of high-performance concrete made with silica fume at various moisture contents". *Materials Journal*, 96(3), 405-409.
- Chandrashekar, A., Ravishankar, A. U., and Girish, M. G. (2010). "Fatigue Behaviour of Steel Fibre Reinforced Concrete with Fly Ash". *Highway Research Journal*, 9-20.
- Chang, J. J. (2003). "A study on the setting characteristics of sodium silicate-activated slag pastes". *Cement and Concrete Research*, 33(7), 1005-1011.
- Cheng, T. W., and Chiu, J. P. (2003). "Fire-resistant geopolymers produced by granulated blast furnace slag". *Minerals Engineering*, 16(3), 205-210.
- Chi, M. (2012). "Effects of dosage of alkali-activated solution and curing conditions on the properties and durability of alkali-activated slag concrete". *Construction and Building Materials*, 35, 240-245.
- Chi, M., and Huang, R. (2013). "Binding mechanism and properties of alkali-activated fly ash/slag mortars". *Construction and Building Materials*, 40, 291-298.
- Collins, F. G., and Sanjayan, J. G. (1999). "Workability and mechanical properties of alkali activated slag concrete". *Cement and Concrete Research*, 29(3), 455-458.
- Collins, F., and Sanjayan, J. G. (2000). "Effect of pore size distribution on drying shrinking of alkali-activated slag concrete". *Cement and Concrete Research*, 30(9), 1401-1406.
- Dattatreya, J. K., Rajamane, N. P., Sabitha, D., Ambily, P. S., and Nataraja, M. C. (2011). "Flexural behaviour of reinforced Geopolymer concrete beams". *International Journal of Civil and Structural Engineering*, 2(1), 138.
- Davidovits, J. (1994). "Properties of Geo-polymer Cements". *First International Conference on Alkaline Cements and Concretes*, Kiev, Ukraine, SRIBM, Kiev State Technical University, 131-149.
- Dhir R K (2009). "Washed copper slag: Use as fine aggregates in concrete". Applying Concrete Knowledge. Birmingham, U.K. Report.HS/ACK/103909.
- Douglas, E., and Brandstetr, J. (1990). "A preliminary study on the alkali activation of ground granulated blast-furnace slag". *Cement and concrete research*, 20(5), 746-756.

Duxson, P., Fernández-Jiménez, A., Provis, J. L., Lukey, G. C., Palomo, A., and Van Deventer, J. S. J. (2007). "Geopolymer technology: The current state of the art". *Journal of Materials Science*, 42(9), 2917-2933.

Fernández-Jiménez, A., and Palomo, A. (2003). "Characterisation of fly ashes - Potential reactivity as alkaline cements". *Fuel*, 82(18), 2259-2265.

Fernández-Jiménez, A., and Puertas, F. (2001). "Setting of alkali-activated slag cement- Influence of activator nature". *Advances in Cement Research*, 13(3), 115-121.

Fernández-Jiménez, A., Garcia-Lodeiro, I., and Palomo, A. (2007). "Durability of alkali-activated fly ash cementitious materials". *Journal of Materials Science*, 42(9), 3055-3065.

Fernández-Jiménez, A., Palomo, A., and Criado, M. (2005). "Microstructure development of alkali-activated fly ash cement-A descriptive model". *Cement and Concrete Research*, 35(6), 1204-1209.

Fernández-Jiménez, A., Palomo, J. G., and Puertas, F. (1999). "Alkali-activated slag mortars - mechanical strength behavior". *Cement and Concrete Research*, 29(8), 1313-1321.

Gambhir, M.L. (2004). "Concrete technology-Theory and practice". Fourth Edition. *Tata McGraw-hill* (Education) Private Limited, New Delhi.

Ganesan, N., Raj, J. B., and Shashikala, A. P. (2013). "Flexural fatigue behavior of self-compacting rubberized concrete". *Construction and Building Materials*, 44, 7-14.

Gary, W.H., McLaughlin, J.F., and Antrim, J.C. (1961). "Fatigue Properties of Lightweight Aggregate Concrete". *ACI Journal*, Proceedings, 258(2), 149-161.

Georgali, B., and Tsakiridis, P. E. (2005). "Microstructure of fire-damaged concrete - A case study". *Cement and Concrete Composites*, 27(2), 255-259.

Ghosh S (2007). "Use of washed copper slag (from ecowise) as partial replacement of same (50% level) for ready mix concrete for structural use". *Holchim*, Singapore.

Glukhovskiy, V. D. (1959). "Soil Silicates". *Kiev, Ukraine: Gastroi Publishers*.

Glukhovskiy, V.D. (1994). "Alkaline cements and concretes". First International Conference, Kiev, Ukraine, 1-8.

- Guerrieri, M., Sanjayan, J., and Collins, F. (2009). "Residual compressive behavior of alkali-activated concrete exposed to elevated temperatures". *Fire and Materials*, 33(1), 51-62.
- Guerrieri, M., Sanjayan, J., and Collins, F. (2010). "Residual strength properties of sodium silicate alkali activated slag paste exposed to elevated temperatures". *Materials and Structures*, 43(6), 765-773.
- Guo, L. P., Carpinteri, A., Spagnoli, A., and Sun, W. (2010). "Experimental and numerical investigations on fatigue damage propagation and life prediction of high-performance concrete containing reactive mineral admixtures". *International Journal of Fatigue*, 32(2), 227-237.
- Haha, M. B., Le Saout, G., Winnefeld, F., and Lothenbach, B. (2011). "Influence of activator type on hydration kinetics, hydrate assemblage and microstructural development of alkali activated blast-furnace slags". *Cement and Concrete Research*, 41(3), 301-310.
- Han, Y., Taylor, J. E., and Pisello, A. L. (2015). "Toward mitigating urban heat island effects: Investigating the thermal-energy impact of bio-inspired retro-reflective building envelopes in dense urban settings". *Energy and Buildings*, 102, 380-389.
- Handoo, S. K., Agarwal, S., and Agarwal, S. K. (2002). "Physico-chemical, mineralogical, and morphological characteristics of concrete exposed to elevated temperatures". *Cement and Concrete Research*, 32(7), 1009-1018.
- Heeralal, M., Kumar, P. R., and Rao, Y. V. (2009). "Flexural fatigue characteristics of steel fiber Reinforced recycled aggregate concrete". *Facta Universitatis Series: Architecture and Civil Engineering*, 7(1), 19-33.
- Hosny H, Abu E (1994). "Fire in Concrete Building", *Egyptian Universities Publishers*.
- Hsu, T. C. C. (1981). "Fatigue of plain concrete". *ACI Materials Journal*, 78 (4), 292-305
- Hughes, D. C. (1985). "Sulphate resistance of OPC, OPC/fly ash and SRPC pastes: pore structure and permeability". *Cement and Concrete Research*, 15(6), 1003-1012.
- Hui, L., Mao-hua, Z., and Jin-ping, O. (2006). "Flexural fatigue performance of concrete containing nano-particles for pavement". *International Journal of Fatigue*, 29 (2), 1292-1301.

Idawati, I., Susan, A. B., John, L. P., Rackel, S. N., David, G. B., Adam, R. K., Sinin, H., and van Deventer, J. S. J. (2013). "Influence of fly ash on the water and chloride permeability of alkali-activated slag mortars and concretes". *Construction and Building Materials*, 48, 1187-1201.

Ismail, I., Bernal, S. A., Provis, J. L., San Nicolas, R., Brice, D. G., Kilcullen, A. R., and Van Deventer, J. S. (2013). "Influence of fly ash on the water and chloride permeability of alkali-activated slag mortars and concretes". *Construction and Building Materials*, 48, 1187-1201.

Jiang, W. (1997). "Alkali-activated cementitious materials - Mechanisms, microstructure and properties". *Ph.D. Thesis, The Pennsylvania State University, Pennsylvania, USA*

Jumppanen, U. M., Diederichs, U., and Hinrichsmeyer, K. (1986). "Material properties of F-concrete at high temperatures".

Kathirvel, P., and Kaliyaperumal, S. R. M. (2016). "Influence of recycled concrete aggregates on the flexural properties of reinforced alkali activated slag concrete". *Construction and Building Materials*, 102, 51-58.

Khoury, G. A. (1992). "Compressive strength of concrete at high temperatures: A reassessment". *Magazine of Concrete Research*, 44(161), 291-309.

Kim, J. K., and Kim, Y. Y. (1996). "Experimental study of the fatigue behavior of high strength concrete". *Cement and Concrete Research*, 26(10), 1513-1523.

Klaiber, F. W., Thomas, T. L., and Lee, D. Y. (1979). "Fatigue Behavior of Air-Entrained Concrete: Phase II". Report, Ames, Iowa, Engineering Research Institute, Iowa State University.

Krivenko, P. D. (1994). "Alkaline cements", The First International Conference on Alkaline Cements and Concrete, October, Kiev, Ukraine, 11-14.

Krizan, D., and Zivanovic, B. (2002). "Effects of dosage and modulus of water glass on early hydration of alkali slag cements". *Cement and Concrete Research*, 32(8), 1181-1188.

Kumar, A.D. (2011). "Performance of geo-polymer concrete mixes under fatigue and elevated temperature". M.Tech Thesis, Department of Civil Engineering, National Institute of Technology Karnataka, Surathkal, India.

Lee, M. K., and Barr, B. I. G. (2004). "An overview of the fatigue behaviour of plain and fibre reinforced concrete". *Cement and Concrete Composites*, 26(4), 299-305.

- Li, H., Zhang, M. H., and Ou, J. P. (2007). "Flexural fatigue performance of concrete containing nano-particles for pavement". *International Journal of Fatigue*, 29(7), 1292-1301.
- Li, M., Qian, C., and Sun, W. (2004). "Mechanical properties of high-strength concrete after fire". *Cement and Concrete Research*, 34(6), 1001-1005.
- Li, Z., and Liu, S. (2007). "Influence of slag as additive on compressive strength of fly ash-based geopolymer". *Journal of Materials in Civil Engineering*, 19(6), 470-474.
- Lye, C. Q., Koh, S. K., Mangabhai, R., and Dhir, R. K. (2015). "Use of copper slag and washed copper slag as sand in concrete: A state of the art review". *Magazine of Concrete Research*, 67(12), 665-679.
- Malhotra, V. M., and Mehta, P. K. (1996). "Pozzolanic and cementitious materials". First edition. *Taylor and Francis*.
- Mangat, P. S., and El-Khatib, J. M. (1992). "Influence of initial curing on sulphate resistance of blended cement concrete". *Cement and Concrete Research*, 22(6), 1089-1100.
- Marceau, M., Nisbet, M. A., and Van Geem, M. G. (2007). "Life cycle inventory of Portland cement concrete". SN3011, *Portland Cement Association*, Skokie, Illinois, PCA, 2007, 121-124.
- Marland, G., Boden, T.A., and Andres R. J., (2007). "Global, regional, and national CO₂ emissions in trends: a compendium of data on global change". Carbon dioxide information analysis center, oak ridge national laboratory, U.S. Department of Energy, Oak Ridge, Tenn., U.S.A, 233-239.
- McGannon, H. (1971). "The making, shaping and treating of steel". United States steel corporation, Ninth Edition.
- Mehta, P. K. (2001). "Reducing the environmental impact of concrete". *Concrete International*, 23(10), 61-66.
- Mejía de Gutierrez, R., Maldonado, J., and Gutiérrez, C. (2004). "Performance of alkaline activated slag at high temperatures". *Materiales De Construccion*, 54(276), 87-92.
- Meyer, A. H., and Ledbetter, W. B. (1970). "Sulfuric acid attack on concrete sewer pipe". *Journal of the Sanitary Engineering Division*, 96(5), 1167-1182.

Mindess, S., Young, J. F., and Darwin, D. (2003). "Concrete". *Second Edition, Prentice-Hall, Upper Saddle River, New Jersey.*

Mohammadi, Y., and Kaushik, S. K. (2005). "Flexural fatigue-life distributions of plain and fibrous concrete at various stress levels". *Journal of Materials in Civil Engineering, 17(6), 650-658.*

Morsy, M. S., Rashad, A. M., and Shebl, S. S. (2008). "Effect of elevated temperature on compressive strength of blended cement mortar". *Building Research Journal, 56(2-3), 173-185.*

Naik, T.R., Singh, S. S., and Congli, Y. (1993). "Fatigue behavior of plain concrete made with or without fly ash". Center for By-Products Utilization, University of Wisconsin-Milwaukee, Department of Civil Engineering and Mechanics, North Cramer Street Milwaukee, WI

Narasimhan, M. C., Nayak, G., Ajith, B. T., and Rao, M. K. (2011). "Development of alternative binders to Portland cement concrete using fly ash and blast furnace slag: Some experiences". Proceedings of the International UKIERI Concrete Congress, New Delhi, India, 43-60.

Oh, B. H. (1986). "Fatigue analysis of plain concrete in flexure". *Journal of Structural Engineering, 112(2), 273-288.*

Oh, B. H. (1991). "Fatigue life distributions of concrete for various stress levels". *Materials Journal, 88(2), 122-128.*

Özge, A. Ç., Oğuzhan, Ç, and Kambiz, R. (2008). "Effect of high temperature on mechanical and microstructural properties of cement mortar". Proceedings of *11 DBMC International Conference on Durability of Building Materials and Components, Istanbul, Turkey, 11-14.*

Pacheco-Torgal, F., Abdollahnejad, Z., Camões, A. F., Jamshidi, M., and Ding, Y. (2012). "Durability of alkali-activated binders: a clear advantage over Portland cement or an unproven issue". *Construction and Building Materials, 30, 400-405.*

Pacheco-Torgal, F., Castro-Gomes, J., and Jalali, S. (2008). "Alkali-activated binders: A review: Part1. Historical background, terminology, reaction mechanisms and hydration products". *Construction and Building Materials, 22(7), 1305-1314.*

Pade, C., Guimaraes, M., Kjellsen, K., and Nilsson, A. (2007). "The CO₂ uptake of concrete in the perspective of life cycle inventory". *International Symposium on Sustainability in the Cement and Concrete Industry, Lillehammer, Norway. 121-124.*

Palacios, M., and Puertas, F. (2005). "Effect of superplasticizer and shrinkage-reducing admixtures on alkali-activated slag pastes and mortars". *Cement and Concrete Research*, 35(7), 1358-1367.

Palomo, A., Grutzeck, M. W., and Blanco, M. T. (1999). "Alkali-activated fly ashes: a cement for the future". *Cement and Concrete Research*, 29(8), 1323-1329.

Petzold, A., Röhrs, M., and Neville A. M. (1971). "Concrete for high temperatures". Maclaren.

Phan, L. T. (1996). "Fire performance of high-strength concrete: A report of the state of the art". US Department of Commerce, Technology Administration, National Institute of Standards and Technology, Office of Applied Economics, Building and Fire Research Laboratory.

Phull, Y. R., and Rao, P. J. (2007). "Assuring Fatigue Adequacy of Concrete Pavements: Some Essential Needs. *Indian Highways*, 35(3), 9-19.

Poon, C. S., Azhar, S., Anson, M., and Wong, Y. L. (2001). "Comparison of the strength and durability performance of normal-and high-strength pozzolanic concretes at elevated temperatures". *Cement and Concrete Research*, 31(9), 1291-1300.

Popovics, S. (1992). "Concrete materials - properties, specifications and testing". *Publication SP-75, S.P. Shah, 2nd Ed., Detroit.*

Pradeep, J., Sanjay, R., and Ashwath, M. U. (2012). "Experimental study on flexural behavior of fly ash and GGBS based geopolymer concrete beams in bending". *International Journal of Emerging Trends in Engineering and Development*, 6(2), 419-428.

Puertas, F. (1995). "Cementos de escorias activada salcalinamente: Situación actualy perspectivas de futuro".

Puertas, F., Martínez-Ramírez, S., Alonso, S., and Vazquez, T. (2000). "Alkali-activated fly ash/slag cements: strength behaviour and hydration products". *Cement and Concrete Research*, 30(10), 1625-1632.

Purdon, A. (1940). "The action of alkalis on blast furnace slag". *Journal of the Society of Chemical Industry*. 59, 191-202.

Rajamane, N.P. (2013). "Studies on ambient temperature cured fly ash and GGBS based geopolymer concrete". Ph.D thesis, Visveshwaraih Technological University, Belgaum, India.

Rashad, A. M. (2013a). "A comprehensive overview about the influence of different additives on the properties of alkali-activated slag: A guide for civil engineer". *Construction and Building Materials*, 47, 29-55.

Rashad, A. M. (2013b). "Properties of alkali-activated fly ash concrete blended with slag". *Iran J Materials Science Engineering*, 10(1), 57-64.

Rashad, A. M., Zeedan, S. R., and Hassan, H. A. (2012). "A preliminary study of autoclaved alkali-activated slag blended with quartz powder". *Construction and Building Materials*, 33, 70-77.

Ravikumar, D., and Neithalath, N., (2013). "Electrically induced chloride ion transport in alkali activated slag concretes and the influence of microstructure". *Cement and Concrete Research*, 47, 31-42.

Ravikumar, D., Peethamparan, S., and Neithalath, N. (2010). "Structure and Strength of NaOH activated concrete containing fly ash or GGBFS as sole binder". *Cement and Concrete Composite*, 32(6), 399-410.

Reddy, B. V. V., (2010). "Embodied energy in buildings". (IISc, Bangalore), [\(www.ese.iitb.ac.in/events/other/renet_files/21/Session%203/Energy%20in%20buildings\)](http://www.ese.iitb.ac.in/events/other/renet_files/21/Session%203/Energy%20in%20buildings). (B.V.V.Reddy). pdf, 47-55.

Richardson, I. G., Brough, A. R., Groves, G. W., and Dobson, C. M. (1994). "The characterization of hardened alkali-activated blast-furnace slag pastes and the nature of the calcium silicate hydrate (CSH) phase". *Cement and Concrete Research*, 24(5), 813-829.

Robin, E. B., and Horst, W. D. (2005). "Modelling acid attack on concrete: Part I. The essential mechanisms centre for building materials". *Cement and Concrete Research*, 35, 2333- 2339.

Rodríguez, E., Bernal, S., Mejía de Gutierrez, R., and Puertas, F. (2008). "Alternative concrete based on alkali-activated slag". *Materiales de Construcción*, 58(291), 53-67.

Roy, D. M. (1999). "Alkali-activated cements opportunities and challenges". *Cement and Concrete Research*, 29(2), 249-254.

Roy, D. M., and Silsbee, M. R. (1992). "Alkali activated materials - an overview". *Materials and Resources*, 245, 153-164.

Roylance, D. (2001). "Fatigue". <http://ocw.mit.edu/courses/materials-science-and-engineering/3-11-mechanics-of-materials-fall-1999/modules/fatigue.pdf>.

- Sakin, R., and Ay, I. (2008). "Statistical analysis of bending fatigue life data using Weibull distribution in glass-fiber reinforced polyester composites". *Materials and Design*, 29(6), 1170-1181.
- Sakkas, K., Nomikos, P., Sofianos, A., and Panias, D. (2013). "Inorganic polymeric materials for passive fire protection of underground constructions". *Fire and Materials*, 37(2), 140-150.
- Sakulich, A. R., Anderson, E., Schauer, C., and Barsoum, M. W. (2009). "Mechanical and microstructural characterization of an alkali-activated slag-limestone fine aggregate concrete". *Construction and Building Materials*, 23(8), 2951-2957.
- Sand, W., and Bock, E. (1984). "Concrete corrosion in the Hamburg sewer system". *Environmental Technology*, 5(12), 517-528.
- Seleem, H. E. H., Rashad, A. M., and Elsokary, T. (2011). "Effect of elevated temperature on physico-mechanical properties of blended cement concrete". *Construction and building Materials*, 25(2), 1009-1017.
- Seto, K. C., Güneralp, B., and Hutyrá, L. R. (2012). "Global forecasts of urban expansion to 2030 and direct impacts on biodiversity and carbon pools". *Proceedings of the National Academy of Sciences*, 109(40), 83-88.
- Shi, C., Krivenko, P. V., and Roy, D. (2006). "Alkali-activated cements and concretes". Taylor and Francis publications, Abingdon, UK.
- Shi, C., Meyer, C., and Behnood, A. (2008). "Utilization of copper slag in cement and concrete." *Conservation and Recycling*, 52(10), 1115-1120.
- Silva, A. C. R., Silva, F. J., and Thaumaturgo, C. "Fatigue behavior of geopolymer concrete".
- Singh, S. P., and Kaushik, S. K. (2001). "Flexural fatigue analysis of steel fiber-reinforced concrete". *Materials Journal*, 98(4), 306-312.
- Sullivan, P. J. E., and Sharshar, R. (1992). "The performance of concrete at elevated temperatures (as measured by the reduction in compressive strength)". *Fire Technology*, 28(3), 240-250.
- Sumajouw, M. D. J., and Rangan, B. V. (2006). "Low-calcium fly ash-based geopolymer concrete reinforced beams and columns". PhD Thesis, *Curtin University of Technology, Australia*.

Varaprasad, G. (2006). "Eco-friendly geopolymers concrete-A preliminary study". M.Tech Thesis, Department of Civil Engineering, National Institute of Technology Karnataka, Surathkal.

Wang, A., Zhang, C., and Sun, W. (2003). "Fly ash effects: I. The morphological effect of fly ash". *Cement and Concrete Research*, 33(12), 2023-2029.

Wang, H. Y. (2008). "The effects of elevated temperature on cement paste containing GGBFS". *Cement and Concrete Composites*, 30(10), 992-999.

Wang, S. D., and Scrivener, K. L. (1995). "Hydration products of alkali activated slag cement". *Cement and Concrete Research*, 25(3), 561-571.

Wang, S. D., Scrivener, K. L., and Pratt, P. L. (1994). "Factors affecting the strength of alkali-activated slag". *Cement and Concrete Research*, 24(6), 1033-1043.

Wei, W., Weide, Z., and Guowei, M. (2010). "Optimum content of copper slag as a fine aggregate in high strength concrete". *Materials and Design*, 31(6), 2878-2883.

Wu, W., Zhang, W., and Ma, G. (2010). "Optimum content of copper slag as a fine aggregate in high strength concrete". *Materials and Design*, 31(6), 2878-2883.

Xiao, J., Xie, M., and Zhang, C. (2006). "Residual compressive behaviour of pre-heated high-performance concrete with blast furnace slag". *Fire Safety Journal*, 41(2), 91-98.

Xu, Y., Wong, Y. L., Poon, C. S., and Anson, M. (2001). "Impact of high temperature on PFA concrete". *Cement and Concrete Research*, 31(7), 1065-1073.

Yang, K. H., Song, J. K., and Song, K. I. (2013). "Assessment of CO₂ reduction of alkali-activated concrete". *Journal of Cleaner Production*, 39, 265-272.

Zuda, L., Pavlík, Z., Rovnaníková, P., Bayer, P., and Černý, R. (2006). "Properties of alkali activated aluminosilicate material after thermal load". *International Journal of Thermophysics*, 27(4), 1250-1263.

ASTM C618-15. "Standard specification for coal fly ash and raw or calcined natural pozzolan for use in concrete". *ASTM International*, West Conshohocken, PA.

ASTM C642-06. "Standard test method for density, absorption and voids in hardened concrete". *ASTM International*, West Conshohocken, PA.

ASTM STP 91: 1963. "A guide for fatigue testing and the statistical analysis of fatigue data". *ASTM Special Technical Publication*, West Conshohocken, PA.

IRC: 21-2000. "Standard specifications and code of practice for road bridges section: III cement concrete (Plain and Reinforced)". Third Revision, *Indian Roads Congress*, New Delhi, India.

IRC: 58-2002. "Guidelines for the design of plain jointed rigid pavements for highways". *Indian Roads Congress*, New Delhi, India.

IRC: 58-2011. "Guidelines for the design of plain jointed rigid pavements for highways". *Indian Roads Congress*, Third Revision, New Delhi, India.

IRC: SP: 62-2004. "Guidelines for the design and construction of cement concrete pavements for rural roads". *Indian Road Congress*, New Delhi, India.

IS: 383-1970. "Indian standard specification for coarse and fine aggregates from natural sources for concrete (Second revision)". *Bureau of Indian Standards*, New Delhi, India.

IS: 456-2000, Reaffirmed 2005. "Plain and Reinforced Concrete - Code of Practice". *Bureau of Indian Standards*, New Delhi, India.

IS: 516-1959. "Methods of tests for strength of concrete". *Bureau of Indian Standards*, New Delhi, India.

IS: 1199-1959. "Method for sampling and analysis of concrete". *Bureau of Indian Standards*, New Delhi, India.

IS: 3812-2003. "Specification for pulverized fuel ash, Part 2: For use as admixture in cement mortar and concrete". *Bureau of Indian Standards*, New Delhi, India.

IS: 2386-1963. "Methods of test for aggregates for concrete". *Bureau of Indian Standards*, New Delhi, India.

IS: 5816-1999. "Splitting Tensile Strength of Concrete - Method of Test". *Bureau of Indian Standards*, New Delhi, India.

IS: 8112-2013. “Ordinary Portland cement, 43 grade-specification (Second revision)”. *Bureau of Indian Standards*, New Delhi, India.

IS: 10262-2009. “Indian standard concrete mix proportioning (First revision)”. *Bureau of Indian Standards*, New Delhi, India.

IS: 12089 - 1987. “Indian standard specification for granulated slag for the manufacture of Portland slag cement”. *Bureau of Indian Standards*, New Delhi, India.

IS -14212-1995. “Sodium and potassium silicates-Methods of test”. *Bureau of Indian Standards*, New Delhi, India.

NT BUILD 443, 1995-11. “Concrete hardened: Accelerated chloride penetration”. *NORD TEST*. Espoo Finland.

APPENDIX - I

Mix Design for OPC Concrete

For the OPC based control concrete mix, OPC 43 grade cement was used as the binder. Sand conforming to Zone - II was used. Locally available crushed stone granite aggregates of 20 mm down size were used. For the mix design, method proposed by IS 10262 – 2009, was followed.

Input parameters

Desired characteristics strength of concrete f_{ck}	=	45 MPa
Grade of cement	=	43
Sp. gravity of cement	=	3.13
Sp. gravity of sand	=	2.64
Sp. gravity of coarse aggregate	=	2.69
Water absorption of sand	=	nil
Water absorption of coarse aggregate	=	nil
Maximum size of aggregate	=	20 mm
Minimum slump required in mm	=	50-75

The aggregates are used in saturated surface dry condition.

Estimation of ingredients for M₄₅ grade concrete

(1) Target mean strength of concrete (TMS)

$$\text{TMS} = f_{ck} + 1.65 * \text{S.D} = 45 + 1.65 * 5 = 53.25 \text{ N / mm}^2$$

(2) Selection of water cement ratio

$$\text{water cement ratio} = 0.40 \text{ (From Table 5, IS: 456 -2000)}$$

(4) Selection of Water content

From Table 2 of IS-10262 - 2009, Max water content for 20mm aggregate = 186 litre
(for 25 – 50mm slump range)

$$\text{Estimated water content for 75mm slump} = 186 + 3/100 * 186 = 191.6 \text{ litre}$$

Based on trials 0.6 % of super plasticizer (as % of cement content) is used and hence the water content is reduced to 176 litre.

$$\text{Water content (w)} = 176 \text{ kg/ m}^3$$

(5) Calculation for cement content

$$\text{Water-cement ratio} = 0.4$$

$$\text{Cement content} = 176/0.4 = 440 \text{ kg/m}^3$$

(6) Proportion of volume of coarse aggregate and fine aggregate content

Coarse aggregate content as percent of aggregate by absolute volume = 62% (From Table 4, IS 10262 - 2000)

For the adopted change in water cement ratio, following adjustments are required

Change in condition: volume adjustment required

For decrease in water cement ratio aggregates	Water content	coarse aggregate in total
--	---------------	---------------------------

by $(0.5 - 0.4) = 0.1$	0	+0.02
------------------------	---	-------

(From section 4.4, IS 10262 - 2009)

Therefore, required Coarse aggregate content as percentage of total aggregate by absolute volume, = $0.62 + 0.02 = 0.64$.

(7) Mix Calculations

(a) Volume of concrete = 1 m^3

(b) Volume of cement = $(\text{Mass of cement}/\text{specific gravity of cement}) * 1/1000$
 $= 440/3140$
 $= 0.140 \text{ m}^3$

(c) Volume of super plasticizer (0.6% by mass of cement)
 $= (\text{Mass of chemical admixture}/ \text{specific gravity of chemical admixture}) * 1/1000$

$$= 2.64/1200$$

$$= 0.0022 \text{ m}^3$$

Water to add = 176 – water present in super plasticizer

$$= 176 - (2.64 \times 0.6) = 174.4 \text{ litres}$$

(d) Volume of water = (Mass of water/sp gravity of water)*1/1000

$$= 174.4/1000 = 0.1744 \text{ m}^3$$

(e) Volume of all in aggregate = [a-(b+c+d)]

$$e = 1 - (0.140 + 0.0022 + 0.1744)$$

$$e = 0.684 \text{ m}^3$$

(f) Mass of coarse aggregate

= e * volume fraction of coarse aggregate * specific gravity of coarse aggregate* 1000

$$= 0.684 \times 0.64 \times 2.69 \times 1000$$

$$= 1177.6 \text{ kg/m}^3$$

(g) Mass of fine aggregate

= e * volume of fine aggregate * specific gravity of fine aggregate* 1000

$$= 0.684 \times 0.36 \times 2.64 \times 1000$$

$$= 650 \text{ kg/m}^3$$

(8) Mix proportions (considering aggregates in SSD condition)

Ingredients of mix	Cement (kg/m ³)	Fine aggregate (kg/m ³)	Coarse aggregate (kg/m ³)	Water (kg/m ³)	Super plasticizer (kg/m ³)
	440	650	1178	174.4	2.64
Relative proportions	1	1.48	2.68	0.396	0.006

APPENDIX - II

Sample Mix Design for Alkali Activated Slag Concrete

For AASC mix 100% OPCC by weight is replaced with GGBFS and alkali solution is used instead of water.

Input parameters

Desired characteristics strength of concrete f_{ck}	=	45 MPa
Specific gravity of GGBS,	=	2.9
Specific gravity of sand	=	2.64
Specific gravity of copper slag	=	3.6
Specific gravity of coarse aggregate	=	2.69
Specific gravity of alkali solution (4% Na ₂ O, Ms 1.25)	=	1.2
Water absorption of sand	=	nil
Water absorption of copper slag	=	nil
Water absorption of coarse aggregate	=	nil
Maximum size of aggregate	=	20 mm
Slump in mm	=	50-75 mm

The aggregates are used in saturated surface dry condition.

Estimation of ingredients for AASC

(1) Target mean strength of concrete (TMS)

$$\text{TMS} = f_{ck} + 1.65 * S = 45 + 1.65 * 5 = 53.25 \text{ N / mm}^2$$

(2) Na₂O dosage required: 4%

Ms required: 1.25

(3) Calculations for alkali solution

Sodium silicate solution having 14.7% Na₂O, 32.8% SiO₂ and 52.5% of water by weight

Hence, 1 kg of sodium silicate contains 0.147 kg of Na₂O, 0.328 kg of SiO₂ and 0.525 kg of water.

$$\text{Ms of sodium silicate} = \text{SiO}_2 / \text{Na}_2\text{O} = 32.8 / 14.7 = 2.23$$

NaOH flakes having Na₂O fraction = $62/80 = 0.775$

1 kg of NaOH contains 0.775 kg of Na₂O

Na₂O required by weight for 440 kg of GGBS at 4% = $440 \times 0.04 = 17.6$ kg

SiO₂ required by weight for 440 kg of GGBS at 1.25 Ms \Rightarrow SiO₂/Na₂O = 1.25

Then SiO₂ required = $1.25 \times \text{Na}_2\text{O}$

$$= 1.25 \times 17.6 = 22 \text{ kg}$$

Amount of Sodium silicate solution required for 22kg for SiO₂

$$= \text{SiO}_2 \text{ required} / \text{SiO}_2 \text{ present in sodium silicate solution}$$

$$= 22 / 0.328 = 67.1 \text{ kg}$$

Na₂O present in 67.1kg sodium silicate solution = $67.1 \times 0.147 = 9.86$ kg

Then Na₂O required from NaOH = $17.6 - 9.86 = 7.74$ kg

NaOH flakes required = $7.74 / 0.775 = 10$ kg

Extra water required to make w/b ratio of 0.2 (for storing in container) = 88 – water present in sodium silicate solution

$$= 88 - (67.1 \times 0.525)$$

$$= 52.8 \text{ kg}$$

Extra water required to make w/b ratio of 0.4 before mixing = 88 kg

Total alkali solution = $67.1 + 10 + 140.8 = 217.9$ kg.

(4) Mix calculations

(a) Volume of concrete = 1 m^3

(b) Volume of GGBS = $(\text{Mass of GGBS} / \text{specific gravity of GGBS}) \times 1/1000$

$$= 440 / 2900$$

$$= 0.152 \text{ m}^3$$

(c) Volume of Alkali Solution

$$= (\text{Mass of Alkali Solution} / \text{specific gravity of Alkali Solution}) \times 1/1000$$

$$= 217.9 / 1180$$

$$= 0.185 \text{ m}^3$$

(d) Volume of all in aggregate = $[a - (b + c)]$

$$= 1 - (0.152 + 0.185)$$

$$= 0.663 \text{ m}^3$$

(e) Mass of coarse aggregate

$$= e * \text{volume fraction of coarse aggregate} * \text{specific gravity of coarse aggregate} * 1000$$

$$= 0.663 * 0.64 * 2.69 * 1000$$

$$= 1141 \text{ kg/m}^3$$

(f) Mass of fine aggregate (sand)

$$= e * \text{volume of fine aggregate} * \text{specific gravity of fine aggregate} * 1000$$

$$= 0.663 * 0.36 * 2.64 * 1000$$

$$= 630 \text{ kg/m}^3$$

(g) Mass of fine aggregates [(75% sand +25% copper slag) by volume]

$$e * \text{volume of sand} * 0.75 * \text{specific gravity of fine aggregate} * 1000$$

$$\text{Mass of sand} = 0.663 * 0.36 * 0.75 * 2.64 * 1000 = 472 \text{ kg/m}^3$$

$$\text{Mass of Copper slag} = 0.663 * 0.36 * 0.25 * 3.6 * 1000 = 216. \text{ kg/m}^3$$

$$\text{Total mass of fine aggregate} = 685.5 \text{ kg/m}^3$$

(8) Mix proportions (considering aggregates in SSD condition)

(All quantities are in kg/m³)

Mix ID	OPC	GGBFS	Fine Aggregates		Coarse Aggregate	LSS	NaOH	Added water	Total water	SP	Total quantity
			Sand	CS							
OPCC	440	-	650	-	1178	-	-	174.4	176	2.64	2445
ACS-0	-	440	630	-	1141	67.1	10	140.8	176	-	2429
ACS-25	-	440	472	216	1141	67.1	10	140.8	176	-	2488
ACS-50	-	440	315	432	1141	67.1	10	140.8	176	-	2547
ACS-75	-	440	156	648	1141	67.1	10	140.8	176	-	2606
ACS-100	-	440	-	864	1141	67.1	10	140.8	176	-	2665

Note: OPCC - Portland cement based control mix; ACS-X - represents AASC mixes with X (% by volume) of sand replaced with copper slag.

APPENDIX-III

Sample Theoretical Calculations for Beams - OPCC

General

Theoretical calculations are carried out in accordance with IS: 465-2000. Theoretical calculations are made for all the beams, but only specimen calculations for one OPCC-based beam are presented for illustrative purposes

Geometric Properties of Beam:

Breadth of beam, $b = 150\text{mm}$ Depth of Beam, $D = 250\text{mm}$

Clear cover to rebars = 25 mm

Effective cover = 31 mm

Effective depth of beam, $d = 219\text{mm}$

Span of the beam = 2250mm

Material Properties

Cube Strength of concrete obtained in the laboratory $f_{ck} = 53\text{ N/mm}^2$

Yield stress of steel TMT $f_y = 460\text{ N/mm}^2$

Elastic modulus of steel $E_s = 200\text{ GPa}$

Tension Reinforcement

Tension reinforcement provided = $3\text{ No, } 12\text{mm}\Phi$

$$A_{st} = 339.29\text{ mm}^2$$

Check for maximum percentage of reinforcement:

From Cl: 26.5.1.1 of IS: 456-2000

Maximum reinforcement = $0.04.b.D$

$$= 0.04 \times 150 \times 250$$

$$= 1500\text{ mm}^2 > \text{Provided } 339.29\text{ mm}^2$$

Check for minimum percentage of reinforcement

Minimum reinforcement = $0.85\text{ bd} / f_y$

$$= 0.85 \times 150 \times 219/460$$

$$= 60.70 \text{ mm}^2 < \text{Provided } 339.29 \text{ mm}^2$$

(i) Calculation of theoretical moment of resistance

According to IS:456-2000, Annex G, with partial safety factors taken as 1.5 for concrete and 1.15 for steel, maximum depth of neutral axis and actual depth of neutral axis are given by,

Maximum depth of neutral axis,

$$\frac{X_{u\max}}{d} = \frac{0.0035}{0.0055 + \frac{0.87f_y}{E_s}}$$

$$= \frac{0.0035}{0.0055 + \frac{0.87 \times 460}{200000}}$$

$$X_{u\max} = 102.2 \text{ mm}$$

Actual depth of neutral axis,

$$X_u = \frac{0.87f_y A_{st}}{0.36f_{ck} b}$$

$$X_u = \frac{0.87 \times 460 \times 339.29}{0.36 \times 53 \times 150}$$

$$X_u = 47.4 \text{ mm} < X_{u\max}; \text{ Hence the beam is under reinforced}$$

Ultimate Moment M_u

$$M_u = 0.87 f_y \cdot A_{st} (d - 0.42X_u)$$

$$= 0.87 \times 460 \times 339.29 (219 - 0.42 \times 47.4)$$

$$= 27.01 \text{ kN-m}$$

Theoretical Ultimate Load Computation

$$\text{Self-weight of beam} = 0.15 \times 0.25 \times 24.5 = 0.91875 \text{ kN/m}$$

$$M_u = \frac{W_{(\text{applied})}L}{6} + \frac{W_{(\text{self weight})}L^2}{8}$$

$$27.01 \times 10^6 = \frac{W_{(\text{applied})} \times 2250}{6} + \frac{0.91875 \times 2250^2}{8}$$

$$W_{(\text{applied})} = 72.0 \text{ kN}$$

Shear Reinforcement Calculations

$$\text{Total ultimate load} = 72.0 + 0.91875 \times 2.25$$

$$= 72.0 + 2.0672$$

$$= 74.2 \text{ kN}$$

$$\text{Ultimate shear force, } V_u = \frac{74.2}{2} = 37.06 \text{ kN}$$

$$V_u = 37.06 \text{ kN}$$

Nominal shear stress,

$$\tau_{vu} = \frac{V_u}{b.d} = \frac{37.06 \times 1000}{150 \times 219}$$

$$= 1.12 \text{ N/mm}^2$$

From Cl. 40.4 and Table 20 of IS 456: 2000, for M45 concrete,

$$\tau_{c_{\max}} = 4 \text{ N/mm}^2$$

$\tau_v < \tau_{c_{\max}}$, Hence OK

Check for Shear Reinforcement

$$\frac{100 \times A_{st}}{b.d} = \frac{100 \times 339.29}{150 \times 219} = 1.032$$

From Table 19, IS: 456-2000, for the above value, for M45 grade concrete, on interpolation,

$$\tau_c = 0.68 \text{ N/mm}^2$$

$\tau_v > \tau_c$ Hence shear reinforcement is required.

Shear force to be resisted by shear reinforcement is

$$\begin{aligned} V_{us} &= V_u - \tau_c \cdot b \cdot d \\ &= 37060 - (0.68 \times 150 \times 219) \\ &= 14.72 \text{ kN} \end{aligned}$$

From clause: 40.4, spacing of 2l, # 8mm bars as vertical stirrups,

$$\begin{aligned} S_v &= \frac{0.87 \cdot f_y \cdot A_{sv} \cdot d}{V_{us}} \\ &= \frac{0.87 \times 460 \times 2 \times 50.26 \times 219}{14.72 \times 10^3} \\ &= 598.5 \text{ mm} \end{aligned}$$

Spacing of the stirrups for minimum shear reinforcement as per Cl: 26.5.1.6 of IS: 456-2000

$$\begin{aligned} S_v &= \frac{0.87 \cdot f_y \cdot A_{sv}}{0.4 \cdot b} \\ &= \frac{0.87 \times 460 \times 2 \times 50.26}{0.4 \times 150} \\ &= 670.46 \text{ mm} \end{aligned}$$

Maximum spacing of shear reinforcement, as per IS: 456-2000, is the minimum of the following

- (i) $0.75d = 0.75 \times 219 = 164.25 \text{ mm}$
- (ii) 300 mm

Considering all the above factors, to be safe in shear; a stirrups-spacing of 125 mm is adopted.

(iii) Check for Lateral Stability

As per IS: 456-2000, slenderness limit for a simply supported beam is minimum of the following. The length of the beam should be less than the value of,

(i) $60 \times b = 60 \times 150 = 9000 \text{ mm}$

(ii) $250 \times \frac{b^2}{d} = 250 \times \frac{150^2}{219} = 25684.93 \text{ mm}$

But the actual test span of 2550 mm is less than 9000 mm. Hence the beam is laterally stable.

(iv) Check for Bond

Maximum stress can be expected at mid span. Available development length with 25 mm cover at the beam-ends, without any hooks is,

$$L_d = \frac{2250}{2} - 25 = 1100 \text{ mm}$$

As per IS: 456 - 2000, required development length for the reference beam, with deformed bars is,

$$L_d = \frac{12 \times 460}{4 \times 3.04} = 453.9 \text{ mm}$$

Available development length is more than required, hence safe.

(v) Calculation of cracking load

From Cl: C-2.1 of IS: 456-2000

$$\text{Cracking moment, } M_{cr} = \frac{f_{cr} \cdot I_{gr}}{y_t}$$

Modulus of rupture, $f_{cr} = 5.1 \text{ M Pa}$

$$I_{gr} = \frac{b \cdot D^3}{12} = \frac{150 \times 250^3}{12} = 195.3125 \times 10^6 \text{ mm}^4$$

$$Y_t = D/2 = 125 \text{ mm}$$

$$M_{cr} = \frac{5.1 \times 195.31 \times 10^6}{125}$$

$$= 7.96 \text{ kN-m}$$

$$\text{First Crack load; } W_{cr} = \frac{6}{L} \left[M_{cr} - \frac{wl^2}{8} \right]$$

where w = self-weight = 0.9375 kN/m

$$W_{cr} = 19.7 \text{ kN}$$

(vi) Deflection for Short term Loading – Calculation under elastic theory

E_c for short term loading, = $33.04 \times 10^3 \text{ N/mm}^2$

$$\text{Modular ratio, } m = \frac{E_s}{E_c} = \frac{2 \times 10^5}{33.04 \times 10^3} = 6.06$$

For actual depth of neutral axis, based on elastic theory, $bx^2/2 = m A_{st} (d-x)$

Solving $x = 64.98 \text{ mm}$

$$I_{gr} = 195.3125 \times 10^6 \text{ mm}^4$$

Now for cracked moment of inertia,

$$I_{cr} = (1/3) bx^3 + m \cdot A_{st} \cdot (d-x)^2$$

$$= (1/3) 150 \times 64.98^3 + 6.06 \times 339.29 \times (219 - 64.98)^2$$

$$I_{cr} = 62.49 \times 10^6 \text{ mm}^4$$

$$I_{cr} < I_{gross}$$

Theoretical service moment,

$$M_{ser} = \frac{27.01}{1.5}$$

$$= 18.0 \text{ kNm}$$

Theoretical service load,

$$W_{ser} = \frac{W}{1.5}$$
$$= \frac{72.0}{1.5}$$

Theoretical service load = 48.0 kN

$$\frac{x}{d} = 0.297$$

$$Z = d - \frac{x}{3} = 197.34 \text{ mm}$$

$$\frac{Z}{d} = \frac{201.17}{219} = 0.90$$

$$\frac{bw}{b} = 1$$

Effective moment of inertia for cracked section:

$$I_{eff} = \frac{I_{cr}}{1.2 - \frac{M_{cr} \cdot Z}{M_{ser} \cdot d} \left| 1 - \frac{x}{d} \right| \frac{bw}{b}}$$

$$I_{eff} = 67.92 \times 10^6 \text{ mm}^4$$

$$I_{gr} > I_{cr} > I_{eff}$$

Total elastic deflection

$$\Delta_{TOTAL} = \Delta_{APPLIED \text{ LOAD}} + \Delta_{SELF \text{ WEIGHT}}$$

$$\Delta = \frac{23 \cdot W \cdot L^3}{1296 \cdot E_c \cdot I_{eff}} + \frac{5 \cdot w \cdot L^4}{384 \cdot E_c \cdot I_{eff}}$$

$$\Delta_{cr} = \frac{23 \times 19.7 \times 10^3 \times 2250^3}{1296 \times 33.04 \times 10^3 \times 195.3125 \times 10^6} + \frac{5 \times 0.91875 \times 2250^4}{384 \times 33.04 \times 10^3 \times 195.3125 \times 10^6}$$

$$\Delta_{cr} = 0.67 \text{ mm}$$

Deflection at theoretical service load = 48.0 kN

$$\Delta_s = \frac{23 \times 48.0 \times 10^3 \times 2250^3}{1296 \times 33.04 \times 10^3 \times 67.92 \times 10^6} + \frac{5 \times 0.91875 \times 2250^4}{384 \times 33.04 \times 10^3 \times 67.92 \times 10^6}$$

$$\Delta_s = 4.47 \text{ mm}$$

PUBLICATIONS BASED ON PRESENT RESEARCH

International/National Journals

1. **Mithun B.M**, and Narasimhan M.C, (2016) “Performance of Alkali Activated Slag Concrete Mixes Incorporating Copper Slag as Fine Aggregate”, *Journal of Cleaner Production, Elsevier*, Vol 112, Part 1, pp. 837-844.
2. **Mithun B.M**, Narasimhan M.C, Nitendra Palankar and Ravishankar A.U. (2015) “Flexural Fatigue performance of Alkali Activated Slag Concrete mixes incorporating Copper Slag as Fine Aggregate”, *SSP - Journal of Civil Engineering, DE GRUYTER* Vol 10, Issue 1, pp. 7-18.
3. **Mithun B.M**, Narasimhan M C and Nitendra Palankar. (2015) “Strength Performance of Alkali Activated Slag Concrete with Copper Slag as Fine Aggregate Exposed To Elevated Temperatures”, *International Journal of Earth Sciences and Engineering*, Vol 8, Issue 2, pp 519-526.
4. **Mithun B.M**, Narasimhan M C and Nitendra Palankar. (2015) “Studies on Alkali Activated Slag Mortar with Copper Slag as Fine Aggregate”, *International Journal of Earth Sciences and Engineering*, Vol 8, Issue 2, pp. 527-531.

International Conferences

1. **Mithun B.M**, Narasimhan M.C, Nitendra Palankar and Ravishankar A.U. (2015) “Experimental investigations on alkali activated slag concrete mixes incorporating copper slag as fine aggregate” UKIERI Concrete Congress-Concrete Research Driving Profit and Sustainability, NIT Jalandar, India.
2. **Mithun B.M** and Narasimhan M.C (2013). “Self-Cured Alkali Activated Slag Concrete Mixes-An Experimental Study”. 8th CUTSE International Conference, Sarawak, Malaysia.

RESUME'

Name : Mr. Mithun B M
Date of Birth : 25 May 1987
Permanent Address : #555, Temple Street, Bettadapura,
Periyapattana (Tq), Mysore (Dist),
571102
Karnataka,
India
Contact Number : +91-9480004877
Email : mithunbm@gmail.com

ACADEMIC QUALIFICATION:

Degree	Specialization	Institute	Duration
Ph.D	Civil Engineering	NITK, Surathkal	2011-2017
M. Tech	Construction Technology and Management	NITK, Surathkal	2008-2010
B E	Construction Technology and Management	SJCE, Mysore	2004-2008

PUBLICATIONS:

Journals:

1. Nitendra Palankar, A.U. Ravishankar and **Mithun B.M** (2017) "Investigations on alkali activated slag/fly ash concrete with steel slag coarse aggregate for pavement structures". *International Journal of Pavement Engineering, Taylor and Francis*, 1-13.
2. **Mithun B.M**, and Narasimhan M.C, (2016) "Performance of Alkali Activated Slag Concrete Mixes Incorporating Copper Slag as Fine Aggregate". *Journal of Cleaner Production, Elseveir*, Vol 112, Part 1, pp. 837-844.
3. Nitendra Palankar, A.U. Ravishankar and **Mithun B.M**, (2016) "Durability of alkali activated slag/fly ash concrete with steel slag coarse aggregate". *Journal of Cleaner Production, Elseveir*, Vol 129, pp. 437-448.
4. **Mithun B.M**, Narasimhan M.C, Nitendra Palankar and Ravishankar A.U. (2015) "Flexural Fatigue performance of Alkali Activated Slag Concrete mixes incorporating

Copper Slag as Fine Aggregate”, *SSP - Journal of Civil Engineering, DE GRUYTER*, Vol 10, Issue 1, pp. 7-18.

5. Nitendra Palankar, A.U. Ravishankar and **Mithun B.M.** (2015) “Studies on eco-friendly concrete incorporating industrial waste as aggregates”, *International Journal of Sustainable Built Environment, Elsevier*, Vol 4, Issue 2, pp. 378–390.
6. Nitendra Palankar, A.U. Ravishankar and **Mithun B.M.** (2015) “Air-cured alkali activated binders for concrete pavements”. *International Journal of Pavement Research and Technology, Elsevier*, Vol 8, Issue 4, pp. 289-294.
7. Nitendra Palankar, A.U. Ravishankar and **Mithun B.M.** “Performance and Fatigue behaviour of Alkali Activated Slag Concrete with Steel Slag as Coarse Aggregate for Concrete Pavement”. *Indian Roads Congress, Accepted for publication, 2015.*
8. **Mithun B.M.**, Narasimhan M C and Nitendra Palankar. (2015) “Strength Performance of Alkali Activated Slag Concrete with Copper Slag as Fine Aggregate Exposed To Elevated Temperatures”. *International Journal of Earth Sciences and Engineering*, Vol 8, Issue 2, pp 519-526.
9. **Mithun B.M.**, Narasimhan M C and Nitendra Palankar. (2015) “Studies on Alkali Activated Slag Mortar with Copper Slag as Fine Aggregate”, *International Journal of Earth Sciences and Engineering*, Vol 8, Issue 2, pp. 527-531.
10. Nitendra Palankar, A.U. Ravishankar and **Mithun B.M.** (2014) “Experimental Investigation on Air-cured Alkali Activated GGBFS-Fly ash Concrete Mixes”. *International Journal of Advanced Structures and Geotechnical Engineering*, Vol 3, Issue 4, pp.326-332.
11. Deepak T.J., Albarra Elsayed., Noor Hassan, Chakravarthy. N, Siow Yun Tong, **Mithun B.M.** (2014). “Investigation on Properties of Concrete with Palm Oil Fuel Ash as Cement Replacement”. *International Journal of Scientific and Technology Research*, Vol 3, Issue 1, pp. 138-142.
12. Sambo A.G., Deepak T.J and **Mithun B.M.** (2013). “Influence of Silica Fume on the Strength of Biostyrene Mixed Concrete”. *International Journal of Earth Sciences and Engineering*, Vol No. 6, Issue 4, pp. 606-611.
13. Sanjeev. S., Prithviraj H.K., **Mithun B.M.**, Mahesh A.M., Ganesh K.S., Sharath M.R., and Adarsh (2013). “Effect of Different Kind of Food Waste in Biogas Production: A Case Study”. *International Journal of Environmental Research and Development*, Vol 3, Issue 5, pp 50-55.

Conferences:

14. **Mithun B.M**, Narasimhan M.C, Nitendra Palankar and Ravishankar A.U. (2015) “Experimental investigations on alkali activated slag concrete mixes incorporating copper slag as fine aggregate”. UKIERI Concrete Congress-Concrete Research Driving Profit and Sustainability, NIT Jalandar, India.
15. **Mithun B.M**, Narasimhan M C and Nitendra Palankar (2015). “Strength Performance of Alkali Activated Slag Concrete with Copper Slag as Fine Aggregate Exposed To Elevated Temperatures”. 2nd International Conference on Earth Sciences and Engineering (ICEE 2015), NIT, Coimbatore, Tamilnadu.
16. **Mithun B.M**, Narasimhan M C and Nitendra Palankar. (2015) “Studies on Alkali Activated Slag Mortar with Copper Slag as Fine Aggregate”. 2nd International Conference on Earth Sciences and Engineering (ICEE 2015), NIT, Coimbatore, Tamilnadu.
17. Nitendra Palankar, A.U. Ravishankar and **Mithun B.M**. (2014) “ Performance of Air-Cured Alkali Activated GGBFS-Fly Ash Concrete Mixes”. 3rd World Conference on Applied Sciences, Engineering and Technology (WCSET 2014), pp. 27-29 September 2014, Kathmandu, NEPAL (Best Paper Award).
18. Prashanth M.H and **Mithun B.M** (2014). “Effect of Curing Compounds on Strength Properties of Concrete Mixes”. 1st Annual Conference on Innovations and Developments in Civil Engineering, NITK Surathkal.
19. **Mithun B.M** and Narasimhan M.C (2013). “Self-Cured Alkali Activated Slag Concrete Mixes-An Experimental Study”. 8th CUTSE International Conference, Sarawak, Malaysia.
20. Subrahmanya Kundapura and **Mithun B.M** (2010). “S–Curve – Tool An Integrated Approach to Earned Value Management”, National Conference on Recent Trends in Emerging Technologies.